Pergamon

Geochimica et Cosmochimica Acta, Vol. 68, No. 19, pp. 3971-4006, 2004

0016-7037/04 $30.00 + .00

doi:10.1016/j.gca.2004.02.026

Geochemistry of Cenozoic microtektites and clinopyroxene-bearing spherules

Billy P. Glass,[1,*] Heinz Huber,[2] and Christian Koeberl[2]

[1]Geology Department, University of Delaware, Newark, Delaware 19716, USA
[2]Department of Geological Sciences, University of Vienna, Althanstrasse 14, A-1090 Vienna, Austria

(*Received July* 1, 2003; *accepted in revised form February* 18, 2004)

Abstract—We have determined the major and trace element compositions of 176 individual microtektites/spherules from the Australasian, Ivory Coast, and North American microtektite and clinopyroxene-bearing (cpx) spherule layers. Trace element contents for up to 30 trace elements were determined by instrumental neutron activation analysis (INAA), and major element compositions were determined using energy dispersive X-ray (EDX) analysis in combination with a scanning electron microscope (SEM). In addition, petrographic data were obtained for the cpx spherules using the SEM and EDX. This is the first trace element study of individual Australasian microtektites, and the data revealed the presence of a previously unrecognized group of Australasian microtektites with high contents of Ni (up to 471 ppm). In previous studies the high-Mg (HMg) Australasian microtektites were thought to be related to the HMg Australasian tektites, but our trace element data suggest that the high-Ni (HNi) Australasian microtektites, rather than the high-Mg microtektites, are related to the high-Mg Australasian tektites. We find that Cenozoic microtektites/spherules from a given layer can be distinguished from microtektites/spherules from other layers as a group, but it is not always possible to determine which layer an individual microtektite/spherule came from based only on trace element compositions. The cpx spherules and most of the microtektites have Cr, Co, and Ni contents that are higher than the average contents of these elements in the upper continental crust, suggesting the presence of a meteoritic component. The highest Cr, Co, and Ni contents are found in the cpx spherules (and low-Si cpx-related microtektites). Unetched to slightly etched cpx spherules have Ni/Cr and Ni/Co ratios that generally lie along mixing curves between the average upper continental crust and chondrites. The best fit appears to be with an LL chondrite. The moderately to heavily etched cpx spherules have values that lie off the mixing curves in a direction that suggests Ni loss, probably as a result of solution of a Ni-rich phase (olivine?). The Ni-rich Australasian microtektites also have Ni values that lie close to mixing curves between the average upper continental crust and chondrites. However, both the cpx spherules and HNi Australasian microtektites appear to have Ir (and to a lesser extent Au) contents that are much too low to have Ni/Ir ratios similar to chondritic values. We have no explanation for the low-Ir and -Au contents except to speculate that they may be the result of a complex fractionation process. The Ivory Coast and North American microtektites do not have high enough siderophile element contents to reach any firm conclusions regarding the presence of, or nature of, a meteoritic component in them. Trace element compositions are consistent with derivation of the Cenozoic microtektite/spherule layers from upper continental crust. The normal Australasian microtektites appear to have been derived from a graywacke or lithic arenite with a range in clay and quartz content. The source rock for the high-Mg Australasian microtektites is not known, but the HMg microtektites do not appear to be normal Australasian microtektites that were simply contaminated by meteorites or ultramafic rocks. The average Ivory Coast microtektite composition can be matched with a mixture of target rocks at the Bosumtwi crater. The average composition of the North American microtektites suggests an arkosic source rock, but with graywacke and quartz-rich end members. However, we could not match the composition of the North American microtektites with lithologies in impact breccias recovered from the Chesapeake Bay impact structure that is believed to be the source crater. Likewise, we could not match the composition of the cpx spherules with mixtures of basement rocks and overlying sedimentary deposits (for which compositional data are available) at the Popigai impact crater that may be the source crater for the cpx spherules. This may be because the cpx spherules were derived, in large part, from clastic surface rocks (sandstones and shales) for which no compositional data are available.

1. INTRODUCTION

Microtektites belonging to the Australasian, Ivory Coast, and North American tektite strewn fields have been found in marine sediments adjacent to the respective tektite strewn fields. In addition, a layer of clinopyroxene-bearing impact spherules has been found in deep-sea sediments just below the North American microtektite layer. Geochemical and petrographic data have confirmed that tektites and microtektites are distal impact ejecta (see e.g., Koeberl, 1994; Montanari and Koeberl, 2000). Australasian microtektites have been recovered from ~50 sediment cores taken in the Indian Ocean, western equatorial Pacific Ocean, and Philippine, Sulu, Celebes, and South China Seas (Peng et al., 1982; Glass and Wu, 1993; Prasad and Sudhakar, 1999; Lee and Wei, 2000). The Australasian microtektites are Middle Pleistocene in age, and the Australasian microtektite layer is closely associated with the Brunhes/Matuyama (B/M) geomagnetic reversal boundary. Based on paleomagnetic stud-

* Author to whom correspondence should be addressed (bglass@UDel.Edu).

ies, the Australasian tektite event appears to have taken place ~12–16 ka before the B/M reversal (Burns, 1989; Schneider et al., 1992; Lee and Wei, 2000), or ~0.8 Ma ago. This age is in agreement with the radiometric ages determined for the Australasian tektites (e.g., Izett and Obradovich, 1992; Kunz et al., 2000; Yamei et al., 2000; Lee et al., 2004). The Australasian strewn field covers nearly 10% of the Earth's surface. The source crater has not been found, but several different lines of evidence suggest that it may be in, or near, Indochina (e.g., Stauffer, 1978; Ford, 1988; Schnetzler, 1992; Glass and Pizzuto, 1994; Koeberl, 1994; Lee and Wei, 2000; Glass, 2003).

The Ivory Coast strewn field is much smaller than the Australasian strewn-field, and Ivory Coast microtektites have been found in only 11 cores in the eastern equatorial Atlantic Ocean (Glass et al., 1991). This layer is also Middle Pleistocene in age, but is slightly older than the Australasian layer. The Ivory Coast microtektite layer is found just above the base of the Jaramillo geomagnetic subchron (Schneider and Kent, 1990) and appears to be ~8 ka younger than the reversal at the base of the Jaramillo subchron (Glass et al., 1991), that has an age of 1.07 Ma (Cande and Kent, 1995). This indicates an age of ~1.1 Ma for the Ivory Coast microtektite layer that is the same, within the errors involved, as the radiometric age of the Ivory Coast tektites (Glass et al., 1991; Koeberl et al., 1997). The source crater for the Ivory Coast strewn field appears to be the 10.5-km-diameter Bosumtwi crater in Ghana, based on geographical location, age, chemical composition, and Sr and Nd isotopic data (e.g., Schnetzler et al., 1966; Schnetzler et al., 1967; Jones, 1985; Koeberl et al., 1997; Koeberl et al., 1998).

North American microtektites have been found in upper Eocene marine sediments on Barbados and in sediment cores recovered from the Gulf of Mexico, Caribbean Sea, and northwestern Atlantic Ocean (e.g., Donnelly and Chao, 1973; Glass et al., 1985; Sanfilippo et al., 1985; Keller et al., 1987; Glass et al., 1998; Glass, 2000). Tektite fragments occurring in the North American microtektite layer on Barbados have Sr and Nd isotopic ratios indistinguishable from North American tektites (Ngo et al., 1985). The North American microtektites are associated with unmelted impact ejecta, including shocked quartz and feldspar with multiple sets of planar deformation features, coesite, stishovite, and reidite (a high-pressure polymorph of zircon) (Glass, 1989; Glass and Wu, 1993; Glass et al., 1998; Glass and Liu, 2001). Radiometric dating of tektite fragments found in the North American microtektite layer at Barbados and at Deep Sea Drilling Project (DSDP) Site 612 (on the upper continental slope off New Jersey) indicates an age of ~35 Ma for this layer (Glass et al., 1986; Obradovich et al., 1989). This age is consistent with the fission-track, K-Ar, and ^{40}Ar-^{39}Ar ages obtained for the North American tektites (Zähringer, 1963; Storzer and Wagner, 1971; Albin and Wampler, 1996). The Chesapeake Bay structure has been suggested as the source of this strewn field based on geographic location, age, composition, and isotopic data (Poag et al., 1994; Koeberl et al., 1996). The size of the Chesapeake Bay structure is generally given as 85 km (Poag et al., 2004); however, some authors suggest that the diameter of the crater before resurge may have been only ~40 km (e.g., Grieve and Therriault, 2004).

The layer of upper Eocene crystal-bearing or clinopyroxene-bearing spherules (cpx spherules) occurs at numerous sites around the globe and may be global in geographic extent (Glass et al., 1985; Keller et al., 1987; Glass et al., 1998; Glass and Koeberl, 1999a; Vonhof and Smit, 1999; Glass, 2000; Liu and Glass, 2001). Where the North American microtektite layer is present, the cpx spherule layer occurs just below it and often the two layers overlap. Based on biostratigraphic data, the cpx spherule layer appears to be ~10 to 20 ka older than the North American microtektite layer (Glass et al., 1998). The cpx spherules are distinguished from microtektites by the presence of crystalline phases in the spherules. The most abundant crystalline phase is clinopyroxene, as indicated by the name, but Ni- and Cr-rich spinel crystals are also present in many of the spherules (e.g., Glass et al., 1985; Glass and Burns, 1987). The cpx spherule layer is associated with a positive Ir anomaly (Glass et al., 1985; Keller et al., 1987; Vonhof and Smit, 1999; Kyte and Liu, 2002) and with the extinction of several species of Radiolaria (Glass et al., 1985; Sanfilippo et al., 1985).

It has been suggested, based on similarity in age and Sr and Nd isotopic compositions, that the source crater for the cpx spherule layer may be the 35.7 ± 0.8 Ma old (Bottomley et al., 1997) 100-km-diameter Popigai impact crater in northern Siberia (Whitehead et al., 2000). Additional support for Popigai as the source of the cpx spherules is found at Massignano, Italy, where shocked quartz and pancake-shaped smectite spherules, containing Ni- and Cr-rich spinel crystals, have been found associated with a positive Ir anomaly in upper Eocene deposits with the same age, as far as can be determined, as the cpx spherule layer (Montanari et al., 1993; Clymer et al., 1996; Pierrard et al., 1998). The pancake spherules appear to be diagenetically altered and flattened cpx spherules. According to Langenhorst (1996), the nature of the shocked quartz is consistent with derivation of this layer, and thus, the cpx spherules from the Popigai crater. At Massignano there is a second Ir anomaly just above the one that is associated with the pancake spherules, that Montanari and Koeberl (2000) suggest could be associated with the North American strewn field.

Microtektites have been found associated with the cpx spherules at several sites in the equatorial Pacific, Indian Ocean, and Atlantic sector of the Southern Ocean. It has been suggested that the microtektites found within the cpx spherule layer at Ocean Drilling Program (ODP) Site 689 in the Southern Ocean (Glass and Koeberl, 1999a; Vonhof and Smit, 1999) and DSDP Site 216 in the Indian Ocean (Glass and Koeberl, 1999b) belong to the North American strewn field. However, more recent Sr and Nd isotopic data suggest that the microtektites in the cpx spherule layer at these sites (and presumably those in the equatorial Pacific Ocean sites) have the same source as the cpx spherules (Whitehead et al., 2000; Liu et al., 2001)

The number of upper Eocene microtektite/spherule layers has been a matter of debate, with estimates ranging from two (Glass et al., 1985; Glass and Burns, 1987), to three (Keller et al., 1987), or six or more (Hazel, 1989). Most of the debate is concerned with the number of cpx spherule layers, but Miller et al. (1991) proposed that the microtektite layer at Site 612, off New Jersey, is older than the microtektite layer on Barbados. However, most authors now agree that there are just two layers: 1) the North American microtektite layer and 2) the cpx spherule layer (Glass, 1990; Wei, 1995; Vonhof and Smit, 1999;

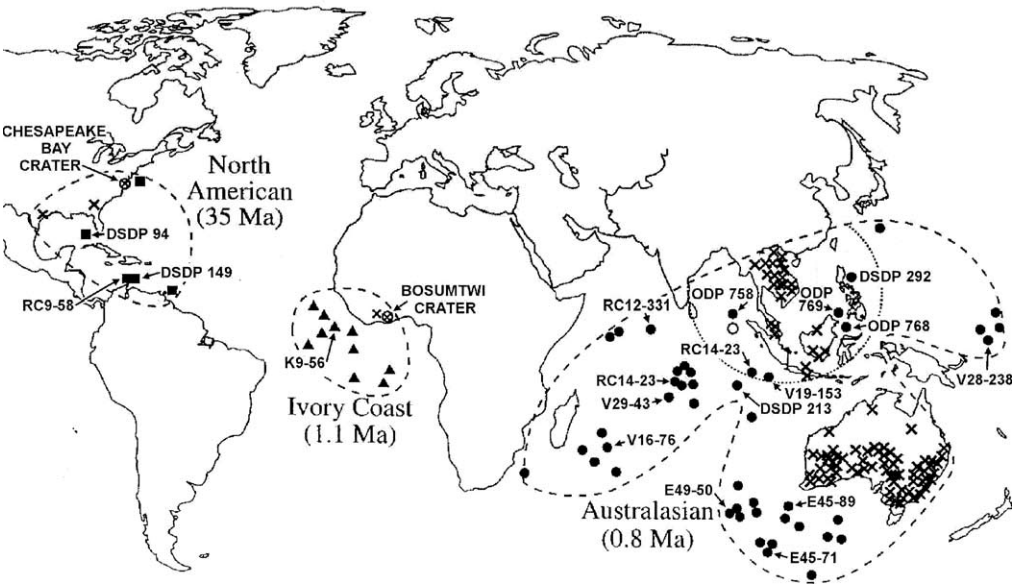

Fig. 1. Map of the Australasian, Ivory Coast, and North American tektite strewn fields. Ages of the strewn fields are given in parentheses. Generalized regions of tektite occurrences on land are indicated by Xs. Australasian, Ivory Coast, and North American microtektite-bearing core sites indicated by solid circles, triangles, and squares, respectively. Dashed lines indicate the known extent of each strewn field. The dotted line inside the Australasian strewn field encircles core sites with the highest concentrations of microtektites and with unmelted ejecta (shocked quartz with planar deformation features, coesite, stishovite) (Glass and Wu, 1993; Glass and Pizzuto, 1994). Core sites for the microtektites used in this study are labeled: DSDP = Deep Sea Drilling Project; ODP = Ocean Drilling Program; E = Eltanin, K = Kane; RC = Robert Conrad, V = Vema. Locations of the proposed source crater for the Ivory Coast and North American strewn fields are also indicated.

Montanari and Koeberl, 2000; Whitehead et al., 2000; Marchand and Whitehead, 2002).

There have been a limited number of previous trace element studies of Cenozoic microtektites and cpx spherules. The first trace element studies of microtektites were done by Frey et al. (1970) and Frey (1977). Due to limitations in the sensitivity of their analytical methods they could not analyze individual microtektites, but had to analyze a group of microtektites. Frey et al. (1970) presented trace element data for a composite of five Australasian microtektites and for a composite of ten Ivory Coast microtektites. Frey (1977) published some trace element data (Sc, Cr, Co, and a few rare earth elements) for a composite of 16 bottle green or high-magnesium (HMg) Australasian microtektites and a composite of 16 HMg Ivory Coast microtektites. Trace element data for four individual Ivory Coast microtektites were reported by Koeberl et al. (1997). Nagasawa et al. (1986) determined the trace element compositions of 11 North American microtektites from the Gulf of Mexico (DSDP Site 94), the Caribbean Sea (DSDP Site 149), and Barbados. Koeberl and Glass (1988) presented trace element data for four individual North American tektite fragments and a composite of two North American microtektites from Barbados and two tektite fragments from the North American microtektite layer at Site 612 in the NW Atlantic Ocean. Glass et al. (1998) reported trace element data for eight tektite fragments in the North American microtektite layer at Site 904, 4 km north of Site 612. Trace element data for eight microtektites from the cpx spherule layer at ODP Site 689 in the South Atlantic sector of the Southern Ocean were published in Glass and Koeberl (1999a).

In this study, we determined the trace element and major element composition of 103 individual (no composites) Cenozoic microtektites and 73 individual cpx spherules. We report here the first trace element analyses of individual Australasian microtektites. The number of Ivory Coast trace element analyses presented here increases the total number of published analyses by a factor of four. The cpx spherule trace element analyses in this report increase the total number of published analyses by more than an order of magnitude and significantly increase the number of sites for which we have trace element data. Furthermore, we present data for up to 30 trace elements, which is as much as two to three times the number in many previous studies.

The objectives of the present study were to: (1) improve the database for Cenozoic microtektite and cpx-spherule compositions; (2) determine how well trace element data can be used to distinguish between microtektite/spherule layers; (3) see what the trace element data indicate about the nature of the source material for the various microtektite/spherule layers; (4) help identify or confirm possible source craters; and (5) help identify meteoritic contamination by the impacting bodies.

2. METHODS

One of us (BPG) has been collecting and studying microtektites and impact spherules from marine sediments for ~36 yr. The microtektites and cpx spherules used in this study were from this collection. We selected microtektites/spherules from as many different sites as possible. The main criterion was that the spherules be large enough to yield statistically valid trace element concentrations. We selected 47 Australasian microtektites (from 15 sites), 16 Ivory Coast microtektites (from one core), 25 North American microtektites (from three sites), 73 cpx spherules (from nine sites), and 15 microtektites from the cpx layer (at four sites) for this project (Figs. 1 and 2). The microtektites used in this study range in size from a 180-μm-diameter spherule to a 600 $\times$ 800 μm fragment of a spherule. Microtektite and spherule weights

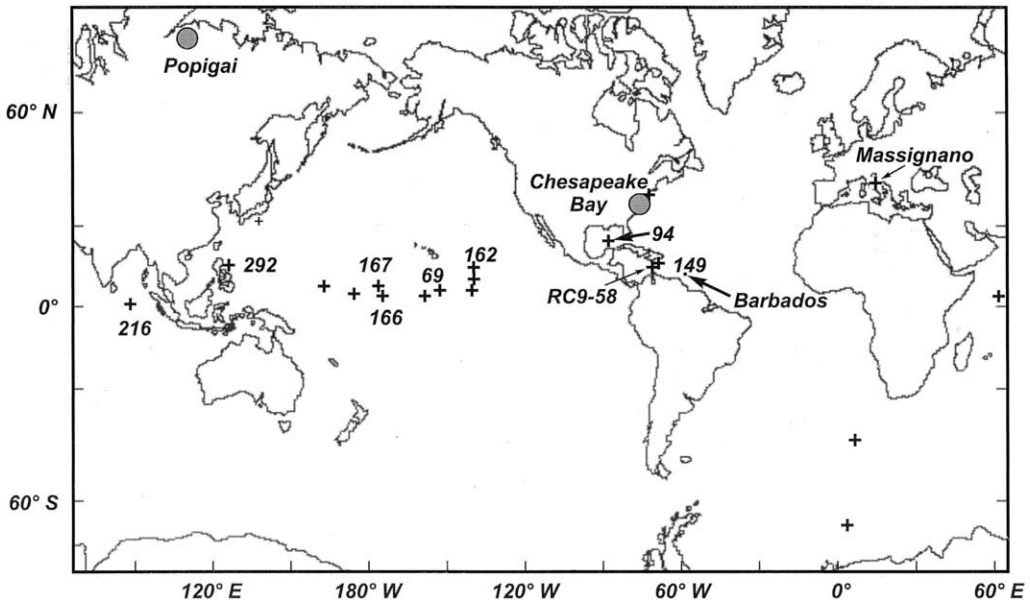

Fig. 2. Clinopyroxene-bearing-spherule sites. Sites containing cpx spherules indicated with plus signs. Core sites for the cpx spherules and cpx-related microtektites used in the study are labeled (Deep Sea Drilling Project sites are indicated by the site number). Microtektites from the cpx-spherule layer (cpx-related microtektites) are from DSDP Sites 162, 167, 216, and 292. Locations of Barbados and Massignano, as well as Chesapeake Bay and Popigai impact structures, are also indicated.

ranged from 0.2 to 258.0 μg (see appendix Table A1 or electronic annex EA1). Compositional data from a few of the smaller microtektites/spherules have large errors and were not used in the calculated averages and standard deviations, or in the figures. Although specimen selection was based primarily on size, there is a wide range in microtektite/spherule sizes, and we see no systematic variation in composition with size which would suggest that selecting the larger specimens might have biased the compositional data.

The microtektites and cpx spherules were analyzed in Vienna for trace element contents using instrumental neutron activation analysis (INAA). The spherules were placed in drilled depressions in high-purity quartz disks and wrapped, together with separately packaged geological reference standards, in aluminum foil for irradiation. In general, because of the small masses, the samples were irradiated for ~100 hr in a high-flux reactor at ~7 x 10^{13} n/cm^{2}s. After irradiation, the samples and standards were weighed using a Mettler UM3 ultramicrobalance (to $\pm$ 0.1 μg). Very long counting times (up to several days) on high-efficiency detectors were used because of the small sample masses. For other details on the procedure (standards, instrumentation, precision, accuracy) see Koeberl (1993). After INAA counting and an appropriate cooling period, the samples were returned to the University of Delaware for major element determinations and petrographic studies. The microtektites/spherules were mounted in epoxy on 1“ diameter glass discs and polished sections were prepared. They were then studied by optical (petrographic) and scanning electron microscopy. Major element contents were determined by energy dispersive X-ray analysis (see Glass (1989) and Glass and Koeberl (1999a) for details). Microtektite compositions were usually determined by averaging five spot analyses, but because of heterogeneity, the cpx compositions were determined by averaging 10–15 spot analyses. Scanning electron microscopy and energy dispersive X-ray (EDX) analysis were used to study the crystalline phases in the cpx spherules and to determine the degree of etching (percent void space on the polished surfaces). The compositions were normalized to 100 wt.% and then small corrections were made based on analyses of glass, used as a standard, that was run at the same time and under the same conditions as the microtektites and cpx spherules.

Major oxide and trace element data are given in Table A1 and EA1. Four of the cpx spherules were lost during preparation of polished sections for SEM/EDX analysis. No major oxide data were obtained for these specimens using SEM/EDX, but the FeO and Na_2O contents determined by INAA are given.

Statistical analyses were used to evaluate the compositional differences between the Australasian, Ivory Coast, and North American microtektites, and cpx spherules and microtektites associated with the cpx spherules (cpx-related microtektites). Levene’s test (Levene, 1960) was used to determine if the microtektites/cpx spherules from each layer were homogeneous in variance. Analysis of variance (ANOVA) was used to determine which elements are the most effective in distinguishing between the different microtektite/spherule groups. Classifications based on these elements were then evaluated, using discriminant analysis, to determine how many microtektites/spherules were classified correctly.

We used an updated version (see Huber (2003)) of the harmonic least-squares mixing program (HMX) by Stöckelmann and Reimold (1989) to perform mixing calculations of target rocks from proposed source craters in attempts to reproduce the compositions of the microtektites/cpx spherules from the respective source craters. This program allows extensive mixing calculations using the average compositions of target rocks and includes measurement and averaging errors. The program is characterized by separate treatment of the different elements, use of a large number of input components (target rocks), and the ability to force the sum to 100% or not. The latter feature can be used to determine whether or not there is a missing component in the input mixture.

3. RESULTS AND COMPARISON WITH PREVIOUS STUDIES

3.1. Australasian Microtektites

Previous studies have shown that the Australasian microtektites can be divided into two end-member groups based on appearance and major element composition: (1) normal and (2) bottle-green or high magnesium (HMg) (Cassidy et al., 1969; Glass, 1972a; Glass, 1972b). Most (~90%) of the microtektites belong to the normal group. These microtektites range from transparent pale-yellow, to transparent yellow-brown, to yel-

low-green, to translucent brown, to opaque black. They have a wide range in major oxide compositions but are generally similar to Australasian tektites in composition (Cassidy et al., 1969; Glass, 1972b). The bottle-green or HMg microtektites are transparent green, have a highly corroded appearance, and have MgO contents as high as 24 wt.% (Cassidy et al., 1969; Glass, 1972a; Glass, 1972b). The microtektites in a third group are transparent yellow-green and have intermediate MgO contents.

In this study, we analyzed 37 normal, five intermediate, and four HMg microtektites (Table A1). In addition, one microtektite was found to contain high aluminum (~32 wt.% Al_2O_3) and low silica (~41 wt.% SiO_2). Similar to the major element contents, the trace element abundances are quite variable (Table 1). Several Australasian microtektites that were originally assigned to the normal group were found to have high-Ni contents (up to ~470 ppm) (Table A1 and Table 1). These high-Ni (HNi) Australasian microtektites are recognized for the first time. The HNi Australasian microtektites also have higher average Co than the normal, intermediate, and HMg Australasian microtektites. Although the averages of most of the other trace element contents are different between the HNi and normal Australasian microtektites, they all exhibit a great degree of overlap (Table 1). The HNi Australasian microtektites are generally transparent to translucent brownish-green to dark brown.

The major oxide compositions of the normal and HNi Australasian microtektites are similar to Australasian tektites, especially australites (Table 1). However, the major oxide contents of the intermediate Australasian microtektites don't match those of any of the Australasian tektites. They have lower SiO_2, Na_2O, and K_2O and higher Al_2O_3, MgO, and CaO contents than do normal Australasian tektites. They also have higher Al_2O_3 and CaO and lower Na_2O and K_2O than the rare HMg Australasian tektites defined by Chapman and Scheiber (1969) that are found mostly in Java (Table 1). The HMg Australasian microtektites also have major oxide compositions that don't match those of any Australasian tektite groups, although previous work (Chapman and Scheiber, 1969; Glass, 1972a) showed that their major oxide compositions overlap smoothly with the compositions of the HMg Australasian tektites.

The trace element contents of the Australasian microtektites are similar to those previously reported for the Australasian tektites (Table 1). However, the normal Australasian microtektites have higher average contents of Ga, REEs, Au, and Th, and lower average U than the Australasian tektites (Table 1) (see footnotes to Table 1 for sources of Australasian tektite data). The trace element contents of the high-Ni (HNi) Australasian microtektites overlap the trace element contents of the Australasian tektites, except for higher Ga and some REEs. The Cr, Co, and Ni contents of the HNi normal Australasian microtektites are higher than in most of the Australasian tektites, but are similar to those of the HMg Australasian tektites (Table 1). In fact, the HNi Australasian microtektites have trace element contents more similar to those of the HMg tektites than do the HMg microtektites (Table 1). Both the intermediate and HMg Australasian microtektites have higher Sc and Cr and lower Rb, Cs, and U contents compared with those of the splash-form and Muong Nong-type (MN) Australasian tektites (Table 1), although the Cr contents of the intermediate Australasian microtektites do overlap with those of the HMg Australasian tektites.

The chondrite-normalized REE patterns of the Australasian microtektites are similar to those of the Australasian tektites (Fig. 3a). The chondrite-normalized REE patterns of the HNi microtektites are similar to, but with slightly lower average values than, the normal Australasian microtektites (Fig. 3b). However, the chondrite-normalized values of the intermediate and HMg groups are higher than those of the normal microtektites, and for many of the REEs, the average chondrite-normalized values of the HMg microtektites are intermediate between those of the normal Australasian microtektites and those of the intermediate Australasian microtektites (Fig. 3b).

3.2. Ivory Coast Microtektites

The Ivory Coast microtektites are generally transparent brownish-green or greenish-brown with scalloped surfaces formed by overlapping shallow solution pits (Glass, 1969; Glass, 1974). They have a restricted range in major and trace element compositions compared with the Australasian and North American microtektites (Tables 1–3), even when considering that only sixteen Ivory Coast microtektites were analyzed and they were all from a single core (site). For example, the silica content of the Ivory Coast microtektites in this study only ranges from ~63 to ~69 wt.%. Earlier studies identified two end members for the Ivory Coast microtektites based on major element compositions: (1) a high-SiO_2, low-MgO end member and (2) a low-SiO_2, high-MgO (up to ~20 wt.%) bottle-green end member (Glass, 1969; Glass, 1972a). These two end members grade into each other and the cutoff point is arbitrary. Unfortunately, none of the Ivory Coast microtektites in this study were of the high-Mg variety. The trace element compositions are relatively uniform (Koeberl et al., 1997) except for some of the more volatile elements such as Ga, As, and Sb (Table A1 and Table 2).

The major oxide compositions of the 16 Ivory Coast microtektites in this report are similar to the major oxide compositions of Ivory Coast microtektites previously reported (Glass, 1969; Glass and Zwart, 1979; Glass et al., 1991; Koeberl et al., 1997) (Table 2). The microtektites have slightly lower average SiO_2 contents, while the average contents of most other oxides are slightly higher than the average for Ivory Coast tektites. However, all of the major oxide contents of the Ivory Coast microtektites in this study overlap the major oxide contents of the Ivory Coast tektites within one standard deviation (Table 2).

The trace element contents of the Ivory Coast microtektites are similar to the trace element contents of Ivory Coast tektites (Table 2). The average content of only two trace elements (Sc, Au) for the microtektites reported in this study do not overlap the average content (plus/minus one standard deviation) reported by Koeberl et al. (1997) for Ivory Coast tektites. The contents of both of these elements are lower than those reported for the Ivory Coast tektites.

3.3. North American Microtektites

Like the Ivory Coast microtektites, the North American microtektites are generally transparent brownish-green or greenish-brown. However, some of the North American mi-

Table 1. Composition of Australasian microtektites and tektites from this paper and various other sources (major elements in wt. % and trace elements in ppm except as otherwise noted).

	Australasian Microtektites (This Study)											Australasian Tektites							
	Normal (30)		High Ni (7)		Intermediate (5)		HMg (4)		High (I)	Australasian Microtektites		Various[c]	MN-Type[d]		MN-Type[e]		Australites[f]	Various[g]	High-Mg[h]
	Ave.	S.D.	Ave.	S.D.	Ave.	S.D.	Ave.	S.D.	Al_2O_3	Normal[a]	HMg[b]	Range	Ave.	S.D.	Ave.	S.D.	Range (15)	Range (51)	Range (8)
SiO_2	69.6	4.4	69.4	1.9	62.3	3.7	54.6	2.1	41.4				72.50	3.89			69.67–77.39	64.76–82.40	67.40–73.15
TiO_2	0.82	0.12	0.75	0.04	0.93	0.15	0.92	0.22	1.38				0.76	0.09			0.6–0.9	0.43–1	0.64–0.76
Al_2O_3	14.9	2.5	13.5	1.0	17.3	2.53	17.4	3.0	32.5				12.94	1.56			9.84–13.96	8.20–17.70	10.90–12.90
FeO[i]	5.08	1.10	5.96	0.57	5.35	0.49	6.01	1.47	2.26				4.76	0.60	4.3	0.5	3.84–5.48	3.09–8.63	5.65–7.82
MgO	3.23	1.05	3.41	0.48	8.41	1.06	15.33	4.96	12.7				2.08	0.39			1.60–2.89	1.13–7.95	3.48–6.38
CaO	3.52	1.19	3.07	0.72	4.55	0.74	4.81	0.62	9.16				2.49	0.80	1.95	0.63	2.39–4.77	0.73–9.77	2.10–3.47
Na_2O	0.92	0.44	1.30	0.22	0.61	0.05	0.63	0.15	0.43				1.42	0.31	1.35	0.15	1.05–1.50	0.62–1.70	0.62–1.22
K_2O	1.83	0.81	2.57	0.28	0.47	0.16	0.11	0.06	0.05				2.64	0.12	2.44	0.17	2.07–2.57	1.34–2.81	1.44–2.23
Sc	14.3	3.7	12.9	1.1	19.3	4.8	21.7	4.5	39.3	11.9	17	10.5–13	7.96	0.87	10.6	1.5	8.2–13		9.6
Cr	128	105	215	100	482	106	962	374	632	81	1100	63–145	64	8	84	22	58–145	41–440	240–390
Co	12	7	26	10	10.2	2.5	11.0	5.9	12.3	9.9	27	11–25	13.5	0.8	13.7	2.7	14–25	8–56	33–52
Ni	39	21	260	110	49.5	29.4	44.3	22.4	67			19–105	46	9	50	33	22–105	14–395	210–395
Zn	13	12	19	17	12	3	8	2	16			2–5.7	50	21	48	26			
Ga	38	34	76	49	17	8	59	49	<6			1–15.3	14.9	4.7	12.5	3.0	4.5–12		
As	1	1	2	1	<1		<0.5		<10				4.6	1.1	3.3	2.1			
Br	0.4	0.5	1.4	0.9	0.6	0.4	1.4	1.9	1.0			0.13–0.23	4.0	1.4	1.6	1.3			
Rb	76	46	122	14	16	6	4	2	6.76	66		80–130	99	24	116	11	75–106		
Sr	200	78	161	35	246	89	235	66	423			90–200	113	19	139	22	150–250		
Zr	315	81	280	67	409	120	358	172	658			252–280	249	68	307	33	238–326	185–390	210–320
Sb	0.26	0.25	0.87	1.13	0.19	0.17	0.25	0.38	0.10			0.06–0.5	0.87	0.21	0.54	0.21			
Cs	4.30	3.11	6.90	1.10	0.73	0.32	0.18	0.10	0.06	2.3		5.7–6.7	4.71	1.08	6.9	1.1	4.2–5.7		4.3
Ba	475	113	452	66	639	188	560	165	793	530		356–390	303	81	408	30	320–380	320–480	320–420
La	48.3	9.5	44.6	4.0	62.4	11.7	56.8	15.2	132	40	56	36.2–36.9	36.7	2.7	42.0	3.4	32.3–37.4		
Ce	95.5	25.6	82.5	5.8	110.5	28.1	95.3	31.5	125	93		73.1–78.6	75.4	5.1	82	8	70.7–80.0		
Nd	43.9	10.6	39.2	5.8	54.9	17.0	48.4	11.8	106	36		33.2–35.0	35.1	6.8	38	6	29.6–35.4		
Sm	8.54	2.00	7.99	1.15	10.10	2.60	9.75	2.58	22.6	7.1	7.1	6.10–6.74	6.01	0.57	6.39	0.60	5.51–6.22		
Eu	1.56	0.43	1.42	0.20	1.87	0.38	1.89	0.49	3.62	1.37	2.00	1.17–1.28	0.88	0.11	1.40	0.17	0.97–1.17		
Gd	7.20	1.52	6.59	0.39	8.80	2.11	8.86	2.44	18.0	5.4		5.24–5.92	6.07	0.92			4.48–5.99		
Tb	1.19	0.32	1.02	0.09	1.43	0.35	1.46	0.42	2.93	0.9		0.84–0.88	1.03	0.12	0.93	0.10	0.70–0.85		
Tm	0.58	0.12	0.53	0.06	0.76	0.21	0.68	0.17	1.60				0.46	0.08					
Yb	3.87	0.83	3.58	0.54	5.07	1.45	4.39	1.06	10.8	2.2		2.80–3.01	3.10	0.45	2.95	0.24	2.43–2.80		
Lu	0.57	0.13	0.52	0.11	0.75	0.23	0.65	0.15	1.67	0.45		0.39–0.54	0.49	0.05	0.45	0.04			
Hf	9.07	2.30	7.60	2.43	10.30	2.19	10.85	4.18	19.2	6.4		6.95–7.95	7.52	1.63	7.21	0.88			5.8
Ta	1.57	0.35	1.48	0.08	1.95	0.37	1.96	0.60	3.78	2.4		1.2–1.6	0.97	0.27	1.18	0.11			

Ir (ppb)	<1		<2		<1		<1		<1				0.02–2											
Au (ppb)	3	2	2	1	5	4	2	2	8				2–2.2	1.2	0.3									
Th	16.0	4.3	13.5	2.3	19.7	4.2	20.1	5.5	43.3	14.5			13.7–15.6	13.26	1.09	15.1	2.7	12.6–15.0						11.1
U	1.76	1.34	2.57	0.76	0.78	0.33	0.58	0.14	1.27				2.07–3.49	2.99	0.31	2.7	0.3	2.02–2.60						1.84
K/U	12205	7064	8943	3234	6191	3968	1459	662	327	-				7416	997	7657	772							
Th/U	16.8	15.1	5.5	1.3	29.4	15.4	36.1	12.2	34.1	-				4.5	0.2	5.7	0.7							
La/Th	3.2	0.9	3.4	0.7	3.2	0.3	2.8	0.1	3.04	2.8				2.8	0.1	2.8	0.1							
Zr/Hf	35	6	38	10	39	4	33	6	34.2	-				33	6	43	3							
Hf/Ta	5.9	1.2	5.1	1.6	5.3	0.3	5.5	0.8	5.09	2.7				7.85	1.32	6.1	0.7							
La_N/Yb_N	8.5	1.1	8.4	0.6	8.6	1.1	8.7	0.4	12.2	12				8.1	0.9	9.6	0.3	8.70–9.60						
Eu/Eu*	0.61	0.09	0.60	0.05	0.62	0.07	0.62	0.04	0.55	0.68				0.43	0.05			0.58–0.64						

Numbers in parentheses indicate number of analyses.
[a] Frey et al. (1970).
[b] Frey (1977).
[c] Koeberl (1986) taken from various sources.
[d] Glass and Koeberl (1989).
[e] Average and S.D. of 52 INAA anaylses of layered (MN) Australasian tektites from Wasson (1991).
[f] Major oxides and some trace elements for 15 australites from Taylor and Sachs (1964); Cs, Ba, Th, U, Zr, Hf, Sc, and REEs for five of the australites from Taylor and McLennan (1979).
[g] Chapman and Scheiber (1969).
[h] High-magnesium tektites (five from Java, one from the Philippines, one from Australia) from Chapman and Scheiber (1969) and one javanite from Taylor and McLennan (1979).
[i] All iron reported as FeO.

crotektites are pale yellow-brown and others are dark brown. The darker brown ones have lower SiO_2 and higher FeO. Some of the North American microtektites are quite vesicular and contain numerous lechatelierite particles. Like the Australasian microtektites, the North American microtektites have a rather wide range in composition, with silica, for example, ranging from ~63 to nearly 82 wt.% (Table A1 and Table 3). The trace element contents are equally variable, especially Cr, Co, and Ni, and the more volatile elements, such as Zn, Ga, As, Sb, and Cs (Table 3).

The North American microtektites in this study came from sites in the Caribbean Sea and Gulf of Mexico (Lamont-Doherty Earth Observatory Core RC9-58 and DSDP Sites 94 and 149) (Fig. 1). Although the average values differ from site to site, our trace element contents for the North American microtektites overlap those of the Barbados microtektites except for higher Sc, Th, and heavy rare earth elements (Table 3). Most likely the variation in average trace element content from site to site is primarily a reflection of the variation in average SiO_2 contents.

The North American microtektites have major and element contents similar to those of the bediasites, but with lower average SiO_2 and slightly higher averages of most of the other major oxides (Table 3). The North American microtektites appear to have lower Na_2O than the bediasites, but this may be at least partly due to different analytical methods (i.e., energy-dispersive X-ray analysis vs. wet chemical analysis). Although the ranges of all the trace elements in the North American microtektites overlap those of the bediasites, the averages are slightly different, even when only the North American microtektites with the same silica range as the bediasites are considered. For example, the average Ga, Rb, Sr, Cs, Ba, Ta, and Th contents of the North American microtektites are between 1.2 and 2.6 times higher than the average values of these trace elements in the bediasites (Table 3).

3.4. Cpx Spherules

The cpx spherules analyzed in this study have a wide variety of crystalline textures (Fig. 4a–f). As in previous studies, the main phase is clinopyroxene (probably diopside). Many of the cpx spherules have crystal-shaped voids representing missing phases that were removed by solution in the seawater (Fig. 4a, e, and f; Glass et al., 1985). The light-colored cpx spherules generally have cryptocrystalline textures with feathery crystals (Fig. 4d). Some light-colored cpx spherules have silica-rich crystals (maybe cristobalite?) (Fig. 4e). The dark cpx spherules often have larger lath-like or chain-like crystals (Fig. 4c) and voids where a phase (or phases) was removed by solution. They also often contain Cr- and/or Ni-rich spinel crystals (e.g., Fig. 4c and f). The cpx spherules have a relatively wide range in composition (Table A1 and Table 4). Except for two outliers, the silica contents range from ~58 to 74 wt.%. The Al_2O_3 content is relatively low and ranges mostly between 5 and 10 wt.%. Generally, either the FeO or the CaO (and often the MgO) contents are higher than the Al_2O_3 contents. The trace element contents of the cpx spherules are highly variable, especially for Cr, Co, Ni, and the volatile elements (Table A1 and Table 4). The cpx spherules generally have high Cr and Ni contents, with an average Cr content of ~991 ± 799 ppm and an average Ni content of ~1495 ± 1249 ppm (Table A1 and

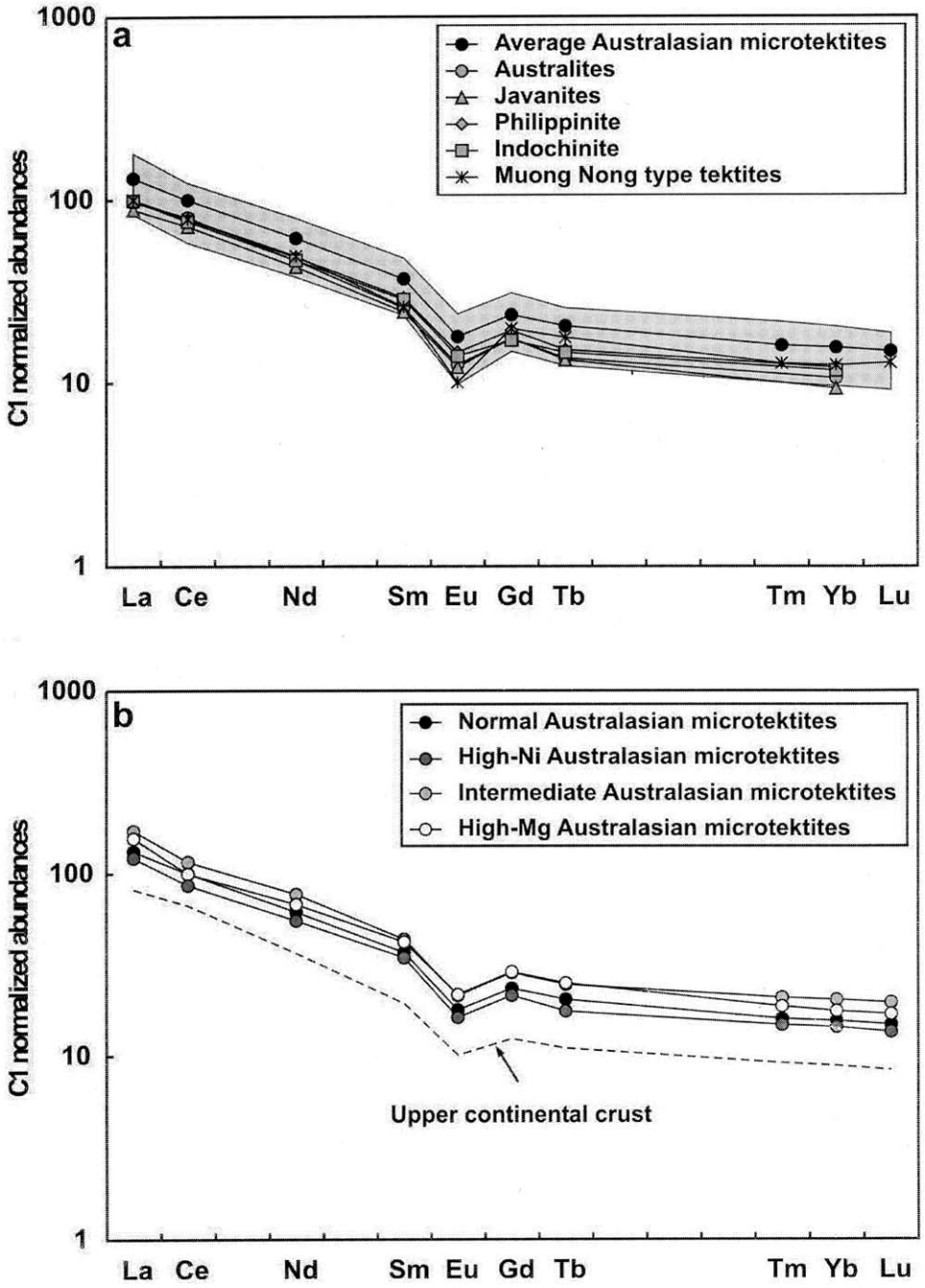

Fig. 3. Chondrite-normalized REE patterns for Australasian microtektites and tektites: (a) Chondrite-normalized REE patterns for average normal Australasian microtektites and Australasian tektites (one philippinite, one indochinite, average of two javanites, five australites, and five Muong Nong-type tektites). The shaded region indicates the range of values for the normal Australasian microtektites; (b) Chondrite-normalized REE patterns for the average normal, high-Ni, intermediate, and HMg Australasian microtektites and average upper continental crust. Tektite data are from Taylor and McLennan (1979) and Glass and Koeberl (1989). Average CI chondrite REE abundances from Taylor and McLennan (1985).

Table 4). The darker-colored cpx spherules generally have lower CaO and higher FeO, Cr, Co, and Ni contents compared with the light-colored cpx spherules (Table 5). In fact, the dark cpx spherules have slightly higher average contents of all the trace elements, except for Ga and As, which are highly variable in abundance.

The average composition of the more heavily etched cpx spherules is slightly different from the average composition of the unetched to slightly etched cpx spherules (Table 5). The greatest percent difference in the major oxides is the higher FeO, Na_2O, and TiO_2 and lower MgO in the highly etched spherules compared with those that are, at most, slightly etched. The heavily etched cpx spherules have higher contents of all the trace elements except for Ni, Sb, and Hf. The greatest percent difference is in the average Cr, As, Br, and Sb contents,

Table 2. Major (wt. %) and trace element (ppm, except where noted) contents of Ivory Coast microtektites and tektites and Bosumtwi impact crater glass.

	Ivory Coast Microtektites[a]		Ivory Coast Microtektites[b]		Ivory Coast Tektites[b]		Suevite Glasses[c]		
	Ave. (16)	S.D.	Ave. (4)	S.D.	Ave. (11)	S.D.	Ave. (3)	S.D.	Impact Glass[d]
SiO_2	66.4	2.0	67.4	1.2	67.58	0.59	65.45	0.25	
TiO_2	0.55	0.04	0.59	0.02	0.56	0.02	0.67	0.05	
Al_2O_3	16.9	0.5	17.1	0.2	16.74	0.37	17.02	0.38	
FeO[e]	6.65	0.58	6.40	0.23	6.16	0.15	5.71	0.55	5.98
MgO	4.27	1.25	3.70	0.86	3.46	0.35	2.02	0.87	
CaO	1.73	0.37	1.22	0.30	1.38	0.11	2.23	0.46	
Na_2O	1.92	0.23	1.63	0.29	1.90	0.16	3.04	0.44	3.73
K_2O	1.60	0.39	1.86	0.27	1.95	0.11	1.92	0.34	1.51
Sc	11.3	1.2	17.9	0.7	14.7	1.2	15	0.0	17.1
Cr	281	139	292	54	244	20	175	16	280
Co	23.3	4.0	32.7	1.7	26.7	2.5	15.0	2.4	24.5
Ni	122	51	224	63	157	52	66.4	20.2	99
Zn	6	2	12	2	23	18			138
Ga	31	34	17	7	21	8	22.0	2.4	45
As	0.3	0.2	0.42	0.13	0.45	0.17			4.59
Br	0.1	0.0	0.4	0.1	0.33	0.32			1.06
Rb	51	15	66.7	13.2	66	10	67.4	23.5	36.6
Sr	256	60	325	31	260	70	258	95	389
Zr	131	25	215	15	134	27	136	21	140
Sb	0.13	0.08	0.21	0.05	0.23	0.09			0.36
Cs	2.53	0.84	3.2	0.2	3.67	0.49	2.4	0.7	2.21
Ba	533	85	620	27	374	94	610	65	609
La	19.4	3.5	25.9	2.3	20.7	2.4			18.9
Ce	41.7	6.9	55.1	5.9	41.9	4.0	46.3	1.6	39.2
Nd	19.8	3.1	27.3	3.3	21.8	2.9	25.9	0.9	18.9
Sm	3.76	0.65	5.10	0.41	3.95	0.57	4.94	0.04	3.59
Eu	1.17	0.23	1.43	0.12	1.20	0.07	1.21	0.01	1.16
Gd	3.18	0.54	4.40	0.16	3.45	0.73	3.81		4.1
Tb	0.50	0.09	0.74	0.04	0.56	0.09			0.71
Tm	0.25	0.04	0.31	0.03	0.30	0.05			0.24
Yb	1.69	0.27	2.07	0.18	1.79	0.23	1.73	0.22	1.39
Lu	0.24	0.04	0.31	0.01	0.24	0.04			0.20
Hf	3.19	0.47	4.28	0.14	3.38	0.29			4.98
Ta	0.34	0.07	0.42	0.04	0.34	0.06			0.48
Ir (ppb)	<2		0.9	0.2	0.4	0.2			
Au (ppb)	3	1	0.8	0.3	41	32			31
Th	3.39	0.53	3.99	0.22	3.54	0.43	3.98	0.11	4.22
U	0.57	0.17	0.64	0.12	0.94	0.27	1.50	0.04	1.44
K/U	24474	9159	21343	1349	18393	6109			8738
Th/U	6.48	2.05	6.52	1.46	4.00	0.97			2.93
La/Th	5.72	0.55	6.48	0.39	5.87	0.23			4.48
Zr/Hf	41.0	5.6	50.3	2.6	40.3	10.4			28.1
Hf/Ta	9.42	1.13	10.30	0.65	10.22	1.42			10.38
La_N/Yb_N	7.70	0.40	8.44	0.32	7.85	0.49			9.19
Eu/Eu*	1.03	0.12	0.92	0.05	1.02	0.16			0.92

Numbers in parentheses indicate number of analyses.
[a] This study.
[b] Koeberl et al. (1997).
[c] Suevite glasses from Bosumtwi impact crater from Jones (1985).
[d] Koeberl et al. (1998).
[e] All iron reported as FeO.

but the average values of most of these elements have large plus/minus values associated with them due to one or two samples with anomalously high contents of these elements. All of the trace element contents exhibit a great deal of overlap between the highly etched and the unetched to slightly etched spherules. The high-Br content of some of the cpx spherules (Table A1) may be due to alteration/contamination by seawater. This hypothesis is supported by the observation that the highest average Br contents occur in the most heavily etched cpx spherules (Table 5).

The cpx spherules with numerous spinel crystals have noticeably higher average FeO and Cr contents than do the cpx spherules that appear to have no spinel crystals (at least none that were visible in scanning electron microscope images of polished interior surfaces). They also have higher average Co and slightly higher average Ni, but there is a great deal of

Table 3. Major oxide (wt. %) and trace element (ppm except where noted) compositions of North American microtektites and tektites.

	Microtektites (25)[a]		North American Microtektites[b]		Barbados Microtektites[c]		Barbados Tektites[d]		Site 612 Tektites[e]		Site 904 Tektites[f]		Bediasites[g]		Georgiaites[h]	
	Ave.	S.D.	Ave.	S.D.	Ave.	S.D.	Ave.	S.D.	Ave.	S.D.	Ave.	S.D.	Ave.	S.D.	Ave.	S.D.
SiO_2	73.4	4.8	69.2	5.2	76.1	2.9	80.4	2.3	72.3	2.6	74.6	2.2	76.36	2.42	81.8	1.0
TiO_2	0.73	0.15	0.59	0.17	0.55	0.12	0.56	0.10	0.78	0.19	0.71	0.08	0.77	0.13	0.51	0.04
Al_2O_3	14.1	2.0	16.9	2.5	12.4	1.3	11.3	1.5	15.4	2.7	13.9	1.2	13.77	1.56	11.2	0.5
FeO[i]	4.37	1.30	5.12	1.24	4.27	2.12	2.75	0.90	4.03	0.99	4.03	0.62	4.01	0.84	2.64	0.40
MgO	1.73	0.87	2.25	1.02	1.08	0.85	0.46	0.15	2.18	3.53	1.22	0.18	0.69	0.21	0.61	0.07
CaO	1.64	0.80	1.65	0.66	1.12	0.30	0.68	0.10	1.42	1.04	1.00	0.21	0.56	0.2	0.45	0.03
Na_2O	1.06	0.23	1.34	0.41	1.18	0.56	1.27	0.11	1.04	0.42	0.65	0.26	1.51	0.2	2.44	0.08
K_2O	2.92	0.47	2.73	0.63	2.69	0.70	2.25	0.24	3.27	1.02	3.21	0.52	2.04	0.28	0.94	0.07
Sc	13.2	5.4			4.6		9.1	0.6	10.0	0.7	12.9	1.8	13.75	4.66	8.7	1.0
Cr	65	51			50		73	29	113	4	46.4	16.8	44.21	13.46		
Co	17.5	9.3			20		16	5	8.3	0.4	13.6	6.0	11.79	2.33	7.5	1.1
Ni	58	57									48	71	13.22	3.60	7.4	1.9
Zn	24	22									8					
Ga	25	35									12	5	12.50	2.33		
As	0.4	0.4			2.5		1	0	0.8	0.2	2.18	3.80	1			
Br	1.4	1.7									0.40	0.28				
Rb	116	49					115	48	88	4	179	37				
Sr	187	72									149	45	63	9	76	5
Zr	213	86							240		284	73	102	34	163	8
Sb	1.96	2.79							1.9	0.2	0.72	0.74	214	37	187	14
Cs	5.70	3.37			6		10	2	5	0	14.3	6.5	2.02	0.43	1.74	0.22
Ba	554	164							700	0	541	122	532	175	572	25
La	42.4	15.6			15		20.8	7.6	29.4	0.1	51.9	14.5	26		20.6	2.0
Ce	79.8	28.3			38		44	24	61	8	102.8	29.7	74.87	13.81	46.2	4.0
Nd	40.6	16.7			20		25	10	37	4	50.7	12.3	37.41	10.57	21.1	2.0
Sm	7.79	2.89			4.5		6.6	2.6	8.5	0.2	9.78	2.22	7.05	1.46	4.07	0.43
Eu	1.58	0.56			0.59		1.11	0.48	0.74	0.01	1.61	0.25	1.55	0.28	0.99	0.09
Gd	6.24	2.28					8	4	7		8.49	1.82			3.44	0.40
Tb	1.01	0.33			0.8		1.3	0.4	1.2	0.1	1.30	0.19	0.96	0.22		
Tm	0.51	0.19					0.5		0.9		0.70	0.08				
Yb	3.48	1.29			3.5		4.1	0.9	4.6	0.6	4.26	0.42	2.89	0.68	1.91	0.17
Lu	0.53	0.19			3		4.3	0.13	0.38	0.04	0.59	0.09	0.46	0.09	0.29	0.03
Hf	5.30	2.18					6.0	1.6	5.9	0.1	7.39	1.05	6.49	0.95	4.64	0.39
Ta	1.30	0.43					3	1	1	0	1.42	0.60	0.70		0.57	0.05
Ir (ppb)	<3										<1					
Au (ppb)	5	5					3		60		0.7	0.3				
Th	11.1	4.1			4		5.8	1.6	9.3		15.6	5.2	7.52	1.19	5.81	0.51
U	2.06	0.94							3.6		3.36	0.85	2.02	0.50	1.46	0.15
K/U	14575	7784									9531	1465			14036	1469
Th/U	5.92	2.17							2.78	1.1	4.67	1.04	3.79	0.43	4.02	0.46
La/Th	3.83	0.44			3.75			0.7	3.2	0.4	3.39	0.24	4.51	0.55	3.64	0.14
Zr/Hf	40.5	6.0					4.3		41.38		38.1	6.3	33.64	2.22	40.3	0.9
Hf/Ta	4.04	1.02									5.68	1.42	9.27		8.12	0.49
La_N/Yb_N	8.19	0.85			2.90		3.4	1.1	4.4	0.6	8.15	1.61	8.03	0.43	7.5	0.2
Eu/Eu*	0.70	0.07					0.4	0.1	0.3		0.55	0.06			0.81	0.04

[a] This study.
[b] 29 microtektites from DSDP Sites 94 and 149 from Glass and Zwart (1979).
[c] Major oxide data for 27 microtektites from this study. Trace element data for a composite of two microtektites from Koeberl and Glass (1988).
[d] Major oxide data for 9 tektites (this study) and trace element data for 4 tektite fragments from Koeberl and Glass (1998).
[e] Major oxide data for 23 microtektites from this study and trace element data for two tektite fragments from Koeberl and Glass (1988).
[f] Major oxide data for 28 microtektites from this study and trace element data for eight tektite fragments from Glass et al. (1998).
[g] Major oxide data for 35 tektites from Chao (1963) and trace element data from Cuttitta et al. (1967); Haskin et al. (1982).
[h] Data for 24 georgiaites from Albin et al. (2000).
[i] All iron reported as FeO.

overlap. In fact, most of the trace elements have higher average contents in the spinel-rich cpx spherules compared to the cpx spherules without any obvious spinel crystals; the only exceptions are Sb and Ta. The generally higher average trace element content of the spinel-rich cpx crystals may simply be due to the lower average SiO_2 content of these spherules.

3.5. Cpx-Related Microtektites

Major and minor element contents were obtained for microtektites found in the cpx spherule layer at four widely spaced sites: DSDP Sites 162, 167, 216, and 292 (Fig. 2). With one exception discussed below, the silica contents of the cpx-

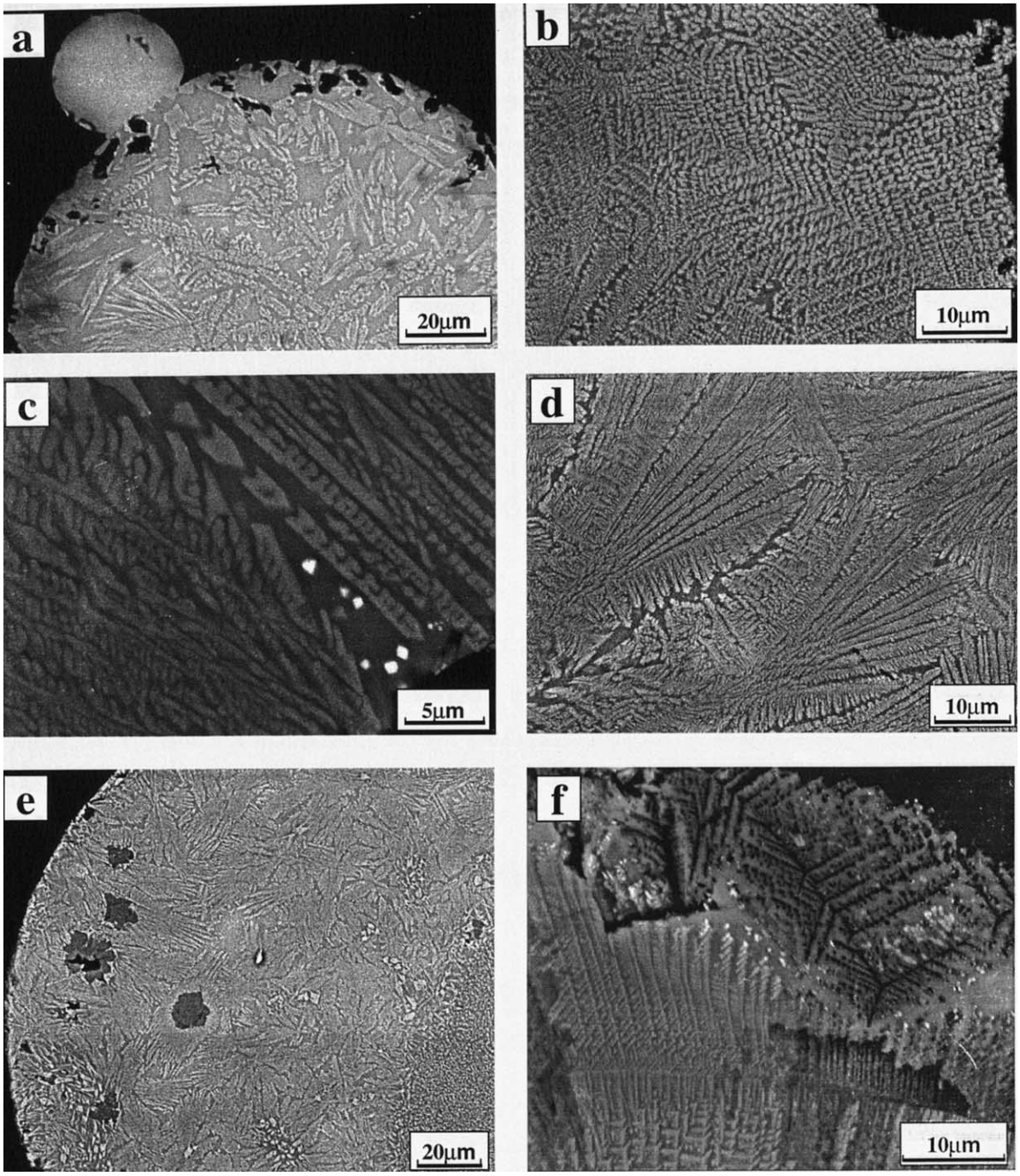

Fig. 4. Scanning electron microscope images of polished interior surfaces of clinopyroxene-bearing spherules: (a) 200 μm diameter opaque white sphere, with a 40 μm diameter transparent brown sphere attached, from Deep Sea Drilling Project (DSDP) Site 166 (Sample 798–2 in Table A1). Note skeletal clinopyroxene crystallites (light grey) in a glass matrix (darker grey). The black regions are where a phase (or phases) has been removed by solution; (b) 240 μm opaque grey to translucent yellow-brown mottled fragment of a sphere with skeletal clinopyroxene crystallites (light grey) in a glass matrix (darker grey) from DSDP Site 216 (sample 770–12 in Table A1); (c) 230 μm diameter opaque dark brown broken sphere with arborescent to chain-like clinopyroxene crystallites (light grey) in a glass matrix (dark grey) from DSDP Site 216 (Sample 770–4 in Table A1). White equant crystallites are Ni- and Cr-rich spinel; (d) 200 $\times$ 300 μm translucent yellow-grey fragment of a sphere with a feathery texture from DSDP Site 166 (Sample 797–6 in Table A1). Light grey feathery crystallites are clinopyroxene in a glass matrix (darker grey); (e) 250 μm diameter mostly opaque dark sphere from DSDP Site 216 (Sample 770–20 in Table A1). Note arborescent clinopyroxene crystallites (light grey) in a glass matrix (dark grey) and large ($\sim$10 μm) darker grey hexagonal silica crystallites (perhaps cristobalite); and (f) 180 μm opaque dark brown to black spherule with a rough surface from DSDP Site 162 (Sample 800–5 in Table A1). Note feathery clinopyroxene microlites (light grey) in a glass matrix (darker grey), spinel crystallites ($<$1 μm) (white), and voids (black arborescent regions) where a phase (or phases) has been removed by solution.

Table 4. Major oxide (wt.%) and trace element (ppm, except where noted) compositions of cpx spherules, cpx-related microtektites, and Popigai impact crater melt rock (tagamite) and impact glass.

	CPX SPHERULES				CPX-RELATED MICROTEKTITES						CPX-RELATED MICROTEKTITES							
	(71)[a]		(15)[b]		Low-SiO_2 (4)[a]		Low-SiO_2 High Al_2O_3	High-SiO_2 (10)[a]			Site 216 High-SiO_2 (9)[c]		Site 689 High-SiO_2 (8)[d]		POPIGAI IMPACT GLASS (4)[e]		POPIGAI IMPACT MELT TAGAMITES (11)[e]	
	Ave.	S.D.	Ave.	S.D.	Ave.	S.D.		Ave.	S.D.		Ave.	S.D.	Ave.	S.D.	Ave.	S.D.	Ave.	S.D.
SiO_2	64.8	4.6	63.3	3.0	67.8	3.1	54.3	79.6	4.90	SiO_2	78.8	5.0	81.6	3.9	62.2	1.7	62.9	2.1
TiO_2	0.31	0.08	0.35	0.14	0.46	0.05	1.54	0.49	0.13	TiO_2	0.45	0.08	0.50	0.16	0.8	0.0	0.7	0.1
Al_2O_3	7.42	1.45	7.90	2.26	10.1	1.3	30.4	13.4	4.0	Al_2O_3	12.1	2.2	12.4	2.2	16.3	1.1	15.4	1.0
FeO[f]	7.18	2.90	10.4	1.9	6.49	0.36	4.06	2.36	2.52	FeO[f]	2.34	2.36	1.71	2.34	7.1	0.4	5.9	0.9
MgO	7.37	2.56	6.56	3.50	5.28	1.90	6.93	0.68	0.25	MgO	0.74	0.25	0.47	0.10	3.7	0.2	3.7	0.5
CaO	9.91	3.12	7.75	2.77	5.14	2.25	1.71	0.68	0.50	CaO	0.79	0.50	0.18	0.13	3.1	0.4	4.1	0.8
Na_2O	0.89	0.33	1.20	0.46	1.75	0.64	0.62	0.15	0.19	Na_2O	0.21	0.24	0.11	0.18	2.4	0.5	2.1	0.2
K_2O	1.85	0.47	2.51	0.98	2.96	1.26	0.34	2.72	0.75	K_2O	2.68	0.56	2.40	0.85	3.0	0.5	2.8	0.2
Sc	8.74	4.44			13.4	2.0	40.9	6.83	1.71	Sc	6.42	1.10	7.06	2.85				
Cr	990	795			482	170	415	28	13	Cr	30	7	44	35				
Co	89	56			72	21	9.15	8.0	4.3	Co	9	3	8.14	4.84				
Ni	1495	1249			1082	622	61	21.5	12.6	Ni	22	13	37.2	47.8				
Zn	42	29			79	50	23	18	10	Zn	19	7	17.2	22.0				
Ga	47	59			21	18	13	52	74	Ga	51	73	7.62	7.39				
As	1.5	2.0			0.6	0.5	0.4	1.7	1.2	As	2.0	1.1	2.86	3.99				
Br	5.3	6.4			0.6	0.3	0.4	0.9	0.6	Br	0.8	0.6	0.11	0.12				
Rb	64	28			122	66	10.3	79	26	Rb	83	15	73.2	27.5	86	6	84.4	8.7
Sr	195	118			200	46	337	199	110	Sr	184	88	139	60	247	12	253	38
Zr	188	93			181	86	853	308	118	Zr	276	83	342	107				
Sb	1.65	3.84			0.53	0.64	<0.1	0.21	0.19	Sb	0.19	0.16	0.75	1.56				
Cs	1.43	1.93			1.71	1.72	0.26	1.51	0.54	Cs	1.55	0.33						
Ba	411	179			495	68	1225	1247	453	Ba	1163	504	1073	381				
La	31.2	12.0			51.1	9.6	109	45.7	9.1	La	43.7	9.7	46.6	16.1				
Ce	56.1	20.0			96.4	23.5	205	79.0	16.6	Ce	75.6	18.0	79.2	27.7				
Nd	23.8	9.0			42.5	7.0	107	36.6	8.4	Nd	35.0	8.6	35.7	15.3	49.3	7.0	41.9	3.4
Sm	4.28	1.68			6.74	0.98	20.6	6.43	1.40	Sm	6.09	1.47	5.99	2.25	8.25	1.26	7.05	0.48
Eu	0.91	0.38			1.47	0.40	4.07	1.39	0.30	Eu	1.32	0.31	1.29	0.49				
Gd	3.47	1.52			5.61	1.16	12.2	4.88	1.12	Gd	4.63	1.00	5.02	1.94				
Tb	0.54	0.23			0.93	0.21	2.75	0.66	0.16	Tb	0.63	0.16	0.73	0.30				
Tm	0.30	0.13			0.50	0.08	1.46	0.36	0.08	Tm	0.34	0.08	0.37	0.17				
Yb	2.06	0.76			3.84	0.94	9.82	2.47	0.56	Yb	2.33	0.54	2.78	1.16				
Lu	0.31	0.12			0.58	0.14	1.58	0.38	0.09	Lu	0.35	0.08	0.42	0.16				
Hf	4.80	1.52			7.35	1.03	25.5	7.27	2.01	Hf	6.80	2.10	9.37	2.81				
Ta	0.49	0.80			0.53	0.20	2.00	0.75	0.20	Ta	0.68	0.11	0.92	0.30				

Ir (ppb)	<2		<5		<1.5	<2		Ir (ppb)			0.2	0.1
Au (ppb)	7	4	7	3	5	5	2	Au (ppb)	5	2	0.4	0.2
Th	7.19	2.52	9.07	1.26	22.8	8.19	1.95	Th	7.60	1.41	8.65	2.59
U	2.06	0.91	1.19	0.62	0.98	1.72	0.64	U	1.70	0.61	2.38	1.33
K/U	8893	6706	24461	14893	2880	15858	11360	K/U	11486	8497	17750	17944
Th/U	4.07	2.18	10.79	8.93	23.3	5.82	3.88	Th/U	4.15	1.40	5.67	4.30
La/Th	4.38	0.82	5.63	0.55	4.78	5.64	0.84	La/Th	5.27	0.87	5.77	0.81
Zr/Hf	38.8	14.8	25.9	14.0	33.5	41.8	5.3	Zr/Hf	36.3	2.8	40.6	4.3
Hf/Ta	13.9	6.17	16.08	7.48	12.8	9.81	1.68	Hf/Ta	10.3	1.1	9.86	1.87
La_N/Yb_N	10.2	1.78	9.06	0.66	11.1	12.60	1.53	La_N/Yb_N	11.6	1.7	12.8	1.6
Eu/Eu*	0.73	0.12	0.72	0.09	0.66	0.76	0.04	Eu/Eu*	0.72	0.04	0.76	0.04

Numbers in parentheses indicate number of analyses.

[a] This study; cpx spherules from Core RC9-58 and DSDP Sites 69, 94, 149, 162, 166, 167, 216, and 292; low-SiO_2 cpx-related microtektites from DSDP Sites 167 and 292; high-SiO_2 cpx-related microtektites from DSDP Sites 167 and 216; HA1 cpx-related microtektite is from Site DSDP Site 162.

[b] D'Hondt et al. (1987); crystal-bearing spherules from Core RC9-58 and DSDP Sites 315, 69, and 216.

[c] Glass and Koeberl (1999a).

[d] Glass and Koeberl (1999b).

[e] Kettrup et al. (2003).

[f] All iron reported as FeO.

related microtektites vary between ~63 and 90 wt.% (Table A1). We divided the cpx-related microtektites into a high-SiO_2 group with SiO_2 >73 wt.% and a low-SiO_2 group with SiO_2 <72 wt.% (Table A1 and Table 4). Most of the cpx-related microtektites belong to the high-SiO_2 (HSi) group, which can be further divided into a high-Fe (>1.5 wt.% FeO) subgroup and a low-Fe (<1 wt.% FeO) subgroup (the oxidation state is not known, but Fe is reported as FeO). The high-iron (HFe) subgroup also has higher Na_2O and generally lower SiO_2 than the low-iron (LFe) subgroup. The cpx-related microtektites in the HFe subgroup are transparent pale brown and the cpx-related microtektites in the LFe subgroup are transparent colorless. The Al_2O_3 content in the HSi group varies inversely with the SiO_2 content. The MgO and CaO contents are generally <1 wt.%, Na_2O is generally <0.2 wt.%, and K_2O is higher than MgO, CaO, and Na_2O combined (Table A1).

The low-SiO_2 (LSi) cpx-related microtektites have higher MgO, CaO, and Na_2O, and usually higher FeO, and all but one have lower Al_2O_3 contents than do the HSi cpx-related microtektites (Table 4). In addition, they have higher Cr, Co, and Ni contents (Table 4). In general, the LSi cpx-related microtektites are similar in composition to the cpx spherules. However, one of the LSi cpx-related microtektites has ~30 wt.% Al_2O_3 and only ~45 wt.% SiO_2 (Table 4).

4. DISCUSSION

4.1. Distinguishing Between Microtektite/Spherule Layers

With the growing number of investigators who are now aware that impact cratering is a major geological process, the number of recognized impact spherule layers in the stratigraphic record will no doubt increase. One of the major problems will be trying to correlate impact spherule layers from one site to another. The debate over the number of upper Eocene microtektite/spherule layers indicates the problems with trying to correlate impact spherule/microtektite layers based on biostratigraphy or radiometric ages, even when the spherules are relatively young and show little alteration. One of the questions that we address here is how easy or difficult it is to distinguish between the presently recognized Cenozoic microtektite/spherule layers based on the major and/or trace element compositions of the microtektites/spherules.

Although there are some minor differences, the four low-Si, low-Al (LSi, Al) cpx-related microtektites have major oxide compositions similar to those of the cpx spherules, and for the purpose of comparing the different spherule layers they have been included with the cpx spherules. In addition, we have combined the four main groups of Australasian microtektites (normal, high-Ni, intermediate, high-Mg) into a single group for the purpose of comparing the Australasian microtektites with microtektites from the other microtektite layers and with the cpx spherules.

The Australasian microtektites can easily be distinguished from the Ivory Coast and high-Si cpx-related microtektites, the Ivory Coast microtektites can be distinguished from the North American and high-Si cpx-related microtektites, and the North American microtektites can be distinguished from the high-Si cpx-related microtektites using major oxide and/or minor and trace element contents (Table 6).

Table 5. Major oxide and trace element compositions of dark- and light-colored cpx-spherules from Site 216 and heavily and slightly etched cpx-spherules from all sites included in this study.

	CPX SPHERULES							
	DARK (10)		LIGHT (11)		HEAVILY ETCHED (18)		SLIGHTLY ETCHED (34)	
	AVE.	S.D.	AVE.	S.D.	AVE.	S.D.	AVE.	S.D.
SiO_2	67.7	6.6	68.7	1.8	62.8	3.6	65.0	4.0
TiO_2	0.30	0.09	0.28	0.05	0.38	0.10	0.28	0.06
Al_2O_3	6.90	1.14	6.83	1.00	8.61	1.90	6.96	0.95
FeO[a]	7.59	2.36	3.69	0.68	9.58	2.12	6.18	2.76
MgO	6.38	2.86	6.83	0.66	5.80	2.88	8.35	2.11
CaO	7.95	3.81	11.4	2.1	9.24	2.90	10.5	2.94
Na_2O	0.90	0.24	0.57	0.13	1.18	0.34	0.75	0.26
K_2O	2.04	0.44	1.64	0.21	2.14	0.61	1.66	0.31
Sc	6.37	2.06	6.17	1.93	9.75	3.70	7.97	2.85
Cr	818	372	250	109	1633	863	727	575
Co	92	32	32	13	97	40	90	68
Ni	1566	704	508	231	1117	859	1779	1527
Zn	40	17	22	8	53	28	37	25
Ga	18	32	70	71	67	82	51	54
As	0.6	0.4	1.1	1.0	3.1	3.0	0.9	1.0
Br	-	-	-	-	7.8	8.3	3.2	3.1
Rb	59.5	23.3	39.8	12.8	84	30	57.0	22.3
Sr	173	50	142	38	244	156	176	96
Zr	146	48	145	47	201	69	192	108
Sb	0.75	0.51	0.27	0.15	0.86	0.87	2.23	4.85
Cs	-	-	-	-	1.30	0.45	1.16	0.61
Ba	328	82	301	101	518	189	400	164
La	26.9	6.8	25.9	8.5	38.0	14.4	29.3	9.3
Ce	50.6	13.7	45.7	14.7	65.0	18.8	53.5	18.4
Nd	19.8	5.7	18.8	5.8	28.1	10.0	22.6	7.7
Sm	3.42	0.89	3.36	0.99	5.13	2.09	4.13	1.3
Eu	0.71	0.21	0.68	0.21	1.05	0.41	0.91	0.38
Gd	3.06	0.67	2.76	0.99	4.17	2.01	3.23	1.03
Tb	0.49	0.15	0.44	0.15	0.64	0.30	0.50	0.14
Tm	0.27	0.09	0.24	0.08	0.37	0.15	0.29	0.10
Yb	1.84	0.58	1.71	0.54	2.38	0.73	2.00	0.60
Lu	0.27	0.09	0.26	0.09	0.36	0.12	0.30	0.09
Hf	3.67	0.85	3.84	1.09	4.90	1.23	5.02	1.56
Ta	0.29	0.12	0.31	0.12	0.50	0.23	0.38	0.18
Ir (ppb)	-	-	-	-	2	2	1	0.4
Au (ppb)	10	7	4	3	7	3	5	3
Th	7.53	2.10	7.31	2.61	8.69	2.59	6.49	2.10
U	2.18	0.77	1.95	0.69	2.24	0.90	1.85	0.78
K/U	10186	10305	7975	4445	7508	3652	9629	6658
Th/U	3.78	1.22	4.01	1.49	3.68	1.32	4.28	2.62
La/Th	3.59	0.20	3.58	0.20	4.31	0.79	4.57	0.80
Zr/Hf	40.0	11.2	33.9	13.2	41.4	11.4	36.6	15.6
Hf/Ta	13.9	3.9	13.0	2.8	11.7	5.4	15.3	6.6
La_N/Yb_N	10.3	1.9	10.3	1.4	10.8	2.3	9.99	1.30
Eu/Eu*	0.67	0.11	0.68	0.04	0.72	0.07	0.76	0.14

Major oxide abundances in wt.% and trace element abundances in ppm, except where noted.
[a] All iron as FeO.

The cpx spherules can be distinguished from the microtektites due to their crystalline textures. However, the cpx spherules have a wide range in composition, and all of the major oxide and minor and trace element contents have ranges which overlap those of the Australasian, Ivory Coast, and North American microtektites. Using only the data in this study, the cpx spherules can be distinguished from the Australasian, Ivory Coast, and North American microtektites by their lower Al_2O_3 contents for a given SiO_2 content (Tables 1–4; Table 6; and Fig. 5a); however, if data from previous studies are included, some overlap is observed. The cpx spherules also have higher CaO for a given SiO_2 content compared with the Ivory Coast and North American microtektites (Fig. 5b). The cpx spherules (and 3 out of 4 LSi cpx-related microtektites) are clearly separated from the Australasian, Ivory Coast, and North American microtektites in an Al_2O_3-CaO-MgO ternary diagram (Fig. 6). The cpx spherules also have higher average Cr, Co, Ni, and Br contents than the Australasian, Ivory Coast, and North American microtektites (Fig. 7) and lower average REE contents and higher average light rare earth element enrichments than the Australasian and North American microtektites (Tables 1, 3, and 4; Fig. 8); but, because of the wide range in trace

Table 6. Compositional comparisons between microtektites/spherules using those oxides, elements, and element ratios that best show the differences between them.

Layers[1]	SiO_2	Al_2O_3	MgO	CaO	Na_2O	TiO_2	Sc	Cr	Co	Ni	Rb	Zr	Ba	REEs[2]	Hf	Ta	Th	U	La/Th	Hf/Ta	La_N/Yb_N	Eu/Eu*	Ba/Sc	Ba/Hf	Ba/Ta	Th/Hf	Ba/Th
Aust./IVC				H/Si	GL	(H)						H		H[2]	H	H	H					L		L	L	H	L
Aust./N.A.												GH			GH		GH			GH				GL	GL		GL
Aust./Cpx		H/Si		GL		(H)				GL							GH			GL					GL		GL
Aust./HSiCM	GL		H	H	GH	GH	GH						GL			GH	GH		GL	GL	L	GL	L	GL	L	GH	L
IVC/N.A.	GL	GH	(H/Si)		(H)			GH			L/Si			GL		L	L/Si	L/Si	H	H		H		GH	H	L	H
IVC/Cpx		(H)		L/Si	GH	GH/Si			GL	GL							GL	GL			GL			GH			H
IVC/HSiCM	L		H	GH	H		H	H	H	H		GL	GL		L	L	L	GL			L	H	L				
N.A./Cpx		(H/Si)	GL	(L/Si)		GH/Si		GL	GL	GL										GL					GL		
N.A./HSiCM			GH		H	(H/Si)							GL						GL	L	L		L		L	H	L
Cpx/HSiCM	GL	L/Si	H	H	GH			H	GH	GH			GL														GL

H = high; L = low; H/Si = high for a given silica content; L/Si = low for a given silica content; G = generally. Parentheses indicate higher or lower values here, but there is overlap in previously published data. Thus, in the first row, Australasian microtektites have a higher CaO content for a given silica content and generally lower Na_2O contents than do the Ivory Coast microtektites. The Australasian microtektites in our data have higher TiO_2 contents than do the Ivory Coast microtektites, but in published data there is some overlap.

[1] Aust = Australasian microtektites including normal, high-Ni, intermediate, and high-Mg. IVC = Ivory Coast microtektites; N.A. = North American microtektites; Cpx = cpx spherules and low-Si cpx-related microtektites (except for the one with low-Si and high Al); HSiCM = High Si cpx-related microtektites. The first layer listed in a row is being compared with the second. Thus, for example, in the first row the Australasian microtektites are being compared with the Ivory Coast microtektites.

[2] High except for Eu.

element contents of the cpx spherules and microtektites, there is some overlap in all the trace elements (Table A1, Tables 1–4).

The presence of crystalline phases in the cpx spherules, but not in the Australasian, Ivory Coast, North American, and HSi cpx-related microtektites, is probably a result of the difference in major oxide compositions. Although the LSi cpx-related microtektites have compositions similar to the compositions of the cpx spherules, they can be distinguished from them by their higher Al_2O_3 contents for a given SiO_2 content (Fig. 5a). This may explain why they did not partially crystallize.

Although the Australasian microtektites and North American microtektites differ in age by ~34 Ma and their strewn fields do not overlap, they are quite similar compositionally and are difficult to distinguish between using major oxide or minor and trace element contents (Table 6), probably due to similar crustal rocks that were sampled in the respective impacts. Both groups have wide ranges in silica content and correspondingly wide ranges in the other major oxides and minor and trace elements (Table A1, Tables 1 and 3). Traditional Harker diagrams cannot be used to distinguish between these two groups of microtektites very well. The Australasian microtektites do have lower average Al_2O_3 and higher average MgO and CaO contents for a given SiO_2 content, but there is a great deal of overlap. A plot of Hf vs. Ba is the best way to distinguish between the two groups, but there is still a minor amount of overlap.

The high-silica microtektites found in the cpx-spherule layer (HSi cpx-related microtektites) are more similar in composition to the North American microtektites than to the cpx spherules and low-silica cpx-related microtektites (Tables 3, 4, and 6). Since the North American microtektite and cpx spherule layers are similar in age and often overlap, the similarity between the HSi cpx-related microtektites and North American microtektites has led to the suggestion that the HSi cpx-related microtektites may belong to the North American microtektite layer (Glass and Koeberl 1999a; Glass and Koeberl 1999b; Vonhof and Smit, 1999). The HSi cpx-related microtektites can be distinguished from the North American microtektites by their lower Na_2O content and by several elemental ratios (Table 6). The compositional differences between the HSi cpx-related microtektites and the North American microtektites were previously attributed to heterogeneities within the target rock. Another possibility is that the HSi cpx-related microtektites belong to a third layer (Vonhof and Smit, 1999). However, more recent Sr and Nd isotopic studies indicate that the HSi cpx-related microtektites (i.e., transparent colorless microtektites recovered from the cpx spherule layer) have a close affinity to the cpx spherules (Whitehead et al., 2000; Liu et al., 2001).

In summary, microtektites and impact spherules from a given layer can have a wide range in compositions, which makes it generally difficult to differentiate between spherule layers based only on major oxide and/or trace element compositions. This appears to be more of a problem for microtektites or microkrystites produced during major impacts because of the greater chance that the target rocks will be heterogeneous. Thus, it may be necessary to obtain isotopic data to correlate or differentiate between impact spherule or microtektite layers (e.g., Sr and Nd).

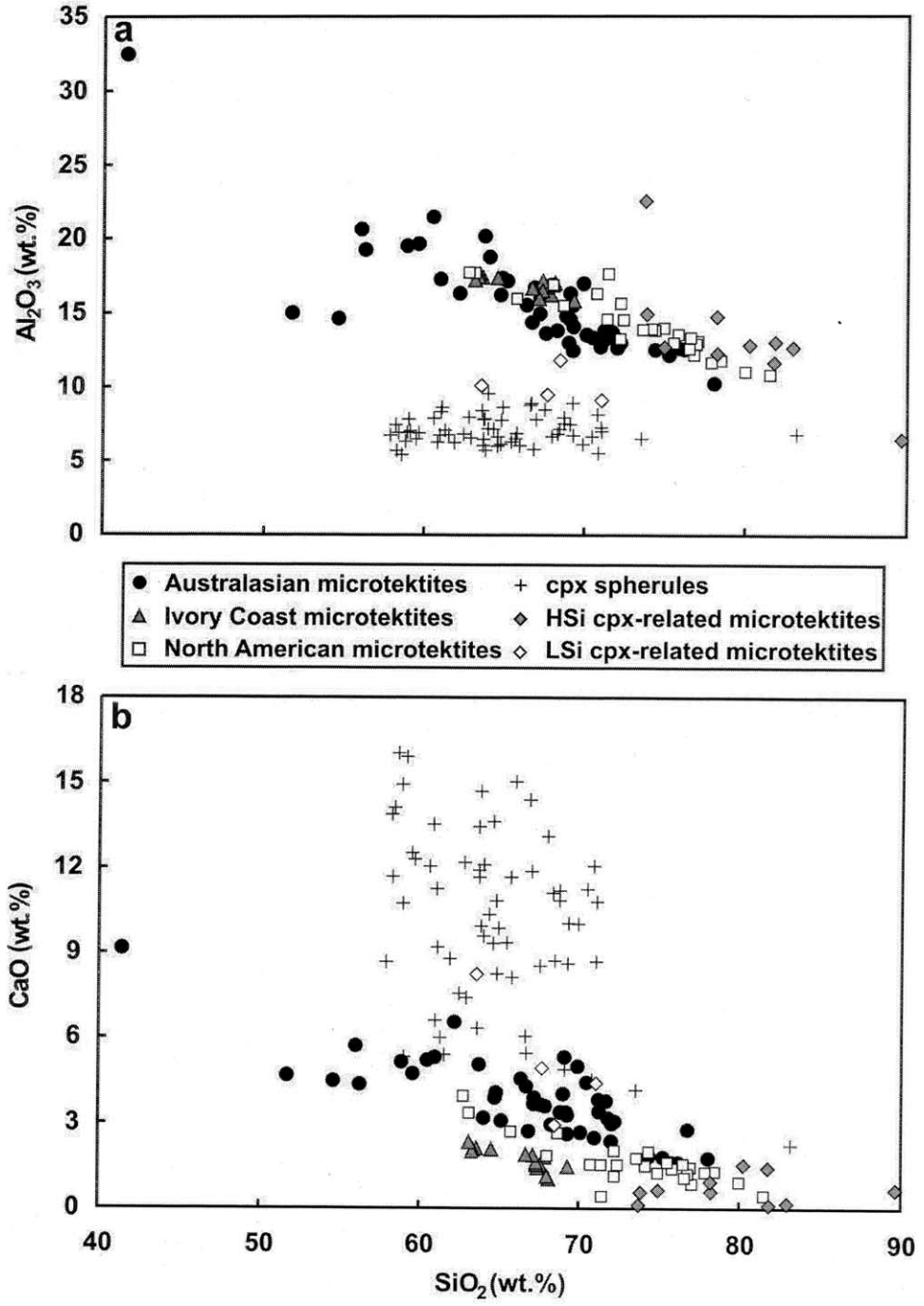

Fig. 5. Oxide variation diagrams for Australasian, Ivory Coast, and North American microtektites, and clinopyroxene-bearing (cpx) spherules and cpx-related microtektites: (a) Al_2O_3 versus SiO_2. Note that the cpx spherules and low-SiO_2 (LSi) cpx-related microtektites have lower Al_2O_3 for a given SiO_2 content compared with the Australasian, Ivory Coast, and North American microtektites; (b) CaO versus SiO_2. Note that the cpx spherules generally have higher CaO for a given SiO_2 content compared with the Australasian, Ivory Coast, and North American microtektites.

4.2. Meteoritic Contamination?

The cpx spherules and Australasian, Ivory Coast, and North American microtektites have elevated Cr, Co, Ni, and Au contents compared to the average upper continental crust (Fig. 7). This suggests the presence of a meteoritic component. The cpx spherules have the highest Cr, Co, Ni, and Au contents, which range up to 3250 ppm, 260 ppm, 5854 ppm, and 28 ppb, respectively. The Ni content of the cpx spherules is positively correlated with FeO, MgO, Cr, and Co and negatively correlated with Al_2O_3, CaO, Na_2O, K_2O, and TiO_2. In a plot of Ni/Co vs. Ni content, the unetched to

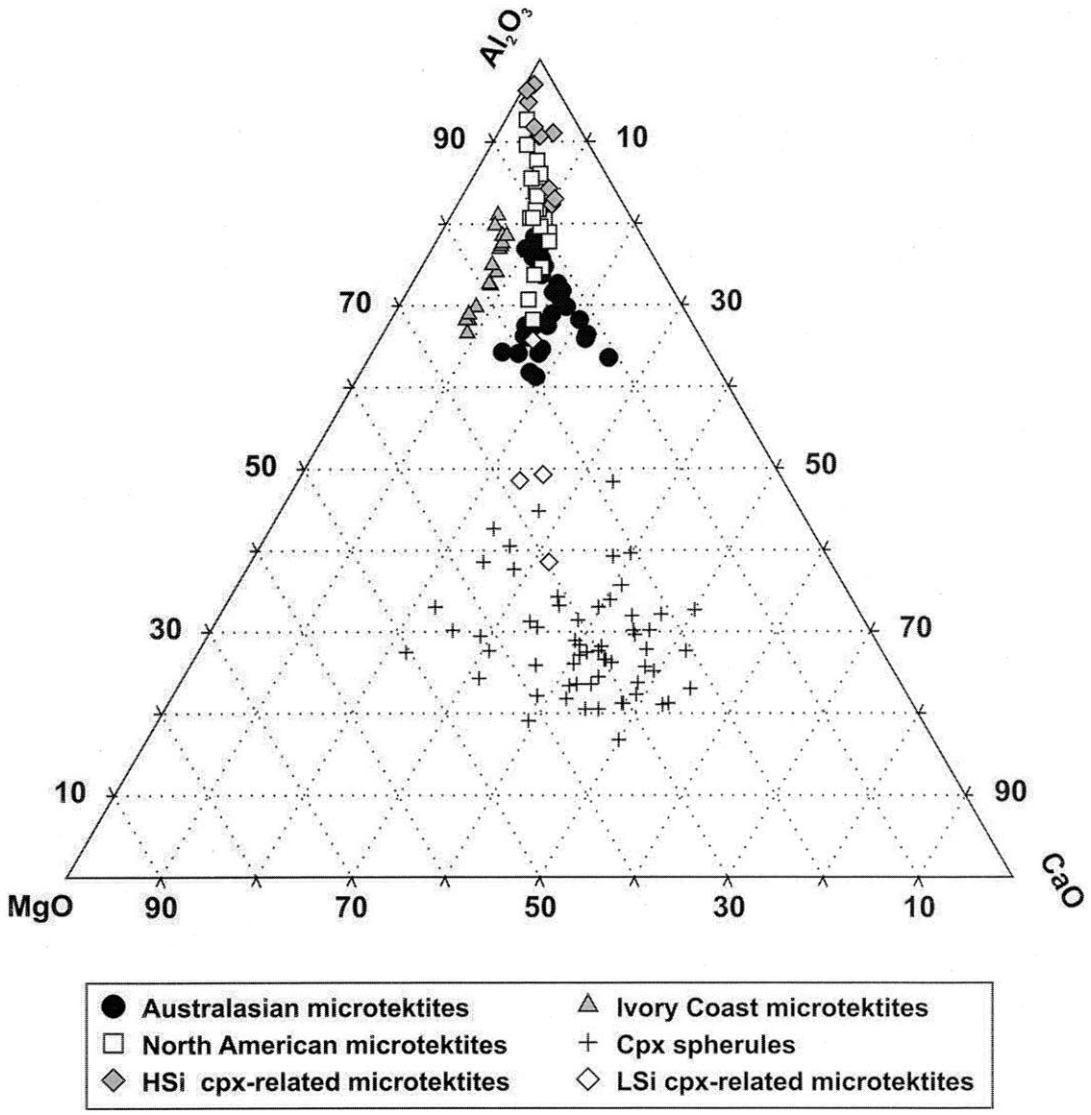

Fig. 6. Al_2O_3-CaO-MgO ternary diagram of Cenozoic microtektite and cpx spherule data. Note that the cpx spherules and three out of four of the low-Si cpx-related microtektites are clearly separated from the Australasian, Ivory Coast, and North American microtektites. Note also that the Ivory Coast microtektites are clearly separated from the Australasian and North American microtektites in this diagram.

slightly etched cpx spherules scatter about a mixing curve between the average upper continental crust and chondritic meteorites (Fig. 9a). The data for unetched to slightly etched cpx spherules also scatter about a mixing curve between the average upper continental crust and chondrite meteorites in a plot of Ni/Cr vs. Ni content (Fig. 9b). However, in this plot there is better separation between the mixing curves, and the cpx spherules fall below the crust-CI chondrite mixing curve, but close to the crust-LL chondrite mixing curve. Mixing curves for the other chondrite types fall between the points for CI and LL chondrites. Variations in the average composition of the target rocks can alter the position of the mixing curves at the low-Ni end, but will not have much effect on the position of the curves at the high Ni (greater than ~3000 ppm Ni) end of the curves. Of greater concern is the possible fractionation of the siderophile elements during spherule formation and later diagenetic alteration of the spherules in the marine environment. Contamination with mantle rocks can not explain the high Ni contents (above 2000 ppm) nor the high Ni/Cr ratios of the cpx spherules.

Tagle and Claeys (2002) concluded that the indigenous-corrected platinum group element ratios of the Popigai melt rocks are similar to those of ordinary chondrites, especially the L type and, to a lesser extent, the LL or H type. On the other hand, Whitehead et al. (2002) stated that the heterogeneity of the target rocks precludes a unique indigenous correction, and they concluded that an L-type chondrite cannot be inferred from the current data. Assuming that fractionation and diagenetic alteration are not problems, and that the cpx spherules were derived from the Popigai impact crater, our data are consis-

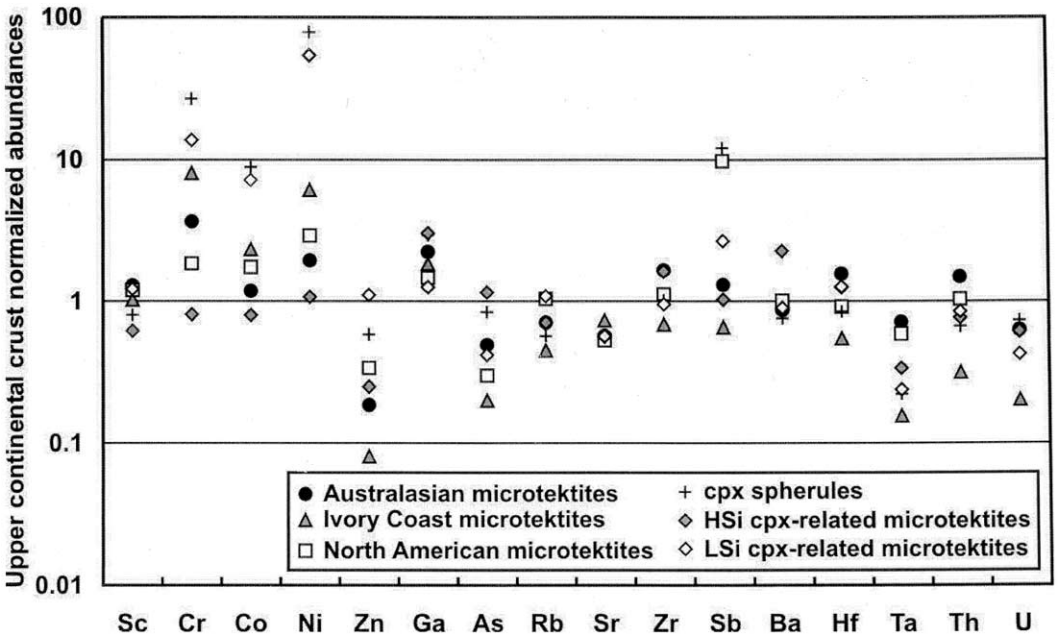

Fig. 7. Comparison of the average trace element compositions of normal Australasian, Ivory Coast, and North American microtektites and clinopyroxene-bearing (cpx) spherules and cpx-related microtektites (HSi = high SiO_2; LSi = low SiO_2) with that of the average upper continental crust. Note the high Cr, Co, and Ni contents of the cpx spherules and LSi cpx-related microtektites compared with the average upper continental crust. Average continental crust values are from Taylor and McLennan (1985).

tent with an LL-type chondrite projectile for the Popigai crater.

In both the Ni/Co and Ni/Cr vs. Ni plots the heavily etched, and most of the moderately etched, cpx spherules lie below the crust-chondrite mixing curves. This suggests that the Ni contents of the heavily to moderately etched cpx spherules may

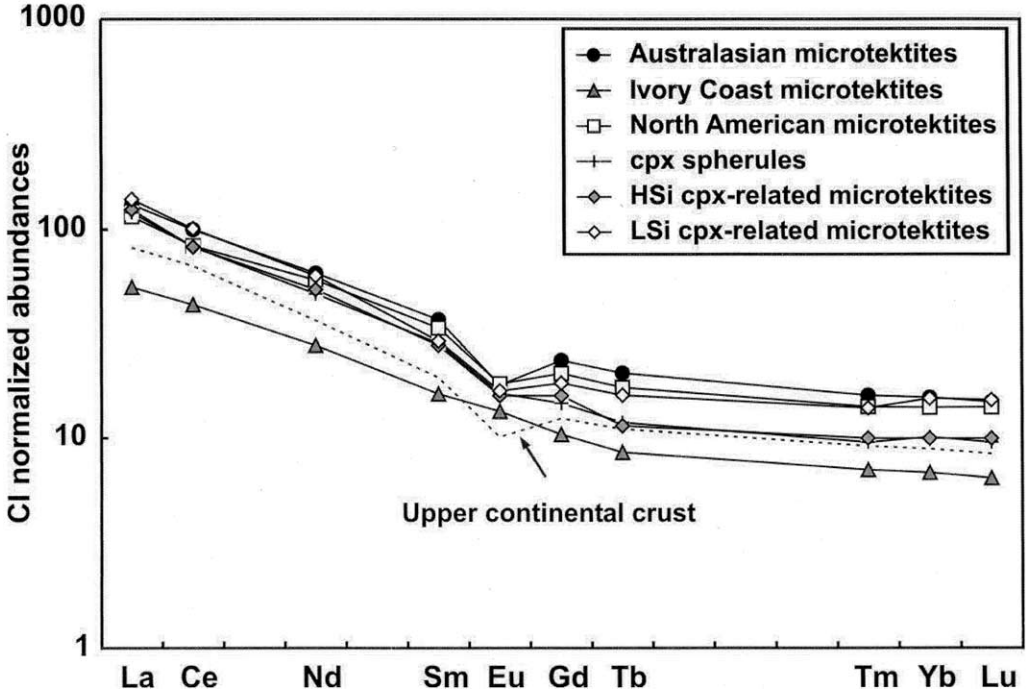

Fig. 8. Chondrite-normalized REE patterns for the average Australasian, Ivory Coast, and North American microtektites, cpx spherules, high-SiO_2 (HSi) and low-SiO_2 (LSi) cpx-related microtektites, and average upper continental crust. Average upper continental crust abundances from Taylor and McLennan (1985).

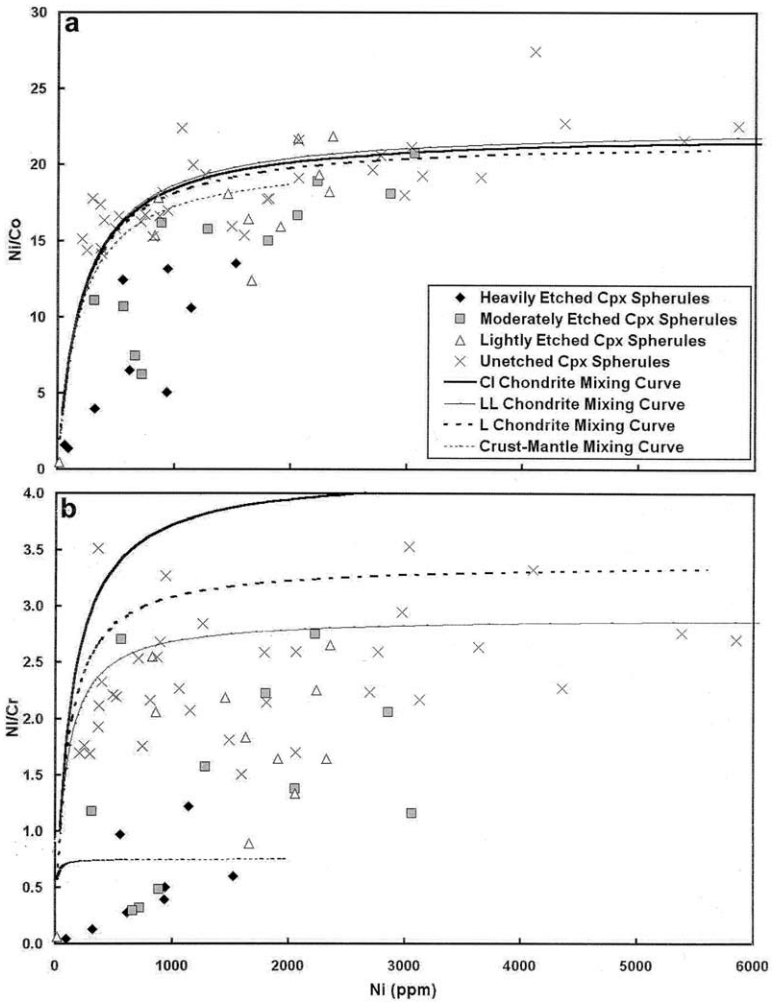

Fig. 9. Ni/Cr and Ni/Co versus Ni content for cpx spherules. Mixing curves between the average upper continental crust and different chondrite groups and the upper mantle are shown for comparison. The heavily-etched cpx spherules exhibit evidence of etching over most of their surfaces in polished sections, while the "unetched" cpx spherules exhibit no etching or, at most, a trace of etching around their peripheries. Average upper continental crust values are from Taylor and McLennan (1985) and mantle values are from Wedepohl (1981). Chondrite meteorite data from Lodders and Fegley Jr (1998).

have been lowered by dissolution of a Ni-bearing phase. Based on the shapes of the voids left by solution and one EDX analysis, it has been suggested that the missing phase may be Mg-rich olivine (Glass et al., 1985). Since Ni goes into the olivine structure more efficiently than Mg does, it is likely that the olivine crystals were Ni-rich. Thus, the removal of olivine by solution may have lowered the Ni/Cr ratio of the heavily to moderately etched cpx spherules. The low-silica (LSi) cpx-related microtektites have similar Cr, Co, and Ni contents compared to those of the cpx spherules and, like the moderately etched cpx spherules, lie close to—but generally below—the crust-chondrite mixing curves in plots of Ni/Co and Ni/Cr vs. Ni content.

We believe that the high Cr, Co, and Ni contents of the cpx spherules and associated low-silica microtektites are the results of chondritic contamination. However, the low-Au and -Ir contents are a problem. None of the low-Si cpx-related microtektites, and only seven cpx spherules, have Ir contents above the detection limits of 1–20 ppm (depending on sample size). The highest Ir content is 5 ppm. Gold contents are higher and generally range between 1 and 12 ppm, with the highest value being 28 ppm. However, there is no correlation between Au (or Ir) contents and Ni or Co content, and the Au and Ir contents are too low compared with the Cr, Co, and Ni contents to yield chondritic ratios. For example, the slightly etched to unetched cpx spherules have an average Ni content of ~1800 ppm Ni. If the impacting body were an average CI chondrite, these cpx spherules should have average Ir and Au contents of ~76 and 24 ppb, respectively, However, the average unetched to slightly etched cpx spherules have <1 ppb Ir and an average of ~5 ppb Au. Thus, the Ir and Au contents are too low by a factor of ~76 and 5, respectively. The results would be similar if the impacting body were an LL chondrite rather than a CI chondrite.

We do not know how to explain the low-Ir and -Au contents, but we note that relatively low-Ir abundances (compared to Cr,

Co, and Ni abundances), as well as low-Au/Ni and -Ir/Ni ratios have been observed in impact glasses from several impact events (e.g., Mittlefehldt et al., 1992; Koeberl et al., 1994). We assume that the low-Ir and -Au contents are the results of fractionation of the meteoritic component before incorporation into the cpx spherules. On the other hand, Ganapathy (personal communication to BPG, 1985) determined the Fe, Cr, Co, Ni, Ir, and Au concentrations in a group of 40 to 50 dark cpx spherules from Core RC9-58 (taken in the Caribbean Sea) using INAA and concluded that they have chondritic ratios within a factor of 3. Thus, additional studies are needed to resolve this problem.

Assuming that the Ni content of the cpx spherules is from the impacting body, we can calculate the percent meteoritic contamination. The average Ni content of the unetched to slightly etched cpx spherules is ~1800 ppm. If we assume that the target rock had an average of 20 ppm Ni (the average for the upper continental crust), then the indigenous corrected Ni content would be 1780 ppm. If the impacting body were a CI chondrite with 11,000 ppm Ni, then the percent contamination would be 16. Using Co indicates a similar amount of contamination (i.e., 15%). However, Cr indicates ~25% contamination from a CI chondrite. On the other hand, if we assume that the impacting body were an LL chondrite with 10,600, 668, and 75 ppm Ni, Cr, and Co, respectively (Lodders and Fegley, 1998), then the amount of contamination would be 17 ± 1% for all three elements. The Ni content of the cpx spherule with the highest Ni content (i.e., 5854 ppm) suggests the presence of as much as 54% chondritic component. This sample has high MgO and FeO content consistent with 54% chondritic component.

The high-Ni (HNi), intermediate, and high-Mg (HMg) Australasian microtektites all have high Cr contents compared with the normal Australasian microtektites. The intermediate and HMg Australasian microtektites have low-Co contents and only slightly elevated Ni contents compared with the normal Australasian microtektites and the average upper continental crust. The HNi Australasian microtektites have higher average Co and Ni contents compared with the normal Australasian microtektites. The Cr, Co, and Ni contents of the HNi Australasian microtektites are all positively correlated with each other and with FeO and MgO and negatively correlated with the other major oxides (Table A1 and Table 1). The HNi Australasian microtektite Ni and Co values lie close to a mixing curve between the average continental crust and the average CI chondrite in a plot of Ni/Co vs. Ni. However, the HNi Australasian microtektite data are about equally close to a mixing curve between the average upper continental crust and ultramafic or mantle rocks. The HNi Australasian microtektite values are also scattered about the mixing curve between the average upper continental crust and chondrite meteorites in a plot of Ni/Cr vs. Ni, but lie above the mixing curve between the average upper continental crust and ultramafic or mantle rocks. The best fit seems to be with an acapulcoite, although most chondrites would do about equally as well.

The average Ni content of the HNi Australasian microtektites indicates ~2% contamination by a CI chondrite meteorite projectile. The Ir content is low by a factor of at least four. The Au content is consistent with ~1–2% chondritic component; however, the Au content could be due entirely to Au in the target rocks, assuming a Au content close to the average for upper continental crust.

The Ivory Coast microtektites have Cr, Co, and Ni contents that are only slightly higher than the target rocks at Bosumtwi. Ni is negatively correlated with Cr and MgO. There is a well-defined trend of decreasing Ni/Cr with increasing Cr content. This trend is not easily explained by contamination with chondrite, or iron meteorites, or mantle rocks, nor can it be explained by vapor fractionation. The best explanation appears to be mixing between a high-Ni, low-Cr end member and a low-Ni, high-Cr end member. However, Cr isotope data for Ivory Coast tektites indicate that Bosumtwi crater, believed to be the source of the Ivory Coast tektites and microtektites, was probably formed by an ordinary chondrite (Koeberl et al., 2004).

The average Cr, Co, and Ni contents of the North American microtektites are only slightly above the average Cr, Co, and Ni contents of upper continental crustal rocks. Cr, Co, and Ni are positively correlated with each other and with all the major oxides except SiO_2. Chromium, Co, and Ni are negatively correlated with SiO_2, and since all the other major oxides are negatively correlated with SiO_2, it is not surprising that Cr, Co, and Ni exhibit weak positive correlations with the other major oxides. The strongest positive correlation is with FeO. The correlation with MgO is not as strong and is about the same as with CaO. Correlation between Ni and Al_2O_3, Na_2O, K_2O, and TiO_2 are all fairly weak. The Ni/Co, Ni/Cr, Ni/Au ratios are close to the ratios for these elements in the upper continental crust. Thus, there is no strong meteoritic signal in the North American microtektites, and correction for the indigenous amounts of Cr, Co, and Ni in the target rock is a major problem.

4.3. Target Rock Compositions

The Cenozoic microtektites generally have trace element (including REEs) contents within a factor of three of the average contents for the upper continental crust (Figs. 7 and 8). Other than the high Cr, Co, and Ni previously mentioned, the largest deviations from the average continental crust are the generally low Zn, As, Ta, and U contents. We do not know if the low abundances of these particular trace elements in microtektites are merely a coincidence or if they are telling us something about the nature of the target rocks that is a prerequisite for tektite formation. The cpx spherules also have lower average Ta contents than the average upper continental crust, but they also have higher average Sb (about and order of magnitude). However, the high Sb average is due to a few really high values, and the mode is only slightly above the average for the continental crust.

4.3.1. Australasian microtektites

In a series of papers, Taylor and colleagues reported the chemical compositions of australites and concluded that the elemental abundances of the australites are similar to well-mixed terrestrial surface materials (not igneous rocks), and in particular, to terrestrial sandstones, such as graywacke, with variable amounts of clay and calcite (Taylor, 1962; Taylor and Sachs, 1964; Taylor, 1966; Taylor and Kaye, 1969). We find, in agreement with Taylor and colleagues, that the compositions of

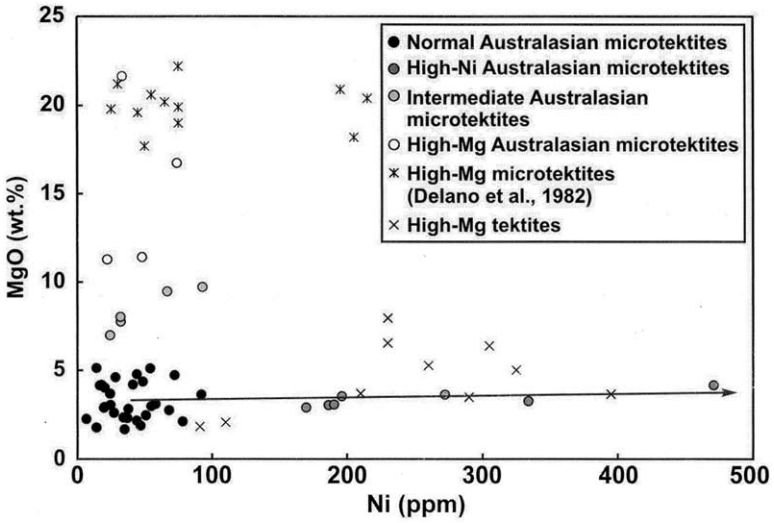

Fig. 10. MgO versus Ni for normal, high-Ni (HNi), intermediate, and high-Mg (HMg) Australasian microtektites and HMg Australasian tektites. The trend line extends from the average Ni and MgO values for normal Australasian microtektites towards the average values for CI chondrites. HMg microtektite data from Delano et al. (1982) were used to supplement our four HMg microtektite analyses. HMg Australasian tektite data from Chapman and Scheiber (1969). CI chondrite values are from Taylor and McLennan (1985).

the normal Australasian microtektites fall on the border between graywackes and lithic arenites based on their Na_2O/K_2O and SiO_2/Al_2O_3 ratios (see Pettijohn et al. 1987).

Delano et al. (1982) graphed refractory lithophile element ratios against each other (Al_2O_3/MgO vs. CaO/TiO_2) and found that the Australasian tektites, in general, plot along two trends (or branches) that converge at a CaO/TiO_2 ratio of ~1. One branch is defined by high-Ca (HCa) philippinites and normal HCa australites (as defined by Chapman and Scheiber (1969)), and the other branch is defined by javanites and HMg microtektites. The Australasian microtektites show a similar pattern, although the high CaO/TiO_2 branch is not well developed. This suggests that three distinct end members are required to explain the observed range in composition for the Australasian tektites and microtektites: (1) a high-Al_2O_3/MgO and low-CaO/TiO_2 end member, (2) a high-Al_2O_3/MgO and high-CaO/TiO_2 end member, and (3) a low Al_2O_3/MgO and intermediate-CaO/TiO_2 (or HMg) end member. Previous studies (Chapman and Scheiber, 1969; Glass, 1972a) indicated that the HMg Australasian microtektites are related to the HMg Australasian tektites as defined by Chapman and Scheiber (1969). However, the trace element data suggest that the high-Ni Australasian microtektites, rather than the HMg Australasian microtektites, are related to the HMg Australasian tektites (see Fig. 10).

The Australasian microtektites, including the HMg variety, have REE patterns consistent with derivation from post-Archean upper continental crust (Fig. 3b). The CI chondrite-normalized REE patterns show light REE enrichments, flat heavy REE distributions, and negative Eu anomalies. However, the REE contents in the Australasian microtektites are enriched above australite values that are themselves enriched above-average continental crustal values (Fig. 3a). The intermediate and HMg Australasian microtektites show the greatest enrichments.

The HMg Australasian microtektites are difficult to explain. They have lower Rb and Cs contents than the cpx spherules and the other Cenozoic microtektites (Tables 1–4). The high Cr and Ni contents of the HMg Australasian microtektites (Table 2) are suggestive of meteoritic contamination, but the average Co content is lower than the average Co content of the normal Australasian microtektites. Addition of a meteoritic component cannot explain the difference in composition between the HMg Australasian microtektites and the normal Australasian microtektites. The elements that have higher abundances in the HMg microtektites (e.g., Al, Mg, Ca, Ti, Sc, Cr) are refractory, and those that have lower abundances (e.g., Na, K, Rb) are volatile. This suggests that the HMg microtektites might have been formed by vapor fractionation of the normal microtektites. However, to increase the average MgO content from 3.2 wt.% for the normal microtektites to 15.3 wt.% for the HMg microtektites would require extensive vapor fractionation, and studies of Mg isotopes in HMg microtektites indicate little or no vapor fractionation during formation of the HMg microtektites (Esat and Taylor, 1987). On the other hand, Li and B isotopic data suggest that the HMg Australasian microtektites may have undergone vapor fractionation of at least some of the more volatile elements (Koeberl et al., 1999).

4.3.2. *Ivory Coast microtektites*

As previously mentioned, most investigators believe that the Ivory Coast tektites (and microtektites) were derived from the Bosumtwi impact crater. Koeberl et al. (1997) pointed out that the Ivory Coast tektites do not exhibit any distinct Eu anomaly in the REE patterns, and that this characteristic, as well as the high La_N/Yb_N ratios of ~8, indicate that Archean rocks are plausible source rocks. The Ivory Coast microtektites have similar chondrite-normalized REE patterns (Fig. 8) and similar La_N/Yb_N ratios as the Ivory Coast tektites (Table 2), and as the

Table 7. Comparison of Ivory Coast microtektite compositions with those obtained from the mixing calculations using Bosumtwi crater rocks.

	Observed			
	Average	Std. Dev.	Calculated[1]	Observed-Calculated
SiO_2	66.4	2.00	66.78	−0.38
TiO_2	0.55	0.04	0.64	−0.09
Al_2O_3	16.9	0.5	17.0	−0.1
FeO	6.65	0.58	6.42	0.23
MgO	4.27	1.25	3.95	0.32
CaO	1.73	0.37	1.64	0.09
Na_2O	1.92	0.23	2.01	−0.09
K_2O	1.60	0.39	1.59	0.01
Sc	11.3	1.2	16.9	−5.6
Rb	51	15	46.9	4.1
Zr	131	25	128	3
La	19.4	3.5	23.1	−3.7
Yb	1.69	0.27	1.69	0.0
Hf	3.19	0.47	3.10	0.09
Th	3.39	0.53	2.90	0.49

Major oxides in wt % and trace elements in ppm.

[1] The best match obtained using major oxide data is shown here and is a mixture of 78.9% average phyllite-graywacke and 21.1% Pepiakese "granite" (sample J508) from Koeberl et al. (1998). The trace element contents were calculated using this same mixture of target rocks.

rocks at the Bosumtwi crater (Koeberl et al., 1998). These data are consistent with the whole rock Rb-Sr age of 1.9 to 2.1 Ga for the country rock at the Bosumtwi crater site (Schnetzler et al., 1966; Shaw and Wasserburg, 1982; Koeberl et al., 1998). The SiO_2/Al_2O_3 and Na_2O/K_2O ratios place the Ivory Coast tektites and microtektites within the graywacke field established by Pettijohn et al. (1987). Using mixing calculations, Koeberl et al. (1998) were able to reproduce the composition of the Ivory Coast tektites reasonably well with a mixture of ~83% phyllite-graywacke and 17% Pepiakese "granite" from the Bosumtwi crater.

To put some constraints on the rocks that might have been melted to form the Ivory Coast microtektites, we performed mixing calculations using the same target rock compositions that Koeberl et al. (1998) used. The best match was a mixture of 79% phyllite-graywacke and 21% Pepiakese "granite" (Table 7), that agrees well with the results obtained using Ivory Coast tektite data (Koeberl et al., 1998). We calculated the content of several trace elements using the same mixture of target rocks (Table 7). There is good agreement between the calculated major oxide and trace element contents and the average major oxide and trace element contents of the Ivory Coast microtektites (especially when the standard deviations are considered), except for the TiO_2 and Sc contents.

4.3.3. North American microtektites

The higher abundance of North American microtektites and tektite fragments and unmelted impact ejecta in the sites off New Jersey indicate that these sites are closer to the source crater than are the sites in the Gulf of Mexico, Caribbean Sea, and Barbados (Glass, 1989; Glass et al., 1998). Furthermore, Sr and Nd isotopic data suggest that the North American tektites were formed from sediments derived from Appalachian age rocks (i.e., Sm-Nd model ages of 0.62–0.67 Ga; Shaw and Wasserburg, 1982). The Chesapeake Bay structure is the correct age and in the right location to be the source crater for the North American microtektites (Poag et al., 1994; Poag and Aubry, 1995; Koeberl et al., 1996).

The North American microtektites have an average La/Th ratio that is more similar to that of Archean rocks than to post-Archean rocks. However, the LREE enrichment, negative Eu anomaly, and Th/Sc and Rb/Sc ratios of the North American microtektites are intermediate between those of Archean and post-Archean crust, but generally closer to post-Archean values. Thus, the REE patterns, and La, Th, Sc, La, and Rb ratios are, in general, consistent with the Chesapeake Bay crater being the source of the North American microtektites.

The average Na_2O/K_2O and SiO_2/Al_2O_3 ratios of the North American microtektites fall mostly into the arkose field but with a weak trend between graywacke and quartz arenite based on Figures 2–14 of Pettijohn et al. (1987). This result is in general agreement with the conclusion of Albin et al. (2000) that the North American tektites required at least three source components: a quartz-rich sandstone (quartz arenite) and two relatively silica-poor and Fe-rich components similar to shale and graywacke.

If the Chesapeake Bay impact structure is the source crater of the North American tektites and microtektites, then the surface deposits at the time of the impact should have been upper/middle-Eocene marine sediments. Undisturbed upper Eocene deposits are missing in and adjacent to the Chesapeake Bay crater. However, upper Eocene sediments in the surrounding region are often fossiliferous and glauconite-rich (Jones, 1989; Miller et al., 1994). The fossiliferous nature of some of the middle/upper-Eocene deposits could be a problem. Since the North American tektites/microtektites average <1.65 wt. % CaO, the presence of more than a few percent biogenic carbonate would result in too high a CaO content. Another possible problem is the high-glauconite content of the upper/middle-Eocene deposits. The high-FeO content (~26 wt.%) and low-Al_2O_3 content (<4 wt.%) of glauconite makes it difficult to add more than a few percent and not make the FeO content too high and the Al_2O_3 content too low. There seems to be two possibilities: (1) glauconite was not present in upper/middle-Eocene sediments at the impact site in any abundance, or (2) the Chesapeake Bay structure is not the source crater for the North American tektites/microtektites.

Koeberl et al. (2001) made a preliminary study of major and trace elements and Sr and Nd isotopes of a suite of seven sediment samples from the environs of the Chesapeake Bay structure that were near-surface preimpact target rocks ranging in age from Paleocene to middle Eocene (but not late Eocene). The samples were clays, silts, and sands (quartz-rich sands with abundant shell fragments). Three of the samples had high CaO (18–27 wt.%). One had high FeO (~16 wt.%) and K_2O (~5.5 wt.%). This sample was glauconite-rich. Only one of the samples had an Al_2O_3 content as high as that of the average North American microtektites and it had only ~59 wt.% SiO_2. The major and trace element, as well as Sr and Nd isotopic compositions of the samples, showed no close similarity with those of the North American tektites. Therefore, mixing calculations using the compositions of the seven samples analyzed by Koeberl et al. (2001) were not able to reproduce the composi-

tion of the North American microtektites very well. Similar poor results were obtained by using compositional data for units of the Exmore breccia from the Chesapeake Bay area (these data are in Poag et al. (2004)). Thus, so far no possible source rocks for the North American microtektites have been identified in the crater-fill breccias from Chesapeake Bay crater. The search for the North American tektite/microtektite source rocks continues.

4.3.4. Cpx spherules and low-silica cpx-related microtektites

The upper Eocene cpx spherule layer appears to occur globally and the cpx spherules have a wide range of textures (Fig. 4) and compositions (Table 4). As discussed above, a number of workers have proposed that the cpx spherules occur in two or more layers; however, we believe that the available data indicate that all upper Eocene cpx spherules belong to a single strewn field. The cpx spherules can be divided into two main groups: (1) translucent to opaque, light-colored spherules with cryptocrystalline textures and high-CaO contents (up to ~19 wt.%); and (2) opaque dark spherules generally with low-CaO contents (usually <10 wt.%). Compositionally, the dark cpx spherules grade smoothly into the light-colored cpx spherules, and the distinction between the two groups is arbitrary. A higher percentage of the cpx spherules from the Indian Ocean and western Pacific Ocean sites are light-colored; and thus, more CaO rich than the cpx spherules from the central equatorial Pacific, Gulf of Mexico, and Caribbean Sea sites. This, and some biostratigraphic data, led Keller et al. (1987) to propose that the cpx spherules (their crystal-bearing spherules) in the Indian Ocean and western Pacific Ocean sites belong to a separate older layer than the cpx spherules in the central equatorial Pacific Ocean, Gulf of Mexico, and Caribbean Sea sites. Light- and dark-colored cpx spherules are found at all the sites, and there is a great deal of overlap in composition from one site to another.

As previously noted, all the high-Ca (HCa) cpx spherules have elevated Cr, Co, and Ni contents, compared with the average upper continental crust, due to contamination by a chondritic projectile. We assume that the HCa cpx spherules with the lowest Ni content have compositions that are closer to that of the target rocks. The four HCa spherules with the lowest Ni contents (<300 ppm) have the following average major oxide composition: 68 wt.% SiO_2, 6.4 wt.% Al_2O_3, 3.5 wt.% FeO, 6.8 wt.% MgO, 12.7 wt.% CaO, 0.5 wt.% Na_2O, 1.6 wt.% K_2O, and 0.3 wt.% TiO_2. This composition is not similar to any common igneous rock type, and the low-Al_2O_3 contents suggest that neither shale nor graywacke was a major source rock.

It is more difficult to determine the source rocks for the dark, LCa cpx spherules. The dark LCa cpx spherules have higher FeO, as well as lower CaO contents compared to the light HCa cpx spherules. In addition, they have ~3 times higher average Co and Ni contents. However, the LCa cpx spherules cannot simply be HCa cpx spherules contaminated by a chondritic meteorite. Only two of the LCa cpx spherules have Ni contents <300 ppm and both of them are heavily etched, indicating a missing phase (or phases), that has altered the compositions. We thus determined the average composition of the unetched to slightly etched LCa cpx spherules and used the average Ni content to correct for the supposed meteoritic contamination. This gave us a composition of: 74 wt.% SiO_2, 9.2 wt.% Al_2O_3, 1.9 wt.% FeO, 3.1 wt% MgO, 8.1 wt.% CaO, 1 wt% Na_2O, 2.4 wt.% K_2O, and 0.4 wt.% TiO_2.

As previously mentioned, the Popagai impact crater may the source of the cpx spherules (and associated microtektites). The target rock at Popigai consists of crystalline basement rock of various gneisses and some dolerite dykes (Kettrup et al., 2003). The basement is overlain by platform deposits consisting of over a kilometer of Upper Proterozoic to Cretaceous clastic rocks (shales, sandstones, and conglomerates) and carbonates (limestones and dolomites) with some volcanogenic rocks and dolerite dykes and sills (Kettrup et al., 2003). Unfortunately, there are no published compositional data for the clastic deposits.

The high-CaO and -MgO contents of the HCa (and to a lesser extent, the LCa) cpx spherules suggest that carbonates were an important source rock. The low Al_2O_3 rules out shale and graywacke as major sources for the cpx spherules, and the relatively low-SiO_2 contents indicate that quartz arenites are not a major component. Arkoses and lithic arenites could have been a major source. We cannot rule out the possibility that the dolerite dykes might have been a minor source.

Impact glasses and melt rocks (tagamites) from the Popigai structure have compositions similar to the basement gneisses (e.g., Whitehead et al., 2002; Kettrup et al., 2003). However, mixing calculations using compositional data for the gneisses, dolerites, quartzite, dolomite, and limestone were not successful in reproducing the composition of the average cpx spherule (Table 4). Nor were they successful in reproducing the compositions of either the low-Ni, HCa or low-Ni, LCa cpx spherules. This is probably because no compositional data are available for the clastic deposits (especially the sandstones) which were probably a major source for the cpx spherules.

In addition to the HCa and LCa end members and the variable degrees of meteoritic contamination, the compositions of the cpx spherules may have been affected by vapor fractionation. Several lines of evidence suggest that the cpx spherules were not formed as melt droplets, but rather were formed by condensation from a vapor. First, teardrop and dumbbell shaped cpx spherules have not been observed, but agglutinated forms are common. Second, vesicles have not been observed in the cpx spherules. Third, lechatelierite particles are not present in the cpx spherules. Fourth, it has been suggested that the spinel crystals found in the Cretaceous/Tertiary (K/T) boundary spherules were crystallized in liquid droplets that formed by condensation from the impact vapor cloud (Kyte and Bohor, 1995). On the other hand, the crustal REE patterns of the cpx spherules show no evidence of vapor fractionation.

Assuming that the source crater for the cpx spherules is the Popigai structure, the sites closer to the source crater have, in general, higher concentrations of spherules and a higher percentage of light-colored cpx spherules with higher Ca and Mg and less meteoritic contamination than the low-Ca, dark-colored cpx spherules. This suggests that the low-Ca end member was at or near the surface at the impact site and the dolomitic source rocks were lower in the section. Spherules produced from the surface deposits were thrown farther and were more heavily contaminated with the projectile, producing the darker cpx spherules with higher average Cr, Co, and Ni contents. Spherules produced from the deeper, more dolomite-rich de-

posits, were generally not thrown as far and are less contaminated by the projectile. This scenario appears to be consistent with impact models. Alternatively, melts with different compositions may have been ejected in different directions. However, such a model is not consistent with the cpx spherules having been formed by vapor fractionation.

The low-SiO_2 cpx-related microtektites have major and trace element contents similar to those of the cpx spherules. They appear to have been derived from similar target rocks and, like the cpx spherules, they appear to be heavily contaminated by the impacting body (Table 4).

4.3.5. High-silica, cpx-related microtektites

As previously mentioned, the cpx-related microtektites can be divided into a high- and a low-SiO_2 group. The high-SiO_2 (HSi) cpx-related microtektites have similar compositions to the North American microtektites, but can be distinguished by their lower Na_2O contents and various elemental ratios (Tables 3, 4, and 6). Furthermore, the HSi cpx-related microtektites have Sr and Nd isotopic values that are more similar to the cpx spherules than to the North American microtektites (Whitehead et al., 2000; Liu et al., 2001); and thus, also seem to have originated from the Popigai impact event.

Compared to the cpx spherules, the HSi cpx-related microtektites generally have higher SiO_2 and higher Al_2O_3 for a given SiO_2 content (Fig. 5a), but lower contents of the other major elements (Table 4). The SiO_2 content varies between 74 and 90 wt.%. The Al_2O_3 content varies inversely with SiO_2 and ranges between 6.5 and 22.5 wt.%. Thus, the HSi cpx-related microtektites have compositions that vary between a high-SiO_2, low-Al_2O_3 (quartz-rich) end member and a low-SiO_2, high-Al_2O_3 (clay-rich) end member. Attempts to produce the composition of the high-silica cpx-related microtektites by mixing of available Popigai target rock compositions were not successful. Again this is probably due to not having compositional data for the clastic rocks from the Popigai crater site.

4.4. High Al_2O_3 (>30 wt.%) Australasian and Cpx-Related Microtektites

One Australasian and one cpx-related microtektite have a high-Al_2O_3 content (>30 wt.%) that distinguishes them from all the other microtektites (and cpx spherules) in this report (Tables 1 and 4). Many of the refractory elements in the high-Al_2O_3 (HAl) Australasian microtektite have contents that are approximately twice as high as in the average normal Australasian microtektites, and many of the more volatile elements are lower. However, not all the refractory elements have higher contents (e.g., U) and not all the volatile elements have lower contents (e.g., Zn). Thus, the HAl Australasian microtektite does not appear to be a normal Australasian microtektite that underwent extreme vapor fractionation. Likewise, some of the refractory element contents (Ti, Al, Sc, Zr, Ba, REEs, Hf, Ta, Th) in the HAl cpx-related microtektite are higher than in the average cpx spherule, and other low-SiO_2 cpx-related microtektites, and some of the volatile element contents (Si, K, Rb) are lower. However, Ca, which is a refractory element, has a lower abundance in the HAl cpx-related microtektite than in the cpx spherules and other LSi cpx-related microtektites; and although some of the volatile elements (e.g., Zn, Ga) have low contents, they are within the range observed for the cpx spherules and other LSi cpx-related microtektites. Thus, despite the generally high refractory element and low volatile element contents, the HAl microtektites probably did not form by vapor fractionation. However, we cannot think of an appropriate source rock for these microtektites, although the high-Al_2O_3 contents suggest that the source rock was clay-rich.

4.5. Silica Range of Microtektites and Size of Source Crater

The compositions of impact generated spherules and microtektites are controlled by the composition of the target rock, the degree of vapor fractionation, and the amount of contamination by the impacting body. The target rock can be heterogeneous and, in general, the degree of variation in the composition of the target rock will increase with the size of the impact. In this study, the sizes of the proposed source craters range from 10.5 km to 100 km. The Ivory Coast microtektites, which were most likely derived from the 10.5-km-diameter Bosumtwi crater, are relatively homogeneous (the SiO_2 content ranges from 63 to 69 wt.%). On the other hand, the SiO_2 content of the cpx spherules and associated microtektites, believed to have originated from the 100-km-diameter Popigai structure, ranges from 54 to 90 wt.%. The North American microtektites, believed to have been derived from the 85-km-diameter (or 40-km-dia.) Chesapeake Bay structure, have an intermediate range in SiO_2 (63–82 wt.%). The source crater for the Australasian microtektites has not been identified, but previous estimates for the size of the source crater range from 17 to 114 km (Baldwin, 1981; Glass and Pizzuto, 1994; Lee and Wei, 2000; Glass, 2003). The large range in SiO_2 content (52–78 wt.%) of the Australasian microtektites (including the HMg group) suggests that the source crater is probably closer to the size of the 85-km-diameter (or 40-km-diameter) Chesapeake Bay structure than to the 10.5-km-diameter Bosumtwi crater. This conclusion is consistent with radial variations in the concentration (number/cm^2) of microtektites with distance from the source craters for these strewn fields.

5. SUMMARY AND CONCLUSIONS

In addition to the previously identified normal, intermediate, and high-Mg (HMg) Australasian microtektites, we have identified a high-Ni (HNi) group. The HNi group appears to be more closely related to the HMg Australasian tektites than are the HMg microtektites. We have divided the microtektites found in the cpx spherule layer into a high-SiO_2 (HSi) group and a low-SiO_2 (LSi) group. The LSi cpx-related microtektites are compositionally similar to the cpx spherules. The HSi cpx-related microtektites are compositionally more similar to the North American tektites, but we believe that the cpx spherules, LSi cpx-related microtektites, and HSi cpx-related microtektites were all produced by the same impact event.

Most of the Cenozoic microtektite/spherule layers can be distinguished based on the major and/or trace element compositions of the microtektites and spherules. However, even though the Australasian and North American microtektites have different ages and occur in different geographic regions, it

is difficult to distinguish between the microtektites in these two strewn fields since all the major oxides and minor elements overlap. Thus, because of the wide range in compositions of microtektites and microkrystites (especially those formed by major impact events), it can be difficult to distinguish between microtektite/impact spherule layers based on major oxide and trace element data alone, and it may be necessary to use isotopic data (e.g., Sr and Nd) as well.

The cpx spherules and most of the microtektites have average Cr, Co, and Ni contents above the average for upper continental crust, suggesting the presence of meteoritic contamination. The highest contents of these elements are found in the cpx spherules and LSi cpx-related microtektites. The slightly etched to unetched cpx spherules lie scattered along mixing lines between upper continental crust and chondrites on plots of Ni/Co and Ni/Cr vs. Ni content. The best match appears to be with LL chondrites, but the validity of such a conclusion is based on the assumption that the Ni/Cr ratios have not been altered due to fractionation during spherule formation or diagenetically altered after deposition. The highly etched cpx spherules lie off the trends in a direction that implies Ni loss. We speculate that Ni loss occurred as a result of solution of a Ni-bearing phase (probably olivine). The HNi Australasian microtektites fall along mixing curves between normal Australasian microtektites and chondrite meteorites; and thus appear to be normal Australasian microtektites that contain a chondritic component. However, the Ir (and, to a lesser extent, Au) contents of the cpx spherules and HNi Australasian microtektites appear to be too low to be consistent with contamination by chondritic projectiles. We do not understand the reason for the low-Ir and -Au contents, but assume that this is the result of fractionation of the meteoritic component before incorporation into the cpx spherules. The Ivory Coast and North American microtektites don't have high enough contents of Co and Ni to reach any firm conclusions about the nature of a meteoritic component, if any, in them.

Assuming that the elevated Ni contents are due to meteoritic contamination, and after correction for possible indigenous Ni, we calculate that the average Ni contents indicate 17% contamination by an LL chondrite and 2% contamination by an average CI chondrite in the cpx spherules and HNi Australasian microtektites, respectively.

The trace element data indicate that all the Cenozoic impact spherule/microtektite layers were derived from upper continental crust, although most exhibit an enrichment in siderophile elements and a depletion in Zn, As, Ta, and U. The normal Australasian microtektites appear to have had a graywacke or lithic arenite source rock, with a range in quartz and clay content. We do not know what the source rock for the HMg Australasian microtektites might have been. They do not appear to be normal microtektites with some meteorite or ultramafic rock added. The average major oxide content of the Ivory Coast microtektite composition can be matched with a mixture of target rocks at the Bosumtwi impact crater (~ 79% phyllite-graywacke, 21% Pepiakese "granite"). The source rock for the North American microtektites may have been something like an arkose, but with a graywacke (clay-rich) end member and a quartz-rich end member. Most investigators believe that the North American tektites/microtektites were derived from the Chesapeake Bay structure, but the apparently calcareous fossil-rich nature and high-glauconite content of the upper/middle-Eocene crater-fill breccia is a problem. We did not have any success in trying to reproduce the North American microtektite composition using published target rock compositions (Koeberl et al., 1996) or compositional data (from Poag et al. (2004)) for clasts in the Exmore breccia from the Chesapeake Bay crater area.

The cpx spherules have a wide range in composition and may have been derived from a mixture of lithic arenite or arkose and dolomite, which produced the low-Ca, dark-colored cpx spherules and the high-Ca, light-colored cpx spherules. Both the light-colored and dark cpx spherules are enriched in siderophile elements and appear to be contaminated by the impacting body. However, the light-colored cpx spherules have lower average siderophile abundances.

The 100-km-diameter Popigai impact structure in northern Siberia appears to be the source crater for the cpx spherules and associated microtektites. The surface and near-surface rocks at the Popigai crater site, at the time of the impact, appear to have been sandstones, shales, and carbonates, which appear to be the appropriate target rocks to produce melts of the correct range in compositions to form low- and high-Ca cpx spherules and the low-and high-SiO_2 cpx-related microtektites. Unfortunately, compositional data are not available for all the target rock lithologies. Mixing calculations involving the crystalline basement rocks, dolerite dikes, quartzite, dolomite, and limestone from the Popigai crater were not successful in reproducing the composition of the cpx spherules or associated microtektites.

We propose that the dark, low-Ca cpx spherules came from near-surface deposits at Popigai and were thrown farther from the crater and were more contaminated by the impacting body, whereas the light-colored, high-Ca cpx spherules were derived from deeper deposits in the target rock and were, therefore, not generally ejected as far or as heavily contaminated by the impacting body.

The HSi cpx-related microtektites appear to have been derived from target material that varies from a quartz-rich end member to a more clay-rich end member.

Two high-Al_2O_3 (>30 wt.%) microtektites (one Australasian and one low-SiO_2 cpx-related microtektite) were analyzed during this study. They generally have higher refractory and lower volatile element contents than the average microtektites or spherules from their respective layers. It is tempting to conclude that they formed by vapor fractionation, but there are some inconsistencies. On the other hand, we cannot think of an appropriate source rock for these unusual glasses.

Acknowledgments—We thank Takako Nagase for EDX analyses of the microtektites and cpx spherules. The Ocean Drilling Program, Lamont-Doherty Earth Observatory, and the Antarctic Core Facility at Florida State University provided core samples from which the microtektites and cpx spherules were extracted. We also thank Ross Taylor, Frank Kyte, and an unknown reviewer for constructive criticism that helped improve the paper. Analytical work was supported by Austrian Science Foundation (FWF) grant Y58-GEO to CK. This research was supported by NSF grant EAR-9903811 to B.P.G.

Associate editor: G. Herzog

REFERENCES

Albin E. and Wampler J. M. (1996) New potassium-argon ages for georgiaites and the upper Eocene Dry Branch Formation (Twiggs Clay Member): Inferences about tektite stratigraphic occurrence (abstract). *Lunar Planet. Sci.* **XXVII,** 5–6.

Albin E. F., Norman M. D., and Roden M. (2000) Major and trace element compositions of georgiaites: Clues to the source of North American tektites. *Meteoritics Planet. Sci.* **35,** 795–806.

Baldwin R. B. (1981) Tektites: Size estimates of their source craters and implications for their origin. *Icarus* **45,** 554–563.

Bottomley R. J., Grieve R. A. F., York D., and Masaitis V. (1997) The age of the Popigai impact event and its relations to events at the Eocene/Oligocene boundary. *Nature* **388,** 365–368.

Burns C. A. (1989) Timing between a large impact and a geomagnetic reversal and the depth of NRM acquisition in deep-sea sediments. In *Geomagnetism and Palaeomagnetism* (eds. Lowes F. J., et al.), pp. 253–261, Kluwer Academic Publishers.

Cande S. C. and Kent D. V. (1995) Revised calibration of the geomagnetic timescale for the Late Cretaceous and Cenozoic. *J. Geophys. Res.* **100,** 6093–6095.

Cassidy W. A., Glass B. P., and Heezen B. C. (1969) Physical and chemical properties of Australasian microtektites. *J. Geophys. Res.* **74,** 1008–1025.

Chao E. C. T. (1963) The petrographic and chemical characteristics of tektites. In *Tektites* (ed. O'Keefe J. A.), pp. 51–94, The University of Chicago Press.

Chapman D. R. and Scheiber L. C. (1969) Chemical investigation of Australasian tektites. *J. Geophys. Res.* **74,** 6737–6776.

Clymer A. K., Bice D. M., and Montanari A. (1996) Shocked quartz from the late Eocene: Impact evidence from Massignano, Italy. *Geology* **24,** 483–486.

Cuttitta F., Clarke R. S., Carron M. K., and Annell C. S. (1967) Martha's Vineyard and Georgia tektites: new chemical data. *J. Geophys. Res.* **72,** 1343–1349.

Delano J. W., Lindsley D. H., and Glass B. P. (1982) Nickel, chromium, and phosphorus in HMg and bottle-green microtektites from the Australasian and Ivory Coast strewnfields (abstract). *Lunar Planet. Sci.* **XIII,** 164–165.

D'Hondt S. L., Keller G., and Stallard R. F. (1987) Major element compositional variation within and between different late Eocene microtektite strewnfields. *Meteoritics* **22,** 61–79.

Donnelly T. W. and Chao E. C. T. (1973) Microtektites of late Eocene age from the eastern Caribbean Sea. *Initial Rep. Deep Sea Drill. Proj.* **15,** 1031–1037.

Esat T. M. and Taylor S. R. (1987) Mg isotopic composition of microtektites and flanged australite buttons (abstract). *Lunar Planet Sci.* **XVII,** 267–267.

Ford R. J. (1988) An empirical model for the Australasian tektite field. *Australian J. Earth Sci.* **35,** 483–490.

Frey F. A. (1977) Microtektites: A chemical comparison of the bottle-green microtektites, normal microtektites and tektites. *Earth Planet. Sci Lett.* **35,** 43–48.

Frey F. A., Spooner C. M., and Baedecker P. A. (1970) Microtektites and tektites: A chemical comparison. *Science* **170,** 845–847.

Glass B. P. (1969) Chemical composition of Ivory Coast microtektites. *Geochim. Cosmochim. Acta*. **33,** 1135–1147.

Glass B. P. (1972a) Bottle green microtektites. *J. Geophy. Res.* **77,** 7057–7064.

Glass B. P. (1972b) Australasian microtektites in deep-sea sediments. In *Antarctic Oceanology II: The Australian-New Zealand Sector, Antarctic Research Series*, (ed. D. E. Hayes), Vol. 19, pp. 335-348, American Geophysical Union.

Glass B. P. (1974) Microtektite surface sculpturing. *Geol. Soc. Am. Bull.* **85,** 1305–1314.

Glass B. P. (1989) North American tektite debris and impact ejecta from DSDP Site 612. *Meteoritics* **24,** 209–218.

Glass B. P. (1990) Chronostratigraphy of Upper Eocene microspherules. Comment and Reply. *Palaios* **5,** 387–390.

Glass B. P. (2000) Cenozoic microtektites and clinopyroxene-bearing spherule layers marine sediments. In *Terrestrial and Cosmic Spherules* (ed. Detre C. H.), pp. 57–71, Akadémiái Kiadó.

Glass B. P. (2003) Australasian microtektites in the South China Sea: Implications regarding the location and size of the source crater (abstract). *Lunar Planet. Sci.* **XXXIV,** #1092. CD ROM.

Glass B. P. and Burns C. A. (1987) Late Eocene crystal-bearing spherules: Two layers or one? *Meteoritics* **22,** 265–279.

Glass B. P. and Koeberl C. (1989) Trace element study of high- and low-refractive index Muong Nong-type tektites from Indochina. *Meteoritics* **24,** 143–146.

Glass B. P. and Koeberl C. (1999a) Ocean Drilling Project Hole 689B spherules and upper Eocene microtektite and clinopyroxene-bearing spherule strewn fields. *Meteorit. Planet. Sci.* **34,** 197–208.

Glass B. P. and Koeberl C. (1999b) North American microtektites in the Indian Ocean? (abstract). *Meteorit. Planet Sci.* **34,** A42–A43.

Glass B. P. and Liu S. (2001) Discovery of high-pressure $ZrSiO_4$ polymorph in naturally occurring shock-metamorphosed zircons. *Geology* **29,** 371–373.

Glass B. P. and Pizzuto J. E. (1994) Geographic variation in Australasian microtektite concentrations: Implications concerning the location and size of the source crater. *J. Geophys. Res.* **99,** 19,075–19,081.

Glass B. P. and Wu J. (1993) Coesite and shocked quartz discovered in the Australasian and North American microtektite layers. *Geology* **21,** 435–438.

Glass B. P. and Zwart M. J. (1979) North American microtektites in Deep Sea Drilling Project cores from the Caribbean Sea and Gulf of Mexico. *Geol. Soc. Am. Bull.* **90,** 595–602.

Glass B. P., Burns C. A., Crosbie J. R., and DuBois D. L. (1985) Late Eocene North American microtektites and clinopyroxene-bearing spherules. Proceedings of the 16th Lunar and Planetary Science Conference, Part 1. *J. Geophys. Res*. **90,** D175–D196.

Glass B. P., Hall C. M., and York D. (1986) $^{40}Ar/^{39}Ar$ laser-probe dating of North American tektite fragments from Barbados and the age of the Eocene-Oligocene boundary. *Chemical Geology* **5,** 181–186.

Glass B. P., Kent D. V., Schneider D. A., and Tauxe L. (1991) Ivory Coast microtektite strewn field: Description and relation to the Jaramillo geomagnetic event. *Earth Planet. Sci. Lett.* **107,** 182–196.

Glass B. P., Koeberl C., Blum J. D., and McHugh C. M. G. (1998) Upper Eocene tektite and impact ejecta layer on the continental slope off New Jersey. *Meteoritics Planet. Sci.* **33,** 229–241.

Grieve R. A. F. and Therriault A. M. (2004) Observations at terrestrial impact structures: Their utility in constraining crater formation. *Meteoritics Planet. Sci.* (in press).

Haskin L. A., Braverman M., and King E. A. (1982) Trace element analyses of some North American tektites (abstract). *Lunar Planet. Sci.* **XIII,** 302–303.

Hazel J. E. (1989) Chronostratigraphy of upper Eocene microspherules. *Palaios* **4,** 318–329.

Huber H. (2003) Application of $\gamma\gamma$-coincidence spectrometry for the determination of iridium in impact-related glasses, tektites, and breccias. Ph.D. Thesis (University of Vienna).

Izett G. A. and Obradovich J. D. (1992) Laser-fusion $^{40}Ar/^{39}Ar$ ages of Australasian tektites (abstract). *Lunar Planet. Sci.* **XXIII,** 593–594.

Jones W. B. (1985) Chemical analyses of Bosumtwi crater target rocks compared with Ivory Coast tektites. *Geochim. Cosmochim. Acta* **49,** 2569–2576.

Jones M. H. (1989) Foraminifera and paleoenvironmental interpretation of the Piney Point Formation (Middle Eocene), Virginia and Maryland. *Southeastern Section Geol. Soc. Am., Abstracts with Programs* **21,** 23.

Keller G., D'Hondt S. L., Orth C. J., Gilmore J. S., Oliver P. Q., Shoemaker E. M., and Molina E. (1987) Late Eocene impact microspherules: Stratigraphy, age, and geochemistry. *Meteoritics* **22,** 25–60.

Kettrup B., Deutsch A., and Masaitis V. L. (2003) Homogeneous impact melts produced by a heterogeneous target? Sr-Nd isotopic evidence from Popigai crater, Russia. *Geochim. Cosmochim. Acta* **67,** 733–750.

Koeberl C. (1986) Geochemistry of tektites and impact glasses. *Ann. Rev. Earth Planet. Sci.* **14,** 323–350.

Koeberl C. (1993) Instrumental neutron activation analysis of geochemical and cosmochemical samples: A fast and proven method

for small sample analysis. *J. Radioanalyt. Nuclear Chem.* **168,** 47–60.

Koeberl C. (1994) Tektite origin by hypervelocity asteroidal or cometary impact: Target rocks, source craters, and mechanisms. In *Large Impacts and Planetary Evolution* (ed. B. O. Dressler et al.), *Geological Society of America Special Paper* **293,** 133–151.

Koeberl C. and Glass B. P. (1988) Chemical composition of North American microtektites and tektite fragments from Barbados and DSDP Site 612 on the continental slope off New Jersey. *Earth Planet. Sci. Lett.* **87,** 286–292.

Koeberl C., Reimold W. U., and Shirey S. B. (1994) Saltpan impact crater, South Africa: Geochemistry of target rocks, breccias, and impact glasses, and osmium isotope systematics. *Geochim. Cosmochim. Acta*. **58,** 2893–2910.

Koeberl C., Poag C. W., Reimold W. U., and Brandt D. (1996) Impact origin of Chesapeake Bay structure and the source of North American tektites. *Science* **271,** 1263–1266.

Koeberl C., Bottomley R., Glass B. P., and Storzer D. (1997) Geochemistry and age of Ivory Coast tektites and microtektites. *Geochim. Cosmoschim. Acta*. **61,** 1745–1772.

Koeberl C., Reimold W. U., Blum J. D., and Chamberlain C. P. (1998) Petrology and geochemistry of target rocks from Bosumtwi impact structure, Ghana, and comparison with Ivory Coast tektites. *Geochim. Cosmochim. Acta.* **62,** 2179–2196.

Koeberl C., Glass B. P., and Chaussidon M. (1999) Bottle-green microtektites from the Australasian tektite strewn field: Did they form by jetting from the top layer of the target surface? *Geol. Soc. Am. Abstracts with Programs* **31**(7), A63–A64.

Koeberl C., Kruger F. J., and Poag C. W. (2001) Geochemistry of surficial sediments near the Chesapeake Bay impact structure and the search for source rocks of the North American tektites (abstract). *Lunar Planet. Sci.* **XXXII,** 1333 CD-ROM.

Koeberl C., Shukolyukov V., and Lugmair G. W. (2004) An ordinary chondrite impactor composition for the Bosumtwi impact structure, Ghana, West Africa: Discussion of siderophile element contens and Os and Cr isotope data (abstract). *Lunar Planet. Sci.* **XXXV,** 1256.

Kyte F. T. and Bohor B. F. (1995) Ni-rich magnesiowüstite in Cretaceous -Tertiary boundary crystalized from ultramafic, refractory silicate liquid. *Geochim. Cosmochim. Acta.* **59,** 4967–4974.

Kyte F. T. and Liu S. (2002) Iridium and spherules in late Eocene impact deposits (abstract). *Lunar Planet. Sci.* **XXXIII,** #1981 CD-ROM.

Kunz J., Bollinger K., Jessberger E. K., and Storzer D. (2000) Ages of Australasian tektites(abstract). *Lunar Planet. Sci.* **XXVI,** 809–810.

Langenhorst F. (1996) Characteristics of shocked quartz in late Eocene impact ejecta from Massignano (Ancona, Italy): Clues to shock conditions and source crater. *Geology* **24,** 487–490.

Lee M.-Y. and Wei K.-Y. (2000) Australasian microtektites in the South China Sea and the West Philippine Sea: Implications for age, size, and location of the impact crater. *Meteoritics Planet. Sci.* **35,** 1151–1155.

Lee Y.-T., Chen J. C., Ho K. S., and Juang W. S. (2004) Geochemical studies of tektites from East Asia. *Geochem. Jour.* **38,** 1–17.

Levene H. (1960) Robust tests for equality of variances. In *Contributions to Probability and Statistics* (eds. I. Olkin et al.), pp. 278–292, Stanford University Press.

Liu S. and Glass B. P. (2001) Upper Eocene impact ejecta/spherule layers in marine sediments: New sites (abstract). *Lunar Planet. Sci.* **XXXII,** #2027 CD-ROM.

Liu S., Glass B. P., Ngo H. H., Papanastassiou D. A., and Wasserburg G. J. (2001) Sr and Nd data for upper Eocene spherule layers (abstract). *Lunar Planet. Sci.* **XXXII,** #1819.

Lodders K. and Fegley Jr. B. (1998) *The Planetary Scientist's Companion.* Oxford University Press.

Marchand E. and Whitehead J. (2002) Statistical evaluation of compositional differences between upper Eocene impact ejecta layers. *Math. Geol*. **34,** 555–572.

Miller K. G., Berggren W. A., Zhang J., and Palmer-Julson A. A. (1991) Biostratigraphy and isotope stratigraphy of Upper Eocene microtektites at Site 612: How many impacts? *Palaios* **6,** 17–38.

Miller K. G., et al. (1994) *Proc. ODP, Init. Repts.*, **150X**. Ocean Drilling Program, College Station, TX. 388 pp.

Mittlefehldt D. W., See T. H., and Hörz F. (1992) Projectile dissemination in impact melts from Meteor Crater, Arizona (abstract). *Lunar Planet. Sci.* **XXIII,** 919–920.

Montanari A. and Koeberl C. (2000) *Impact Stratigraphy: The Italian Record.* Springer.

Montanari A., Asaro F., Michel E., and Kennett J. P. (1993) Iridium anomalies of Late Eocene age at Massignano (Italy), and in ODP Site 689B (Maud Rise, Antarctica). *Palaios* **8,** 420–437.

Nagasawa H., Fukuoka T., and Glass B. P. (1986) Trace element concentrations in microtektites from Barbados and DSDP cores from the Caribbean Sea and Gulf of Mexico (abstract). *Lunar Planet. Sci.* **XVII,** 597–598.

Ngo H. H., Wasserburg G. J., and Glass B. P. (1985) Nd and Sr isotopic compositions of tektite material from Barbados and their relationship to North American tektites. *Geochim. Cosmochim. Acta*. **49,** 1479–1485.

Obradovich J. D., Snee L. W., and Izett G. A. (1989) Is there more than one glassy impact layer in the late Eocene? *Geol. Soc. Amer. Abstracts with Programs* **21**(6), A134.

Peng H., Zhao K., and Chen S. (1982) The evidence for 'CHO1' in sediment core samples of Pacific Ocean collected among FGGE. *J. Geophys. Res.* **87,** 5563–5565.

Pettijohn F. J., Potter P. E., and Siever R. (1987) *Sand and Sandstone, 2nd Ed.* Springer-Verlag.

Pierrard O., Robin E., Rocchia R., and Montanari A. (1998) Extraterrestrial Ni-rich spinel in upper Eocene sediments from Massignano, Italy. *Geology* **26,** 307–310.

Poag C. W. and Aubry M.-P. (1995) Upper Eocene impactites of the U.S. East Coast: Depositional origins, biostratigraphic framework, and correlation. *Palaios* **10,** 16–43.

Poag C. W., Powars D. S., Poppe L. J., and Mixon R. B. (1994) Meteoroid mayhem in Ole Virginny: Source of the North American tektite strewn field. *Geology* **22,** 691–694.

Poag C. W., Koeberl C., and Reimold W. U. (2004) *Chesapeake Bay Crater–Geology and Geophysics of a Late Eocene Submarine Impact Structure.* Springer-Verlag.

Prasad M. S. and Sudhakar M. (1999) Australasian minitektites discovered in the Indian Ocean. *Meteoritics Planet. Sci.* **34,** 179–184.

Sanfilippo A., Riedel W. R., Glass B. P., and Kyte F. T. (1985) Late Eocene microtektites and radiolarian extinctions on Barbados. *Nature* **314,** 613–615.

Schneider D. A. and Kent D. V. (1990) Ivory Coast microtektites and geomagnetic reversals. *Geophys. Res. Lett.* **17,** 163–166.

Schneider D. A., Kent D. V., and Mello G. A. (1992) A detailed chronology of the Australasian impact event: Brunhes/Matuyama geomagnetic polarity reversal, and climate change. *Earth Planet. Sci. Lett.* **111,** 395–405.

Schnetzler C. C. (1992) Mechanism of Muong Nong-type tektite formation and speculation on the source of the Australasian tektites. *Meteoritics* **27,** 154–165.

Schnetzler C. C., Pinson W. H., and Hurley P. M. (1966) Rubidium-strontium age of the Bosumtwi crater area, Ghana, compared with the age of the Ivory Coast tektites. *Science* **151,** 817–819.

Schnetzler C. C., Philpotts J. A., and Thomas H. H. (1967) Rare earth and barium abundances in Ivory Coast tektites and rocks from Bosumtwi crater area, Ghana. *Geochim. Cosmochim. Acta.* **31,** 1987–1993.

Shaw H. F. and Wasserburg G. J. (1982) Age and provenance of the target materials for tektites and possible impactites as inferred from Sm-Nd and Rb-Sr systematics. *Earth Planet. Sci. Lett.* **60,** 155–177.

Stauffer P. H. (1978) Anatomy of the Australsian tektite strewnfield and the probable site of its source crater. *3rd Regional Conference on Geology and Mineral Resources of Southeast Asia, Bangkok,* 285-289.

Stöckelmann D. and Reimold W. U. (1989) The HMX mixing calculation program. *Math. Geol.* **21,** 853–860.

Storzer D. and Wagner G. A. (1971) Fission track ages of North American tektites. *Earth Planet. Sci. Lett.* **10,** 435–440.

Tagle R. and Claeys P. (2002) An L-chondrite origin for the Popigai crater (abstract). *Geol. Soc. Am. Abstracts with Programs*. **34**(6), 318.

Taylor S. R. (1962) The chemical composition of australites. *Geochim. Cosmochim. Acta* **26,** 685–722.

Taylor S. R. (1966) Australites, Henbury impact glass, and subgreywacke: A comparison of 51 elements. *Geochim. Cosmochim. Acta* **30,** 1121–1136.

Taylor S. R. and Kaye M. (1969) Genetic significance of the chemical composition of tektites: A review. *Geochim. Cosmochim. Acta* **33,** 1083–1100.

Taylor S. R. and McLennan S. M. (1979) Chemical relationships among irghizites, zhamanshinites, Australasian tektites and Henbury impact glasses. *Geochim. Cosmochim. Acta* **43,** 1551–1565.

Taylor S. R. and McLennan S. M. (1985) *The Continental Crust: Its Composition and Evolution.* Blackwell Scientific Publication.

Taylor S. R. and Sachs M. (1964) Geochemical evidence for the origin of australites. *Geochim. Cosmochim. Acta* **28,** 235–265.

Vonhof H. B. and Smit J. (1999) Late Eocene microkrystites and microtektites at Maud Rise (Ocean Drilling Project Hole 689B; Southern Ocean) suggest a global extension of the approximately 35.5 Ma Pacific impact ejecta strewn field. *Meteoritics Planet. Sci.* **34,** 747–755.

Wasson J. W. (1991) Layered tektites: a multiple impact origin for Australasian tektites. *Earth Planet. Sci. Lett.* **102,** 95–109.

Wedepohl K. H. (1981) Der primære Erdmantel (Mp) und die durch Krustenbildung verarmte Mantelzusammensetung (Md). *Fortschr. Mineral.* **59,** 203–205.

Wei W. (1995) How many impact-generated microspherule layers in the Upper Eocene? *Palaeogeogr. Palaeoclimatol. Palaeoecol.* **114,** 101–110.

Whitehead J., Papanastassiou D. A., Spray J. G., Grieve R. A. F., and Wasserburg G. J. (2000) Late Eocene impact ejecta: geochemical and isotopic connections with the Popigai impact structure. *Earth Planet. Sci. Lett.* **181,** 473–487.

Whitehead J., Grieve R. A. F., and Spray J. G. (2002) Mineralogy and petrology of melt rocks from the Popigai impact structure, Siberia. *Meteoritics Planet. Sci.* **37,** 623–647.

Yamei H., Potts R., Baoylin Y., Zhengtang G., Deino A., Wei W., Clark J., Guangmao X., and Weiwen H. (2000) Mid-Pleistocene Acheulean-like stone technology of the Bose Basin, South China. *Science* **287,** 1622–1626.

Zähringer J. (1963) K-Ar measurements of tektites. In: *Radioactive Dating. Proceedings of the International Atomic Energy Agency Symposium, Nov. 19-23, 1962* International Atomic Energy Agency, Vienna. pp. 289-305.

SUPPLEMENTARY DATA

Supplementary data associated with this article can be found, in the online version, at doi:10.1016/j.gca.2004.02.026.

Table A1. Major and trace element contents of Cenozoic microtektites and clinopyoxene-bearing spherules.

Australasian Microtektites
Normal

Site	E45-71	E45-89	E45-50	E45-89	E45-89	E45-50	ODP 769A	ODP 769A	RC14-23	V29-43	V28-238	V16-76	DSDP 292	DSDP 292	DSDP 292	ODP 758B	ODP 758B	ODP 768B	ODP 768B	V19-153	V19-153	DSDP 292
No.	802-2	803-2	803-3	804-1	804-2	804-3	805-3	806-1	807-1	810-1	810-3	810-4	810-6	810-7	810-8	811-1	811-2	811-4	811-5	812-1	812-2	812-3
weight	3.9	62.4	178.0	70.1	195.9	54.2	64.9	61.5	144.1	14.9	13.9	26.4	28.0	47.8	64.3	91.0	135.8	73.5	73.3	9.9	23.5	37.3
SiO_2	68.82	69.07	69.89	72.22	76.77	60.48	66.84	65.14	64.81	69.19	67.87	63.73	75.82	74.39	76.19	67.18	69.06	64.03	68.26	62.17	71.24	78.05
TiO_2	0.76	0.81	0.95	0.79	0.71	1.18	0.83	0.84	0.93	0.83	0.97	1.14	0.73	0.77	0.77	0.82	0.92	0.91	0.78	0.67	0.78	0.64
Al_2O_3	14.80	14.55	16.99	12.98	12.75	21.46	16.71	17.15	17.33	15.48	16.88	20.17	12.64	12.52	12.55	15.99	16.31	18.76	13.82	16.33	13.23	10.25
FeO	6.20	6.32	2.90	5.49	3.04	5.87	5.65	6.11	5.82	5.87	5.37	3.85	3.80	4.34	3.48	5.41	4.24	5.69	6.41	7.23	4.60	3.55
MgO	4.17	3.64	2.91	3.09	2.27	4.43	2.62	2.99	4.80	4.10	2.75	4.61	2.15	2.11	1.82	5.07	2.92	3.12	4.71	2.79	2.33	1.67
CaO	3.39	3.38	4.99	3.07	2.79	5.21	2.72	3.09	4.07	3.38	3.60	5.07	1.63	1.85	1.63	3.90	5.32	3.18	2.96	6.56	3.41	1.78
Na_2O	0.63	0.79	0.44	0.72	0.39	0.28	1.39	1.58	0.68	0.22	1.06	0.72	0.94	1.38	1.09	0.54	0.28	1.33	1.16	1.69	1.70	1.14
K_2O	1.18	1.35	0.91	1.61	1.26	1.06	3.21	3.05	1.52	0.91	1.50	0.67	2.25	2.62	2.37	1.05	0.88	2.96	1.80	2.50	2.69	2.86
Sc	13.7	14.9	17.7	10.8	11.6	15.6	19.3	16.3	18.4	11.4	14.5	20.2	11.0	11.0	10.5	16.5	16.7	20.8	15.3	21.9	11.0	7.43
Cr	402	386	112	153	66.7	56.5	74.0	75.4	154	106	65.2	107	102	109	53.1	224	46.4	121	348	118	58.1	54.8
Co	16.7	31.3	3.11	16.0	4.41	9.12	12.0	11.9	13.7	7.07	8.55	2.86	7.26	12.5	5.56	10.1	3.82	10.4	22.4	21.0	10.7	8.00
Ni	17	92	19	24	7	48	27	55	44	18	38	28	< 10	78	14	14	20	58	72	68	37	35
Zn	7	< 5	11	< 4	< 6	3	16	26	7	12	5	6	5	7	7	8	6	13	11	60	27	23
Ga	4	14	6	4	< 1	4	28	42	56	13	14	20	20	15	77	108	85	122	48	19	20	18
As	< 3	< 1	< 1	< 1	< 0.3	< 0.7	1.1	0.9	0.9	0.3	< 1	0.3	< 0.4	< 0.3	< 0.4	< 0.4	0.3	< 1	< 1	1.7	1.5	0.1
Br	0.8	< 1.5	< 2	0.2	< 0.4	< 0.9	0.3	0.2	0.4	0.4	0.6	< 0.5	< 0.3	0.2	< 0.3	0.5	0.1	0.8	< 2	0.2	0.2	0.2
Rb	54.3	75.9	38.2	68.7	55.8	33.0	168	153	69.4	30.7	58.6	22.7	82.7	112	92.1	26.9	37.3	152	75.1	184	107	8.82
Sr	248	181	313	131	198	242	153	144	236	146	268	324	120	102	147	195	272	190	195	468	142	138
Zr	344	305	393	206	312	302	241	247	317	216	261	415	407	277	271	272	436	269	235	508	280	273
Sb	< 0.5	0.09	0.13	0.07	0.06	0.01	0.56	1.02	0.18	0.11	0.30	< 0.1	< 0.1	0.14	< 0.1	< 0.1	0.10	0.18	0.10	0.68	0.53	0.50
Cs	2.68	4.13	2.21	4.01	2.64	1.70	12.1	10.7	3.68	1.64	2.76	0.98	3.41	5.19	3.98	1.33	1.86	8.81	3.49	11.2	6.15	4.38
Ba	512	495	603	338	553	506	521	461	547	454	332	618	475	274	383	669	605	628	419	658	432	276
La	52.1	50.2	66.8	39.0	48.2	52.0	50.8	47.2	55.9	38.9	56.1	69.9	44.6	40.3	36.7	56.1	56.9	54.4	42.4	62.7	44.3	30.9
Ce	97.7	94.6	120	75.9	89.6	105	98.3	92.7	105	106	136	112	84.2	70.0	69.9	101	106	125	86.5	140	72.2	56.1
Nd	46.2	44.9	57.0	31.6	43.1	45.6	43.1	39.7	45.0	38.9	51.3	50.7	38.9	37.9	30.9	58.2	55.4	68.1	38.2	56.6	37.5	27.1
Sm	8.91	8.61	11.2	6.64	7.93	8.89	8.59	8.11	9.22	8.14	10.6	12.1	7.67	7.46	6.23	9.07	11.9	12.1	7.52	10.6	7.49	5.43
Eu	1.61	1.58	2.08	1.20	1.44	1.68	1.63	1.60	1.83	1.05	1.44	2.03	1.34	1.36	1.12	1.56	2.70	2.05	1.50	2.55	1.45	0.86
Gd	7.63	7.58	9.54	5.98	7.10	7.72	7.49	7.65	8.41	5.41	7.46	10.4	6.86	6.07	5.33	7.25	9.19	8.71	7.01	10.2	5.83	4.56
Tb	1.25	1.23	1.49	0.99	1.17	1.27	1.20	1.30	1.39	0.84	1.09	1.68	1.12	0.95	0.88	1.12	1.40	1.28	1.17	1.73	0.88	0.72
Tm	0.61	0.61	0.78	0.45	0.56	0.58	0.56	0.63	0.66	0.40	0.66	0.82	0.54	0.66	0.43	0.56	0.70	0.56	0.50	0.83	0.51	0.36
Yb	4.04	4.01	5.06	2.93	3.68	3.94	3.61	4.15	4.29	2.58	4.61	5.37	3.56	4.79	2.88	3.74	4.65	3.60	3.16	5.39	3.48	2.38
Lu	0.56	0.59	0.71	0.43	0.54	0.56	0.53	0.81	0.60	0.39	0.65	0.79	0.51	0.73	0.41	0.55	0.69	0.52	0.44	0.82	0.53	0.35
Hf	8.82	7.74	10.4	6.04	8.19	6.80	6.32	6.17	8.20	7.25	7.28	13.0	11.9	8.76	8.24	10.4	12.9	8.22	9.09	14.9	7.99	7.75
Ta	1.75	1.73	2.14	1.22	1.66	1.74	1.79	1.74	5.00	1.14	1.58	2.14	1.69	1.36	1.27	1.69	2.04	1.73	1.54	2.33	1.31	0.97
Ir (ppb)	< 1	< 1	< 1	< 1	< 1	< 1	< 1	< 1	< 1	< 2	1	< 1	< 2	< 1	< 1	< 1	< 1	< 1	< 1	2	< 1	< 1
Au (ppb)	10	6	< 7	2	2	7	2	< 2	4	2	< 9	3	< 7	2	1	< 5	2	3	7	< 4	< 9	1
Th	19.7	19.4	23.8	14.7	17.4	20.7	19.5	17.7	20.2	11.9	12.3	22.1	15.5	9.66	12.5	13.3	20.9	19.3	14.4	23.8	12.7	10.4
U	0.58	1.01	1.43	1.09	0.48	0.28	3.01	2.74	0.60	0.48	1.30	1.84	0.79	1.82	1.30	0.64	1.47	4.22	0.57	4.85	3.35	2.46
K / U	16687	11096	5233	12162	21618	31356	8798	9208	20892	16168	9854	3023	23538	12003	14815	13749	5026	5783	26361	4232	6609	9724
Th / U	33.8	19.2	16.7	13.5	36.3	74.5	6.48	6.46	33.7	24.9	9.46	12.0	19.6	5.31	9.62	20.8	14.2	4.57	25.3	4.91	3.78	4.24
La / Th	2.65	2.59	2.81	2.66	2.77	2.51	2.61	2.66	2.77	3.27	4.57	3.16	2.88	4.17	2.94	4.22	2.72	2.82	2.94	2.64	3.49	2.97
Zr / Hf	39.0	39.4	37.6	34.1	38.1	44.4	38.1	40.0	38.7	29.8	35.8	31.9	34.2	31.7	32.9	26.2	33.8	32.7	25.9	34.0	35.1	35.3
Hf / Ta	5.04	4.47	4.88	4.95	4.93	3.90	3.53	3.55	1.64	6.37	4.61	6.07	7.04	6.44	6.49	6.15	6.32	4.75	5.90	6.42	6.11	8.00
La_N/Yb_N	12.9	12.5	13.2	13.3	13.1	13.2	14.1	11.4	13.0	15.1	12.2	13.0	12.5	8.40	12.7	15.0	12.2	15.1	13.4	11.6	12.7	13.0
Eu/ Eu*	0.60	0.60	0.61	0.58	0.59	0.62	0.62	0.62	0.64	0.49	0.50	0.55	0.56	0.62	0.59	0.59	0.79	0.61	0.63	0.75	0.67	0.53

Table A1. (Cont.).

	Australasian Microtektites																						
	Normal								High-Ni							Intermediate					High-Mg			
Site	ODP 758B	ODP 768B	V19-153	DSDP 292	V19-153	DSDP 213	DSDP 213	DSDP 292	ODP 769A	RC14-46	RC14-46	ODP 769A	ODP 768B	ODP 758B	ODP 768B	E45-71	E45-71	ODP 769A	V29-43	V16-76	E45-89	RC12-331	RC14-46	DSDP 213
No.	812-4	812-7	813-1	813-2	814-1	814-3	815-1	815-2	805-2	805-5	805-6	806-2	811-3	812-5	812-6	802-1	802-4	805-1	810-2	810-5	803-1	805-4	806-3	814-2
weight	20.7	94.6	26.8	28.3	56.9	86.5	258.0	141.0	69.5	49.3	49.4	45.4	72.9	24.8	30.8	3.4	10.7	83.2	16.9	34.7	82.0	71.3	15.1	83.5
SiO_2	68.82	72.28	70.46	75.25	71.69	66.35	71.21	71.82	70.09	67.17	69.25	72.01	69.27	66.69	70.97	60.96	58.87	64.72	67.56	59.58	54.69	56.05	51.83	56.35
TiO_2	0.76	0.71	0.80	0.73	0.80	0.85	0.75	0.77	0.75	0.80	0.69	0.75	0.75	0.81	0.72	0.97	1.07	0.87	0.71	1.05	0.75	1.17	0.72	1.05
Al_2O_3	14.80	13.05	13.35	12.16	13.71	15.52	13.80	13.36	13.54	14.94	12.48	12.65	14.07	14.37	12.73	17.28	19.51	16.21	13.63	19.66	14.66	20.66	15.05	19.28
FeO	6.20	4.72	5.10	4.10	4.73	6.06	5.28	4.88	5.74	5.97	6.77	5.11	5.78	6.62	5.75	4.87	4.85	5.39	5.74	5.93	7.78	4.50	5.16	6.64
MgO	4.17	2.15	2.46	1.88	3.70	5.07	3.92	2.36	3.02	3.07	4.17	2.90	3.27	3.89	3.52	9.43	9.61	7.77	7.22	7.99	16.76	11.34	21.82	11.53
CaO	3.39	2.99	4.43	1.81	3.78	4.56	3.83	3.18	2.68	3.68	3.29	2.37	2.63	4.30	2.50	5.31	5.15	3.90	3.66	4.73	4.48	5.72	4.69	4.37
Na_2O	0.63	1.40	1.18	1.21	0.57	0.68	0.29	1.20	1.37	1.59	1.04	1.31	1.47	0.98	1.32	0.59	0.59	0.62	0.69	0.58	0.79	0.43	0.71	0.61
K_2O	1.78	2.69	2.19	2.83	0.94	0.83	0.91	2.41	2.77	2.79	2.22	2.86	2.73	2.25	2.36	0.52	0.26	0.48	0.70	0.39	0.08	0.13	0.04	0.17
Sc	12.5	12.1	8.85	10.1	14.0	17.5	15.4	11.9	11.8	12.8	13.0	11.2	14.3	12.9	14.0	16.7	20.2	19.7	13.4	26.3	15.0	24.7	24.1	23.0
Cr	24.1	94.5	57.8	54.0	217	302	22.3	87.1	135	140	381	98.6	209	273	272	583	568	316	472	472	1167	455	1306	919
Co	28.4	13.0	10.9	8.74	7.76	14.4	11.3	12.1	17.3	16.8	42.3	16.7	29.2	32.6	27.0	12.9	12.2	7.40	8.00	10.6	18.0	3.90	9.5	12.5
Ni	41	44	51	47	24	54	20	34	186	190	471	170	334	272	196	67	93	32	24	32	74	22	33	48
Zn	6	23	16	10	11	9	4	17	16	57	13	14	14	9	12	< 11	14	8	13	13	6	7	10	< 3
Ga	73	102	13	20	22	61	25	49	37	79	171	57	42	69	n.d.	13	7	24	25	14	14	126	62	34
As	< 0.1	1.7	0.6	0.1	0.3	< 0.3	0.3	1.0	1.0	2.7	1.0	< 0.1	0.5	< 1	2.6	< 6	< 1	< 0.1	< 1	0.5	0.3	< 0.6	< 1	< 0.3
Br	0.2	0.1	2.4	0.2	< 1	0.5	0.1	< 1	0.3	2.4	1.3	< 0.1	1.6	< 3	< 2	< 7	0.3	1.0	0.4	< 1	< 4	0.1	2.7	< 0.1
Rb	77.7	131	72.0	101	37.3	25.9	37.0	108	128	133	120	118	140	97.5	119	10.4	11.2	18.2	16.1	26.3	3.72	4.90	1.11	5.62
Sr	108	145	170	131	250	247	218	180	140	176	213	186	108	168	137	220	272	197	156	387	159	276	204	303
Zr	463	326	171	286	321	442	370	296	274	324	255	205	382	198	322	363	413	430	255	586	224	438	208	562
Sb	0.15	0.39	0.27	0.44	< 0.1	0.07	0.02	0.20	0.58	3.13	0.70	0.41	0.27	0.10	< 0.2	0.13	0.04	0.47	0.22	0.07	0.02	0.10	0.82	0.07
Cs	8.12	6.60	3.85	5.54	1.62	1.43	1.72	1.21	7.67	8.20	6.74	7.47	7.08	4.83	6.32	0.54	0.37	0.97	0.64	1.14	0.06	0.23	< 1	0.25
Ba	402	500	259	352	479	556	457	473	403	403	448	370	465	535	540	571	757	556	415	897	363	656	491	730
La	37.1	48.3	50.4	32.2	47.7	53.7	38.5	45.1	42.0	44.1	45.5	40.8	53.0	42.5	44.0	58.9	77.0	60.0	46.2	70.0	36.8	69.5	53.0	67.8
Ce	71.0	87.1	56.8	62.7	92.5	172	96.8	84.0	79.6	83.0	85.0	71.7	90.4	85.6	81.9	106	126	109	67.8	143	62.3	117	74.8	127
Nd	30.8	40.4	32.6	27.0	48.5	64.9	38.4	47.8	34.1	38.3	36.9	32.6	49.8	42.9	40.1	51.6	64.9	50.3	31.3	76.4	34.9	62.1	43.5	53.0
Sm	6.36	8.50	5.66	5.73	7.62	12.2	6.63	9.23	7.12	7.55	7.70	7.12	10.4	8.40	7.66	9.89	12.9	10.2	5.98	11.5	6.35	11.5	9.14	12.0
Eu	1.05	1.32	1.00	1.08	1.77	1.78	1.87	1.26	1.32	1.33	1.34	1.26	1.72	1.26	1.68	1.85	1.89	1.92	1.31	2.38	1.20	2.26	1.89	2.21
Gd	6.58	7.29	4.75	5.08	6.64	8.91	6.88	6.45	6.18	6.53	6.48	6.10	6.99	6.69	7.14	8.27	10.3	9.05	5.51	10.9	5.90	10.7	7.83	11.0
Tb	2.24	1.14	0.76	0.82	1.07	1.32	1.21	0.93	0.98	1.04	1.03	0.90	0.99	1.03	1.19	1.31	1.62	1.49	0.91	1.83	0.98	1.78	1.24	1.84
Tm	0.50	0.57	0.48	0.40	0.57	0.79	0.53	0.49	0.47	0.51	0.52	0.49	0.67	0.53	0.54	0.66	0.87	0.74	0.48	1.03	0.46	0.80	0.62	0.82
Yb	4.38	3.81	3.42	2.65	3.86	5.50	3.37	3.31	3.12	3.40	3.42	3.31	4.77	3.55	3.49	4.41	5.84	4.86	3.19	7.03	3.04	5.22	4.04	5.26
Lu	0.47	0.52	0.52	0.40	0.58	0.83	0.48	0.49	0.44	0.48	0.48	0.44	0.75	0.52	0.51	0.62	0.90	0.71	0.47	1.05	0.46	0.79	0.58	0.76
Hf	7.73	9.58	6.31	7.85	11.5	12.7	10.5	9.50	6.26	5.71	6.70	5.78	12.4	7.10	9.26	8.67	11.2	10.9	7.64	13.2	6.14	12.6	8.95	15.7
Ta	1.05	1.37	0.96	1.25	1.58	1.84	1.62	1.31	1.52	1.38	1.53	1.45	1.49	1.41	1.61	1.80	2.05	2.08	1.42	2.41	1.17	2.50	1.82	2.35
Ir (ppb)	< 2	< 1	< 1	< 1	< 1	< 2	< 1	< 1	1	1	1	< 1	< 1	< 2	< 1	< 1	< 1	< 1	< 1	< 2	< 1	< 1	< 5	1
Au (ppb)	3	< 6	< 6	3	< 2	4	1	2	1	2	1	< 2	2	< 10	< 9	12	5	2	3	4	4	1	< 7	< 2
Th	12.8	15.9	7.37	11.1	12.3	17.4	17.1	14.0	15.4	15.4	15.3	9.60	12.0	11.8	14.9	20.0	24.6	21.2	13.1	19.5	13.5	24.7	17.6	24.5
U	1.41	3.68	2.53	2.50	0.42	0.79	0.58	4.61	2.25	2.37	2.40	1.56	3.95	2.29	3.14	0.84	0.88	0.38	0.55	1.24	0.67	0.51	0.42	0.73
K / U	10418	6113	7193	9446	18580	8827	13311	4322	10297	9784	7679	15219	5716	7613	6292	5151	2447	10486	10264	2607	995	2116	793	1933
Th / U	9.07	4.32	2.92	4.43	29.3	22.0	29.5	3.04	6.84	6.52	6.38	6.15	3.04	5.15	4.75	23.9	27.8	55.8	23.8	15.7	20.2	48.4	42.1	33.6
La / Th	2.90	3.04	6.84	2.92	3.88	3.09	2.25	3.22	2.73	2.86	2.97	4.25	4.42	3.60	2.95	2.94	3.13	2.83	3.53	3.59	2.73	2.81	3.01	2.77
Zr / Hf	59.9	34.0	27.1	36.4	27.9	34.8	35.2	31.2	43.8	56.7	38.1	35.5	30.8	27.9	34.8	41.8	37.0	39.4	33.4	44.5	36.5	34.8	23.2	35.8
Hf / Ta	7.37	6.99	6.56	6.29	7.28	6.90	6.48	7.25	4.13	4.13	4.38	3.98	8.32	5.04	5.75	4.81	5.43	5.24	5.38	5.47	5.26	5.04	4.92	6.68
La_N/Yb_N	8.48	12.7	14.7	12.2	12.4	9.76	11.4	13.6	13.4	13.0	13.3	12.3	11.1	12.0	12.6	13.4	13.2	12.3	14.5	10.0	12.1	13.3	13.1	12.9
Eu /Eu*	0.50	0.51	0.59	0.61	0.76	0.52	0.85	0.50	0.61	0.58	0.58	0.58	0.62	0.51	0.69	0.62	0.50	0.61	0.70	0.65	0.60	0.62	0.68	0.59

Table A1. (Cont.).

	Aust. Micro. HAl	Ivory Coast Microtektites																North American Microtektites									
Site	E45-71	K9-56	K9-56	K9-56	K9-56	K9-56	K9-56	K9-56	K9-56	K9-56	K9-56	K9-56	K9-56	K9-56	K9-56	K9-56	K9-56	DSDP 94	DSDP 94	DSDP 94	DSDP 94	DSDP 94	DSDP 94	DSDP 94	DSDP 94	DSDP 94	DSDP 94
No.	802-3	857-1	857-2	857-3	857-4	857-5	857-6	858-1	858-2	858-3	858-4	858-5	858-6	858-7	858-8	858-9	858-10	771-3	771-4	771-5	771-6	772-1	772-2	772-3	772-4	772-5	772-6
weight	2.2	14.0	31.9	26.4	23.6	52.5	27.6	69.7	85.0	119.4	90.7	113.2	56.9	108.0	73.2	84.0	75.2	16.9	25.2	25.2	19.2	56.1	56.7	36.5	45.8	40.0	27.5
SiO_2	41.41	64.53	63.32	66.69	63.12	63.60	67.42	63.38	69.30	67.35	67.33	67.12	67.38	68.11	67.86	68.00	67.59	75.53	74.16	68.66	76.95	71.44	77.87	74.36	78.47	73.60	81.51
TiO_2	1.38	0.57	0.60	0.53	0.58	0.62	0.56	0.57	0.47	0.54	0.58	0.50	0.52	0.54	0.53	0.58	0.54	0.66	0.69	0.92	0.61	0.90	0.60	0.74	0.60	0.76	0.46
Al_2O_3	32.49	17.37	17.48	16.67	17.24	17.42	16.83	17.62	15.82	17.15	16.50	15.97	16.89	17.02	16.23	16.90	16.73	12.97	13.92	15.49	12.90	17.62	11.66	13.82	11.78	13.87	10.82
FeO	2.26	7.13	7.25	6.49	7.49	7.40	6.12	7.44	5.67	6.39	6.48	6.53	6.31	6.67	6.34	6.55	6.19	3.71	3.88	5.63	3.34	5.98	3.09	3.51	3.12	4.17	2.28
MgO	12.72	5.44	5.87	4.36	6.30	5.98	3.17	6.15	3.25	3.13	3.86	4.20	3.31	2.91	3.84	3.15	3.37	1.51	1.58	2.62	1.29	0.95	1.10	1.68	1.23	1.76	0.80
CaO	9.16	2.09	2.02	1.90	2.34	2.12	1.43	2.09	1.48	1.56	1.63	1.88	1.54	1.05	1.81	1.14	1.54	1.64	1.51	2.66	1.45	0.43	1.29	2.01	1.30	1.78	0.45
Na_2O	0.43	1.61	2.19	1.93	1.81	1.82	2.47	1.67	2.10	1.98	1.96	1.96	2.09	1.60	1.80	1.72	2.03	1.22	1.35	1.46	0.77	1.05	1.22	1.25	0.94	1.32	0.92
K_2O	0.05	1.24	1.24	1.40	1.00	1.00	2.00	1.03	1.89	1.90	1.65	1.82	1.96	2.03	1.54	1.95	1.96	2.76	2.86	2.54	2.68	1.64	3.16	2.60	2.52	2.74	2.74
Sc	39.3	10.9	11.7	10.5	9.00	11.6	13.2	11.2	10.4	10.4	11.9	10.9	9.74	11.9	13.6	11.6	11.8	12.4	13.1	17.5	9.81	11.0	6.57	12.4	6.58	13.8	4.22
Cr	632	429	460	327	419	146	560	470	235	147	210	161	182	201	181	172	200	40.0	40.0	85.0	35.0	48.5	21.7	30.0	23.1	49.0	12.4
Co	12.3	19.0	20.3	19.9	21.1	18.4	31.0	21.0	22.9	20.5	25.0	31.0	20.5	24.4	28.9	24.3	24.7	13.7	20.4	22.9	10.5	9.9	7.44	11.2	6.81	17.0	5.92
Ni	67	75	50	90	72	132	99	69	142	130	128	197	153	225	119	192	87	45	45	60	35	36	16	45	12	35	17
Zn	16	9	< 4	< 4	< 4	3	< 4	< 2	5	< 3	5	4	6	4	8	4	8	20	17	33	6	32	6	19	5	14	4
Ga	< 6	17	67	11	39	7	12	32	31	25	9	12	95	9	119	7	9	27	153	26	13	12	1	17	7	73	2
As	< 10	0.4	0.1	0.8	0.7	< 0.2	0.5	0.2	< 0.2	0.1	0.3	< 0.1	0.1	0.2	0.3	0.1	< 0.1	0.1	1.4	0.7	<2	0.3	<0.27	0.1	<1	0.2	0.4
Br	1.0	< 0.1	0.05	0.1	0.1	0.02	0.1	< 0.1	< 0.1	< 0.1	< 0.1	< 0.1	< 0.1	0.02	< 0.1	0.01	0.02	5.6	2.6	0.4	0.5	<2.0	0.7	<1	2.0	2.5	0.2
Rb	6.76	26.6	37.8	36.7	28.1	55.0	41.7	27.1	57.8	59.2	52.1	57.2	63.8	67.0	66.4	63.4	69.5	96.5	120	98.1	88.1	34.0	67.9	83.8	49.6	109	44.3
Sr	423	211	251	240	324	160	374	270	262	206	236	255	242	233	387	200	251	230	215	180	195	65.5	73.3	130	124	205	68.3
Zr	658	101	115	107	80.7	104	172	140	113	128	138	149	135	152	160	155	139	155	215	170	160	165	95.0	165	89.5	200	66.2
Sb	0.10	0.11	0.17	0.12	0.24	< 0.5	0.05	0.02	0.09	0.03	0.10	0.10	0.31	0.23	0.17	< 0.1	0.09	0.26	0.48	0.34	0.09	0.27	0.07	0.17	0.08	0.22	0.07
Cs	0.06	1.40	1.57	2.01	1.28	2.74	1.89	1.32	3.06	3.12	2.66	2.62	3.00	3.86	3.38	3.19	3.47	3.95	n.d.	n.d.	3.58	n.d.	2.50	n.d.	2.30	3.98	1.08
Ba	793	456	604	488	618	373	734	513	548	497	494	434	494	556	559	609	556	540	630	550	575	223	342	565	335	620	290
La	132	15.5	20.1	15.8	16.9	14.2	26.6	17.5	22.0	16.4	18.8	17.4	20.1	23.4	24.4	22.4	19.1	32.9	43.8	38.7	36.9	29.9	17.7	38.8	22.1	40.8	12.8
Ce	125	33.9	41.5	34.0	36.8	33.5	56.9	38.5	41.4	39.9	40.6	37.1	41.8	54.5	46.2	48.3	42.8	66.9	81.2	78.4	67.5	61.6	38.4	70.4	39.5	82.8	26.1
Nd	106	15.3	20.7	15.2	17.0	16.4	23.2	18.2	21.7	18.5	18.1	18.6	19.7	23.9	22.9	25.5	21.2	29.6	39.8	36.5	31.5	27.6	17.6	29.9	19.2	34.7	10.6
Sm	22.6	3.03	3.88	2.95	3.24	2.94	5.21	3.47	4.16	3.24	3.69	3.41	3.98	4.50	4.60	4.18	3.68	6.21	7.69	7.23	6.48	5.82	3.45	6.54	3.71	7.74	2.41
Eu	3.62	0.90	1.04	1.09	1.01	1.01	1.48	1.02	1.04	0.98	1.07	1.16	0.97	1.51	1.63	1.46	1.31	1.39	1.63	1.72	1.37	1.28	0.79	1.45	0.81	1.60	0.51
Gd	18.0	2.56	3.23	2.58	3.24	2.37	4.45	3.18	3.20	2.79	2.78	3.04	2.98	3.64	3.99	3.55	3.37	4.91	7.12	7.02	5.14	4.90	2.97	4.64	3.18	5.87	1.85
Tb	2.93	0.40	0.50	0.41	0.47	0.36	0.70	0.52	0.48	0.44	0.41	0.49	0.44	0.56	0.63	0.56	0.55	0.89	1.19	1.25	0.82	0.84	0.56	1.05	0.52	1.11	0.36
Tm	1.60	0.22	0.27	0.22	0.23	0.19	0.34	0.25	0.26	0.22	0.24	0.23	0.25	0.28	0.32	0.28	0.25	0.38	0.43	0.44	0.38	0.28	0.26	0.49	0.20	0.44	0.21
Yb	10.8	1.44	1.89	1.44	1.53	1.28	2.26	1.64	1.78	1.47	1.67	1.47	1.74	1.89	2.16	1.82	1.59	2.69	3.31	3.05	2.57	2.36	1.78	3.31	1.45	3.12	1.36
Lu	1.67	0.21	0.27	0.21	0.22	0.19	0.33	0.23	0.27	0.22	0.25	0.21	0.21	0.28	0.32	0.26	0.23	0.41	0.53	0.48	0.48	0.37	0.27	0.50	0.25	0.47	0.21
Hf	19.2	2.99	2.98	2.80	3.04	2.45	4.58	3.41	3.03	2.96	3.16	3.01	2.91	3.38	3.76	3.33	3.18	4.25	4.50	4.24	4.25	3.08	2.51	3.97	2.35	4.75	1.72
Ta	3.78	0.28	0.27	0.36	0.33	0.29	0.48	0.36	0.31	0.32	0.30	0.27	0.32	0.42	0.46	0.31	0.39	1.05	1.63	1.75	1.40	0.69	0.81	1.49	0.78	1.56	0.50
Ir (ppb)	< 1	< 1	< 4	< 4	< 6	< 2	< 4	< 2	< 2	< 3	< 1	< 2	< 2	< 3	< 1	< 2	< 3	1	1	1	1	1	< 1	1	< 1	1	<2
Au (ppb)	8	5	3	2	2	4	< 11	4	4	2	1	2	3	1	4	2	6	1	1	1	<1	1	1	1	<1	1	<1
Th	43.3	2.89	3.53	2.89	3.32	2.53	4.91	3.39	3.15	3.30	3.38	3.16	3.19	3.92	3.76	3.59	3.35	9.11	11.6	11.3	9.34	6.45	6.41	10.2	4.90	11.1	3.51
U	1.27	0.35	0.61	0.45	0.46	0.51	0.89	0.49	0.77	0.55	0.67	0.28	0.75	0.75	0.36	0.49	0.69	1.62	2.67	3.57	2.71	2.37	0.96	1.08	0.73	2.29	0.65
K / U	327	26565	16009	24904	17589	15243	18196	17065	20592	27621	20196	51588	22027	23023	33897	33375	23701	13528	8612	5790	7965	5707	27128	19293	28195	9860	34833
Th / U	34.1	8.26	5.83	6.42	7.18	5.00	5.54	6.98	4.09	6.00	5.04	11.3	4.25	5.23	10.3	7.33	4.86	5.62	4.34	3.17	3.45	2.72	6.67	9.44	6.74	4.85	5.44
La / Th	3.04	5.36	5.69	5.47	5.09	5.59	5.41	5.15	6.98	4.97	5.56	5.51	6.30	5.97	6.49	6.24	5.70	3.61	3.78	3.42	3.95	4.63	2.76	3.80	4.51	3.68	3.64
Zr / Hf	34.2	33.8	38.5	38.2	26.5	42.4	37.5	41.2	37.3	43.2	43.7	49.5	46.4	45.0	42.5	46.5	43.7	36.5	47.8	40.1	37.6	53.5	37.9	41.6	38.0	42.1	38.6
Hf / Ta	5.09	10.7	10.9	7.78	9.26	8.35	9.51	9.33	9.77	9.25	10.5	11.1	9.09	8.05	8.12	10.7	8.15	4.05	2.76	2.42	3.04	4.45	3.08	2.66	3.00	3.04	3.43
La_N/Yb_N	12.2	10.8	10.7	11.0	11.0	11.0	11.7	10.7	12.4	11.2	11.3	11.8	11.6	12.4	11.3	12.3	12.0	12.2	13.2	12.7	14.4	12.6	9.94	11.7	15.2	13.1	9.39
Eu / Eu*	0.55	0.99	0.90	1.21	0.95	1.17	0.94	0.93	0.87	1.00	1.02	1.10	0.86	1.14	1.16	1.16	1.14	0.77	0.67	0.74	0.73	0.73	0.75	0.80	0.72	0.73	0.74

Table A1. (Cont.).

	North American Microtektites														Cpx Spherules							
Site	DSDP 94	DSDP 149	DSDP 149	DSDP 149	RC9-58	RC9-58	RC9-58	RC9-58	RC9-58	RC9-58	RC9-58	RC9-58	RC9-58	RC9-58	DSDP 216	DSDP 216	DSDP 216	DSDP 216	DSDP 216	DSDP 216	DSDP 216	DSDP 216
No.	772-7	775-1	775-2	775-3	792-1A	792-1T	792-2	792-3	792-4	792-5	792-7	792-8	793-1	793-2	793-3	770-1	770-2	770-3	770-4	770-5	770-6	770-7	770-8
weight	32.0	35.0	39.9	47.9	43.1	43.1	43.8	56.0	30.1	21.4	40.0	32.5	6.3	8.8	24.0	10.1	6.1	15.4	7.7	12.0	10.4	7.5	12.5
SiO_2	79.97	71.38	72.22	70.72	76.79	72.40	77.05	75.82	76.50	76.59	63.11	74.92	72.20	65.73	62.74	66.68	66.90	68.69	58.87	64.07	64.82	65.96	83.17
TiO_2	0.51	0.73	0.85	0.84	0.58	0.76	0.62	0.65	0.68	0.60	1.00	0.73	0.72	0.89	1.00	0.48	0.40	0.34	0.21	0.24	0.29	0.26	0.22
Al_2O_3	11.03	14.57	15.63	16.30	12.17	14.53	13.08	13.55	12.58	13.34	17.70	14.00	13.25	15.97	17.72	8.77	8.92	7.16	5.44	5.74	6.66	6.87	6.79
FeO	2.78	4.29	4.90	4.68	3.88	4.98	3.09	3.73	3.47	3.43	6.66	3.98	5.74	6.62	6.65	11.44	9.13	5.67	6.20	7.57	8.80	9.51	3.01
MgO	0.96	1.95	1.48	1.68	1.25	1.70	0.97	1.36	1.49	1.07	4.00	1.41	1.73	2.96	4.32	3.27	5.54	6.89	10.69	10.16	7.44	5.17	1.18
CaO	0.94	1.55	1.15	1.56	1.23	1.54	0.88	1.41	1.57	1.09	3.36	1.26	2.05	2.70	3.95	6.06	5.48	8.76	16.11	9.99	9.37	8.16	2.24
Na_2O	0.78	1.24	0.89	1.01	1.04	1.10	1.11	0.62	0.70	0.91	1.36	0.93	0.72	1.42	0.98	1.07	1.09	0.79	0.81	0.69	0.90	1.47	0.67
K_2O	3.02	4.30	2.86	3.20	3.04	2.95	3.19	2.86	2.98	2.98	2.78	2.75	3.59	3.70	2.64	2.22	2.55	1.69	1.68	1.54	1.72	2.61	2.71
Sc	4.57	16.7	18.4	17.8	13.3	-	9.24	12.7	11.5	11.2	26.9	13.1	11.6	21.0	20.9	4.74	8.73	8.15	6.25	6.86	7.86	4.08	2.34
Cr	15.1	112	57.6	59.5	58.9	-	31.8	61.4	51.6	38.5	169	48.3	82.3	188	194	207	810	665	890	1060	1160	816	266
Co	5.64	19.2	18.7	19.1	18.9	-	13.2	14.1	15.4	14.8	35.0	15.4	32.2	41.6	30.2	52.5	118	80.5	108	104	120	81.4	28.2
Ni	26	71	52	46	39	-	26	18	33	33	162	37	249	172	92	560	2230	1455	2360	1595	1910	1283	312
Zn	9	25	25	20	23	-	9	19	25	10	44	29	27	109	49	26	41	70	24	34	30	44	28
Ga	89	14	18	15	6	-	19	3	7	15	7	4	6	55	9	2	3	4	5	9	10	106	4
As	<2	< 0.7	< 0.8	< 0.8	0.3	-	< 0.5	0.1	< 0.4	< 0.7	0.4	< 1	1.0	0.6	0.2	0.7	0.8	0.3	<0.9	0.4	<1	0.8	0.1
Br	0.1	< 0.6	2.3	4.8	0.6	-	0.1	0.1	< 0.3	0.2	< 0.7	0.3	0.5	< 1	< 0.1	n.d.	n.d.	n.d.	n.d.	n.d.	n.d.	n.d.	n.d.
Rb	52.0	201	141	134	129	-	141	121	108	122	178	114	189	216	158	55.1	58.8	50.3	67.1	44.4	56.3	108	17.4
Sr	59.6	168	151	195	240	-	232	214	211	188	306	215	199	324	287	153	171	229	219	143	<110	250	96.3
Zr	59.6	248	297	303	360	-	278	249	195	205	350	209	258	300	314	157	210	180	95	205	130	135	58.9
Sb	0.16	0.35	< 0.1	0.17	8.25	-	9.29	3.56	2.59	6.47	1.27	0.98	4.16	4.63	1.07	1.12	1.10	0.42	0.29	0.32	0.41	1.57	0.37
Cs	2.28	10.2	6.10	6.64	5.30	-	4.02	4.78	4.87	4.00	10.7	4.74	11.7	13.0	8.33	n.d.	n.d.	n.d.	n.d.	n.d.	n.d.	n.d.	n.d.
Ba	226	614	752	666	620	-	704	629	499	645	824	544	479	699	733	384	440	345	240	310	285	410	168
La	14.1	52.0	68.2	54.6	43.6	-	57.3	47.5	42.7	45.4	69.8	45.0	43.6	53.4	65.2	27.8	36.6	33.1	21.4	26.3	27.6	29.5	11.6
Ce	26.5	92.8	120	103	82.3	-	100	90.5	77.5	84.7	137	80.1	80.1	111	116	52.1	70.1	61.4	40.7	46.8	50.3	58.2	19.4
Nd	12.2	44.2	59.6	52.7	44.5	-	54.5	46.2	45.8	44.1	71.3	43.9	45.1	60.9	71.8	18.6	26.8	24.8	16.6	22.0	25.3	19.5	7.02
Sm	2.75	9.74	13.2	10.5	7.98	-	10.1	8.73	7.67	8.50	12.6	8.42	7.75	9.75	12.0	3.13	4.37	4.19	2.98	3.48	3.64	4.03	1.27
Eu	0.59	1.75	2.37	1.96	1.69	-	1.46	1.61	1.47	1.62	2.90	1.68	1.86	2.42	2.05	0.71	1.00	0.87	0.51	0.67	0.89	0.82	0.27
Gd	2.16	7.58	10.3	7.99	6.34	-	7.23	6.87	6.35	6.46	10.2	6.36	6.09	8.88	9.25	2.49	3.35	3.46	3.44	3.05	3.86	n.d.	1.72
Tb	0.39	1.12	1.51	1.31	0.97	-	1.06	1.05	1.00	0.97	1.59	0.96	0.93	1.46	1.41	0.36	0.58	0.51	0.54	0.44	0.52	0.75	0.19
Tm	0.22	0.51	0.83	0.67	0.60	-	0.62	0.62	0.56	0.57	0.87	0.54	0.56	0.70	0.81	0.25	0.38	0.23	0.28	0.23	0.32	0.41	0.08
Yb	1.35	3.85	5.44	4.65	3.86	-	4.78	4.11	3.37	3.90	5.96	3.71	3.62	4.26	5.62	1.69	2.69	2.12	1.68	1.65	1.95	2.48	0.54
Lu	0.21	0.57	0.84	0.67	0.59	-	0.74	0.60	0.49	0.59	0.87	0.59	0.55	0.66	0.90	0.24	0.41	0.35	0.26	0.27	0.28	0.35	0.08
Hf	1.51	6.61	7.11	6.70	6.05	-	7.04	6.65	5.83	5.39	10.0	6.04	5.90	8.12	8.63	3.58	4.56	4.66	3.70	3.06	3.74	4.05	1.65
Ta	0.54	1.39	1.70	1.61	0.98	-	1.45	1.36	1.17	1.30	2.35	1.30	1.31	1.66	1.48	0.25	0.32	0.40	0.48	0.25	0.19	0.26	0.08
Ir (ppb)	< 1	< 3	< 3	< 2	< 3	-	1	< 4	< 4	< 1	< 4	< 3	< 18	< 10	< 4	<2	<4	<1	<4	<1	<3	<1	<1
Au (ppb)	<1	7	12	4	2	-	10	4	4	15	5	1	10	13	12	8	9	5	5	9	28	9	10
Th	3.87	13.0	14.8	14.2	10.2	-	13.9	13.5	13.0	11.1	19.7	11.4	10.6	15.7	17.6	7.15	10.8	9.80	6.12	6.81	7.43	8.22	3.11
U	1.00	2.33	1.28	2.47	1.50	-	2.78	1.98	1.58	1.11	3.07	1.89	2.27	3.33	4.12	1.48	2.11	1.94	2.12	2.93	2.72	3.32	0.57
K / U	22395	15346	18399	10702	16771	-	9709	11930	15155	21922	7323	11696	13155	8962	5415	11881	9797	6932	6344	4250	5188	6326	38815
Th / U	3.87	5.60	11.5	5.74	6.76	-	5.00	6.84	8.24	10.0	6.42	6.02	4.66	4.71	4.27	4.82	5.12	5.05	2.89	2.32	2.73	2.48	5.49
La / Th	3.63	4.00	4.61	3.84	4.28	-	4.13	3.51	3.28	4.08	3.54	3.96	4.12	3.40	3.70	3.89	3.39	3.38	3.50	3.86	3.71	3.59	3.74
Zr / Hf	39.6	37.6	41.8	45.2	59.4	-	39.5	37.5	33.4	38.0	34.8	34.6	43.7	36.9	36.4	44.0	46.1	38.6	25.7	67.0	34.8	33.3	35.7
Hf / Ta	2.79	4.75	4.17	4.17	6.15	-	4.85	4.88	4.97	4.14	4.26	4.65	4.50	4.91	5.81	14.6	14.3	11.7	7.71	12.2	19.7	15.6	19.9
La_N/Yb_N	10.4	13.5	12.5	11.7	11.3	-	12.0	11.6	12.7	11.6	11.7	12.1	12.1	12.5	11.6	16.5	13.6	15.6	12.7	15.9	14.2	11.9	21.7
Eu / Eu*	0.74	0.62	0.62	0.65	0.73	-	0.52	0.63	0.64	0.67	0.78	0.70	0.83	0.80	0.60	0.77	0.80	0.70	0.49	0.63	0.73	n.d.	0.55

Table A1. (Cont.).

	Cpx Spherules																						
Site	DSDP 216	DSDP 216	DSDP 216	DSDP 216	DSDP 216	DSDP 216	DSDP 216	DSDP 216	DSDP 216	DSDP 216	DSDP 216	DSDP 216	DSDP 216	DSDP 94	DSDP 94	DSDP 94	DSDP 94	DSDP 94	DSDP 69A	DSDP 69A	DSDP 69A	DSDP 69A	DSDP 69A
No.	770-9	770-10	770-11	770-12	770-13	770-14	770-15	770-16	770-17	770-18	770-19	770-20	770-21	771-1	771-2	771-7	771-8	771-9	773-1	773-2	773-3	773-4	773-5
weight	9.3	8.4	22.3	7.4	8.8	9.4	7.2	13.7	9.4	9.2	7.8	10.5	10.0	5.6	3.6	3.3	4.0	8.1	5.2	9.8	6.2	7.1	6.8
SiO_2	65.63	73.73	67.61	66.88	68.81	67.03	n.d.	71.14	66.02	70.92	70.01	70.56	68.40	64.51	71.43	64.14	65.26	65.89	64.45	61.95	65.08	62.11	64.99
TiO_2	0.26	0.26	0.37	0.22	0.34	0.31	n.d.	0.30	0.22	0.22	0.26	0.31	0.29	0.61	0.37	0.45	0.56	0.51	0.29	0.29	0.35	0.25	0.37
Al_2O_3	6.30	6.51	8.46	5.78	7.94	7.80	n.d.	7.26	6.03	5.52	6.12	6.65	6.82	11.58	10.48	10.85	12.22	11.61	7.17	6.81	8.65	6.26	7.77
FeO	8.29	6.53	4.78	3.54	3.47	3.83	3.54	4.31	3.23	2.47	4.36	3.12	3.81	8.77	6.02	8.55	6.94	9.51	10.46	10.23	7.30	11.05	7.60
MgO	7.46	6.19	7.64	7.25	6.01	6.60	n.d.	6.01	7.33	7.04	6.91	5.93	7.61	2.78	2.02	3.43	2.96	2.25	4.69	12.51	5.72	9.09	8.83
CaO	9.39	4.18	8.56	14.40	10.87	11.89	n.d.	8.72	15.04	12.09	10.04	11.27	11.13	7.51	5.04	9.05	7.00	7.05	10.38	5.44	9.90	8.83	8.29
Na_2O	0.82	0.74	0.83	0.41	0.66	0.71	1.73	0.53	0.54	0.42	0.46	0.50	0.61	1.62	1.12	1.42	1.80	0.95	0.78	1.25	1.13	0.98	0.80
K_2O	1.84	1.86	1.74	1.50	1.90	1.84	2.93	1.73	1.59	1.32	1.82	1.65	1.32	2.60	3.53	2.10	3.27	2.22	1.79	1.53	1.86	1.43	1.36
Sc	8.01	6.64	9.40	5.98	7.08	7.35	7.14	7.66	2.83	5.33	6.77	3.49	4.82	15.2	7.20	12.3	6.78	1.88	11.9	11.0	9.15	10.4	10.8
Cr	1415	890	415	280	145	190	230	425	175	170	375	121	222	2550	2370	2400	575	87.6	2274	1948	1499	2165	1211
Co	128	99.2	48.0	43.7	20.7	25.2	29.6	44.6	16.6	24.2	53.1	13.6	31.1	80.9	69.5	185	44.7	40.7	89.3	249	124	260	138
Ni	2330	1630	855	710	285	365	435	745	296	395	810	205	490	320	95	935	555	64	664	5386	2058	5854	2702
Zn	70	33	30	14	23	33	30	27	6	24	22	13	19	56	76	48	22	28	84	93	90	78	63
Ga	10	27	0	162	9	161	24	52	26	143	17	8	164	2	2	11	1	16	8	12	8	14	11
As	0.4	1.3	<4	<5	<2	2.5	<1.5	<2	0.4	1.0	0.4	<1.5	<8	6.0	3.1	2.2	1.5	3.0	< 1.1	0.6	1.4	0.6	< 1.1
Br	n.d.	n.d.	n.d.	n.d.	n.d.	n.d.	n.d.	n.d.	n.d.	n.d.	n.d.	n.d.	n.d.	2.74	3.18	3.1	1.2	<2	16	6.1	5.8	2.5	0.1
Rb	58.8	78.4	62.1	45.8	36.9	42.0	44.4	54.0	20.6	35.3	47.0	24.6	25.5	119	81.8	66.5	64.8	62.7	87.6	69.8	46.8	61.2	54.9
Sr	140	154	143	189	115	181	173	160	55.9	121	169	123	136	280	<195	105	152	206	291	n.d.	209	134	150
Zr	120	170	190	125	205	170	160	165	76.7	90.0	195	74.9	145	230	165	260	66.3	182	208	93.5	222	122	141
Sb	0.40	1.48	0.22	0.11	0.26	0.47	0.60	0.24	0.07	0.18	0.29	0.22	0.31	0.25	0.14	0.66	0.04	0.08	0.27	0.14	0.25	0.42	0.10
Cs	n.d.	n.d.	n.d.	n.d.	n.d.	n.d.	n.d.	n.d.	n.d.	n.d.	n.d.	n.d.	n.d.	n.d.	n.d.	n.d.	<2	n.d.	1.30	0.78	0.75	0.83	1.20
Ba	320	375	385	300	435	430	365	255	126	260	330	159	265	605	420	620	351	492	531	417	415	287	468
La	24.6	30.0	38.2	27.6	32.5	34.5	31.3	29.0	10.9	20.7	26.0	14.4	20.3	44.4	25.7	51.3	21.4	25.9	44.6	29.1	33.4	26.8	34.4
Ce	49.2	57.5	70.2	46.3	57	57.2	53.0	51.3	20.0	37.3	48.5	26.3	35.9	88.7	47.9	74.8	40.0	49.3	81.4	54.0	58.1	46.1	64.4
Nd	16.5	21.0	27.9	20.2	22.3	20.7	22.1	22.4	7.85	21.3	15.2	11.2	15.5	36.0	19.1	24.4	16.6	20.7	31.0	23.2	25.5	22.5	24.3
Sm	3.18	3.90	4.72	3.84	3.85	4.25	3.99	3.72	1.57	2.86	3.64	2.04	2.48	6.06	3.54	6.61	3.04	2.94	5.27	4.26	4.28	4.11	5.25
Eu	0.73	0.67	0.94	0.71	0.74	0.86	0.87	0.74	0.29	0.67	0.77	0.34	0.57	1.31	1.10	1.37	0.65	0.55	1.12	0.84	0.90	0.97	1.26
Gd	3.11	2.72	3.71	3.05	2.84	3.91	3.41	2.69	1.22	2.45	3.19	1.23	2.25	5.32	4.67	7.52	2.34	1.63	4.50	3.15	2.91	3.06	3.68
Tb	0.48	0.50	0.61	0.47	0.42	0.64	0.44	0.50	0.18	0.43	0.59	0.24	0.35	1.01	0.52	1.16	0.43	0.41	0.61	0.49	0.43	0.44	0.54
Tm	0.28	0.29	0.33	0.26	0.26	0.23	0.33	0.26	0.11	0.26	0.33	0.14	0.17	0.52	0.28	0.55	0.25	0.22	0.36	0.29	0.23	0.26	0.33
Yb	1.76	1.82	2.23	1.65	1.78	2.50	1.97	1.83	0.73	1.80	2.14	0.97	1.21	3.60	1.81	3.79	1.69	1.46	2.49	1.93	1.69	1.74	2.21
Lu	0.27	0.20	0.42	0.23	0.28	0.31	0.30	0.26	0.11	0.27	0.32	0.15	0.18	0.55	0.24	0.56	0.24	0.19	0.39	0.30	0.25	0.24	0.34
Hf	3.67	4.06	5.39	3.92	4.26	4.40	4.50	4.69	1.73	3.79	4.20	2.23	3.10	5.15	3.16	4.76	2.52	3.40	4.83	3.62	4.24	3.63	5.19
Ta	0.26	0.43	0.50	0.45	0.36	0.29	0.36	0.38	0.15	0.20	0.35	0.14	0.25	1.03	0.57	0.54	0.47	0.56	0.32	0.28	0.57	0.12	0.49
Ir (ppb)	<2	<1	<1	<2	<3	<4	<2	<1	<1	<2	<4	<1	<4	1	3	5	1	1	< 7	< 2	< 7	< 7	< 9
Au (ppb)	9	12	6	4	2	1	8	2	3	5	11	3	4	5	7	5	5	<1	8	6	5	7	2
Th	7.32	8.53	11.9	6.95	9.29	9.81	8.63	8.20	2.91	5.78	7.20	4.25	5.46	12.8	7.48	10.6	5.94	7.62	8.64	7.18	6.29	6.11	7.36
U	2.15	2.43	1.75	2.31	2.53	2.85	1.80	2.61	1.33	2.06	2.45	0.70	1.05	2.89	2.82	3.96	1.51	1.61	2.96	1.68	1.51	1.58	2.96
K / U	6448	5876	7969	5283	5906	5185	16421	5343	8908	5158	6133	19548	10316	7095	9361	3983	16411	10462	4909	7341	9670	7535	3640
Th / U	3.40	3.51	6.80	3.01	3.67	3.44	4.79	3.14	2.18	2.81	2.94	6.11	5.18	4.43	2.65	2.68	3.93	4.73	2.92	4.26	4.17	3.88	2.48
La / Th	3.36	3.52	3.21	3.97	3.50	3.52	3.63	3.54	3.75	3.58	3.61	3.38	3.72	3.47	3.44	4.84	3.60	3.40	5.16	4.06	5.31	4.38	4.68
Zr / Hf	32.7	41.9	35.3	31.9	48.1	38.6	35.6	35.2	44.3	23.7	46.4	33.6	0.1	44.7	52.2	54.6	26.3	53.5	43.2	25.8	52.5	33.7	27.2
Hf / Ta	14.1	9.44	10.8	8.71	11.8	15.2	12.5	12.3	11.6	19.0	12.0	16.3	12.3	5.00	5.54	8.81	5.35	6.08	15.2	12.8	7.42	31.4	10.6
La_N/Yb_N	14.0	16.5	17.1	16.7	18.3	13.8	15.9	15.8	15.0	11.5	12.1	14.8	16.8	12.3	14.2	13.5	12.6	17.8	17.9	15.1	19.8	15.4	15.5
Eu / Eu*	0.71	0.63	0.69	0.63	0.68	0.64	0.72	0.71	0.64	0.77	0.69	0.65	0.74	0.71	0.83	0.59	0.74	0.76	0.70	0.70	0.78	0.84	0.88

Table A1. (Cont.).

	Cpx Spherules																					
Site	DSDP 69A	DSDP 149	DSDP 149	DSDP 149	DSDP 149	DSDP 149	DSDP 149	DSDP 149	DSDP 149	DSDP 149	DSDP 292	DSDP 292	DSDP 292	DSDP 292	DSDP 292	DSDP 292	DSDP 292	RC9-58	DSDP 166	DSDP 166	DSDP 167	DSDP 167
No.	773-6	776-1'	776-2	776-3	776-4	776-5	776-6	776-7	776-8	776-9	789-2	789-3	789-5	789-6	789-7	789-8L	789-10	792-6	797-1	797-10R	797-11	797-12
weight	2.5	4.1	5.7	2.6	8.5	4.6	7.2	8.6	4.0	5.4	3.8	22.3	0.2	12.9	20.1	45.0	32.2	43.6	3.2	8.3	3.9	15.0
SiO_2	62.69	69.36	58.99	59.95	59.66	65.82	64.95	63.91	58.54	60.63	69.38	71.16	n.d.	68.01	69.36	71.44	68.80	61.66	n.d.	63.82	64.71	64.08
TiO_2	0.28	0.40	0.33	0.32	0.26	0.26	0.23	0.25	0.30	0.40	0.27	0.31	n.d.	0.24	0.33	0.36	0.31	0.26	n.d.	0.20	0.23	0.22
Al_2O_3	6.85	8.93	6.34	6.92	6.51	6.53	6.14	6.49	6.94	7.88	6.72	7.00	n.d.	6.65	7.49	8.21	7.53	6.64	n.d.	6.06	6.01	7.20
FeO	9.97	4.88	10.55	7.46	7.45	5.11	6.52	6.06	8.66	10.75	3.67	3.02	4.56	3.33	7.69	5.80	3.61	7.76	14.60	4.78	4.81	5.57
MgO	10.29	5.13	6.24	10.12	10.87	8.42	9.22	9.02	8.08	4.16	7.02	5.41	n.d.	6.72	6.09	6.45	6.26	10.18	n.d.	9.86	8.70	8.01
CaO	7.60	8.65	14.97	12.37	12.57	11.70	10.87	11.96	14.15	12.06	10.07	10.83	n.d.	13.12	4.91	4.58	11.21	11.17	n.d.	13.48	13.66	12.14
Na_2O	0.83	0.61	1.10	0.76	0.81	0.62	0.59	0.48	1.29	1.79	0.68	0.49	2.97	0.49	1.51	1.19	0.61	0.86	2.33	0.44	0.55	1.14
K_2O	1.49	2.03	1.49	2.09	1.88	1.52	1.47	1.83	2.04	2.32	2.22	1.77	n.d.	1.44	2.62	1.98	1.67	1.48	n.d.	1.37	1.34	1.63
Sc	15.5	11.3	11.9	10.4	8.66	6.66	6.71	6.79	9.95	15.6	8.44	7.72	14.8	7.24	12.5	11.2	10.1	7.89	15.7	2.70	4.17	5.15
Cr	1012	341	2288	937	1237	844	995	1217	1869	2559	468	142	893	237	862	796	224	1447	1639	177	325	325
Co	165	52.3	117	108	150	102	116	108	134	113	47.3	17.4	135	31.3	144	95.7	29.7	163	175	26.5	43.2	54.0
Ni	2978	869	723	1142	4109	1807	2241	2063	1658	1525	1059	250	2030	520	3041	2066	459	3133	4030	374	20	828
Zn	7	70	28	82	14	98	20	18	18	62	46	48	104	30	32	37	48	39	59	12	9	18
Ga	17	16	44	189	74	61	34	71	96	284	12	13	94	33	121	7	31	12	44	21	11	12
As	0.4	1.7	< 1.3	12	3.0	0.1	0.8	0.9	2.7	3.6	1.2	0.1	2.8	0.4	0.7	0.1	0.1	< 1	1.3	0.6	0.3	< 1
Br	3.5	9.0	19	29	1.6	11	12	2.4	23	1.9	0.9	0.6	3.1	2.6	< 0.9	1.1	0.7	< 1	4.4	3.5	2.0	1.8
Rb	99.7	70.9	109	135	89.3	69.9	58.0	69.0	91.3	146	61.8	62.0	110	55.3	138	72.1	59.7	58.1	136	35.0	32.1	44.5
Sr	579	102	286	777	107	171	251	392	179	218	262	167	520	232	168	150	284	297	226	136	186	172
Zr	478	253	157	390	176	345	142	163	304	149	136	181	315	225	179	216	282	128	387	79.2	188	220
Sb	0.45	0.26	0.99	3.70	0.38	0.39	0.36	0.16	0.42	0.67	1.59	0.47	0.40	0.13	0.61	0.03	0.09	1.22	46.4	3.81	0.83	1.68
Cs	< 0.9	2.82	1.66	1.93	2.16	2.28	1.25	1.48	1.50	2.05	1.64	1.07	13.4	1.32	1.25	0.65	1.00	1.16	2.30	0.54	0.47	0.98
Ba	998	519	432	1200	467	584	453	411	512	540	361	572	476	416	430	414	464	4.15	978	309	244	395
La	61.9	47.1	43.9	80.5	28.3	31.3	26.5	25.4	36.9	53.4	36.0	32.9	54.5	32.9	40.4	36.7	38.3	32.1	54.3	13.8	15.9	27.3
Ce	109	81.3	76.2	111	49.7	52.6	44.5	45.5	71.9	86.1	72.8	69.7	98.5	68.4	86.3	77.9	78.4	58.2	93.6	22.1	36.3	51.8
Nd	46.3	35.9	38.3	57.5	18.4	22.9	29.6	19.9	29.9	39.2	28.9	26.8	35.7	28.8	31.7	31.0	34.1	25.9	44.5	11.0	14.2	17.8
Sm	8.69	6.64	6.58	11.7	4.29	4.95	3.81	3.88	5.79	7.19	4.68	4.48	7.05	4.58	5.21	5.08	5.74	4.52	9.26	1.81	2.38	3.44
Eu	1.83	2.13	1.22	2.22	1.15	1.10	0.86	0.95	0.83	1.69	1.34	0.99	1.25	0.96	1.34	1.17	1.12	0.91	1.73	0.33	0.52	0.73
Gd	5.51	4.79	4.64	9.66	3.15	3.49	2.60	3.07	3.97	5.29	3.52	4.29	7.90	4.24	4.57	4.46	4.81	2.91	7.17	0.62	1.93	2.41
Tb	0.65	0.70	0.74	1.44	0.51	0.58	0.39	0.42	0.54	0.75	0.57	0.71	1.39	0.70	0.74	0.76	0.81	0.40	1.11	0.24	0.32	0.34
Tm	n.d.	0.39	0.44	n.d.	n.d.	n.d.	0.22	0.21	0.33	0.44	0.34	0.37	n.d.	0.39	0.44	0.43	0.38	0.27	0.55	0.15	0.19	0.22
Yb	3.46	2.61	3.28	3.25	1.80	2.11	1.47	1.45	2.12	3.19	2.33	2.45	4.83	2.64	3.09	2.94	2.57	1.92	3.66	1.03	1.35	1.43
Lu	0.55	0.42	0.51	0.49	0.26	0.32	0.24	0.21	0.34	0.49	0.35	0.35	0.74	0.40	0.47	0.44	0.39	0.30	0.47	0.16	0.19	0.22
Hf	7.90	5.57	5.22	5.79	4.09	4.89	3.71	3.93	4.07	5.58	6.09	5.48	5.85	5.82	5.58	5.65	6.38	4.72	8.63	3.45	2.45	6.80
Ta	0.53	0.88	0.62	1.03	0.47	0.55	0.49	0.18	0.21	0.31	0.74	0.49	6.90	0.76	0.50	0.50	0.74	0.50	1.30	0.15	0.30	0.31
Ir (ppb)	< 20	< 13	< 6	< 10	< 8	< 9	< 15	< 2	< 11	< 15	< 5	< 3	< 6	< 6	< 6	< 2	< 3	1	< 9	< 2	< 3	< 1
Au (ppb)	<1	10	3	<1	<1	<1	11	<1	10	12	6	3	< 4	7	3	3	< 3	6	5	5	< 17	8
Th	12.5	12.8	8.80	13.9	6.32	5.62	5.52	5.43	7.33	12.2	5.53	5.71	9.15	5.17	7.50	7.19	6.79	6.44	11.1	3.14	8.36	5.43
U	3.01	1.98	2.72	3.49	2.76	2.92	1.63	2.12	3.75	3.57	1.31	0.78	2.09	0.75	1.00	0.49	0.66	2.19	4.49	1.51	1.37	1.32
K / U	3914	8257	4449	4754	5651	4235	7333	7100	4470	5353	13941	19152	n.d.	16390	21319	32541	20645	5530	n.d.	7241	7451	10100
Th / U	4.15	6.45	3.23	3.98	2.29	1.92	3.38	2.57	1.95	3.41	4.22	7.32	4.38	6.90	7.52	14.8	10.2	2.94	2.47	2.08	6.10	4.13
La / Th	4.95	3.68	4.99	5.80	4.48	5.57	4.80	4.68	5.03	4.39	6.52	5.77	5.96	6.36	5.39	5.10	5.64	4.98	4.89	4.40	1.90	5.02
Zr / Hf	60.4	45.5	30.1	67.4	43.0	70.6	38.4	41.6	74.8	26.6	22.3	32.9	88.0	38.7	32.1	38.3	44.2	27.2	44.8	23.0	76.5	32.3
Hf / Ta	14.8	6.35	8.37	5.64	8.76	8.91	7.65	22.3	19.3	18.0	8.19	11.2	0.85	7.63	11.1	11.3	8.61	9.47	6.64	23.6	8.20	22.1
La_N/Yb_N	17.9	18.0	13.4	24.8	15.7	14.8	18.0	17.6	17.4	16.7	15.5	13.4	7.62	12.5	13.1	12.4	14.9	16.8	14.8	13.5	11.8	19.1
Eu / Eu*	0.81	1.15	0.68	0.64	0.96	0.81	0.84	0.84	0.53	0.84	0.94	0.69	0.51	0.66	0.84	0.75	0.65	0.76	0.65	0.94	0.74	0.77

Table A1. (Cont.).

	Cpx Spherules																			Cpx-Related Microtektites High-Si		
Site	DSDP 167	DSDP 166	DSDP 166	DSDP 166	DSDP 166	DSDP 166	DSDP 166	DSDP 166	DSDP 166	DSDP 162	DSDP 162	DSDP 162	DSDP 162	DSDP 162	DSDP 162	DSDP 162	DSDP 162	DSDP 162	DSDP 162	DSDP 162	DSDP 216	DSDP 216	DSDP 216
No.	797-14	797-2	797-3	797-4	797-5	797-6	797-7	797-9	798-2	800-1A	800-2	800-3	800-4	800-5	800-6	800-7	800-8	801-2	801-3A	774-1	774-2	774-3
weight	12.1	15.5	16.9	42.4	26.3	4.9	3.9	57.9	9.5	33.9	6.3	4.0	4.2	6.1	5.8	5.7	5.7	9.5	5.2	40.7	25.4	42.3
SiO_2	n.d.	63.19	63.77	63.80	63.78	62.86	58.56	59.19	61.03	59.10	59.33	61.26	58.24	61.32	61.28	61.66	n.d.	64.05	58.31	78.22	78.24	74.96
TiO_2	n.d.	0.27	0.38	0.29	0.23	0.32	0.22	0.27	0.24	0.27	0.33	0.33	0.26	0.27	0.32	0.30	n.d.	0.45	0.37	0.48	0.45	0.46
Al_2O_3	n.d.	6.60	8.44	7.83	7.85	7.97	5.72	7.04	6.28	6.94	7.87	8.64	6.78	6.78	8.35	7.11	n.d.	9.56	7.46	14.72	12.24	12.69
FeO	1.98	11.06	10.19	5.07	2.64	5.61	9.17	4.88	6.15	12.32	13.61	9.45	11.12	11.60	6.88	11.85	14.02	8.52	11.68	2.10	4.51	6.92
MgO	n.d.	7.59	7.62	8.90	7.90	8.64	12.49	10.22	10.69	8.86	10.62	8.15	12.39	9.55	9.20	10.37	n.d.	4.97	5.58	0.49	0.65	0.65
CaO	n.d.	7.45	6.36	11.69	14.69	12.21	11.75	15.93	13.57	10.78	5.34	9.23	8.74	6.65	11.31	6.04	n.d.	9.61	13.90	0.95	0.60	0.65
Na_2O	0.70	1.06	1.12	0.74	1.13	0.72	0.84	1.19	0.68	0.67	1.25	1.10	0.99	1.39	0.87	0.79	2.09	0.82	0.98	0.39	0.11	0.57
K_2O	n.d.	2.77	2.13	1.67	1.77	1.67	1.26	1.28	1.36	1.05	1.65	1.83	1.47	2.43	1.78	1.88	n.d.	2.02	1.72	2.62	3.20	3.08
Sc	1.98	7.53	7.36	6.06	5.45	6.33	7.01	8.05	7.64	10.3	10.9	11.6	10.2	10.2	8.43	10.6	12.0	12.3	13.0	8.38	6.12	8.10
Cr	178	1547	823	333	102	287	1070	444	556	1889	1390	811	1920	2660	1850	1380	3250	691	2240	46.3	33.7	46.4
Co	24.5	94.9	93.5	49.0	20.7	55.3	135	65.3	57.6	71.4	158	120	192	148	55.0	190	115	101	95.3	2.69	10.0	13.7
Ni	5	2060	1487	890	359	937	2774	1262	1150	939	2860	1800	4360	3070	889	3640	2390	1790	617	11	26	49
Zn	9	21	65	29	30	10	16	42	48	35	36	55	74	119	17	17	141	50	49	5	18	19
Ga	10	16	20	6	11	16	75	18	28	16	80	168	122	98	96	156	36	32	< 40	50	156	216
As	0.53	< 0.8	< 0.7	0.7	4.3	0.2	1.6	< 0.2	0.4	1.9	< 3	< 5	< 5	< 1	1.5	< 4	< 2	0.2	< 5	< 1.6	< 2.6	1.1
Br	2.9	0.3	0.5	< 0.2	< 0.3	0.3	0.4	< 0.2	< 1	3.8	3.3	2.5	< 3	7.9	2.5	4.3	7.3	7	15	0.7	2.3	0.6
Rb	14.8	92.0	49.6	40.7	61.2	53.3	40.8	39.6	52.2	48.6	62.8	70.7	58.6	114	58.6	68.2	106	68.9	81.3	91.7	97.4	108
Sr	75	< 65	123	124	201	107	136	83.8	157	282	236	228	150	< 230	113	173	245	220	119	424	217	355
Zr	73.1	104	37.8	206	443	136	216	424	354	191	271	238	114	227	147	141	244	302	228	249	174	275
Sb	0.62	15.6	26.0	4.33	6.12	4.25	7.01	10.77	3.35	0.67	1.08	1.33	0.88	1.64	0.49	0.68	0.41	0.25	0.44	0.72	0.25	0.08
Cs	0.39	0.59	0.59	0.68	1.69	0.40	0.59	0.87	0.80	1.12	0.94	1.50	1.35	0.98	0.78	0.54	1.6	1.13	1.25	1.61	2.03	2.31
Ba	116	369	470	358	553	347	29.6	423	458	517	539	563	422	345	515	480	465	551	455	1470	1040	1230
La	10.1	21.0	28.9	24.1	26.5	25.3	20.0	31.0	30.7	30.1	33.2	48.8	28.8	26	30.3	30.1	31.1	32.4	32.9	50.4	44.5	47.3
Ce	18.1	43.7	45.9	38.3	48.1	41.6	35.1	53.0	55.5	49.2	58.6	77.6	49.7	51.3	48.6	56.7	58.5	66.1	61.3	90.9	70.8	85.5
Nd	5.23	20.6	19.4	17.4	18.9	18.5	16.2	28.7	22.2	23.0	28.8	33.3	19.3	22.8	27.7	20.1	26.7	35.1	24.1	45.5	35.0	36.1
Sm	1.12	3.25	4.29	3.52	4.10	3.81	3.15	4.35	4.54	4.25	4.51	6.01	3.64	3.96	4.30	3.91	4.57	4.84	4.98	6.35	6.37	6.61
Eu	0.26	0.74	0.62	0.68	0.80	0.86	0.78	0.60	1.03	1.01	0.84	1.09	0.89	0.70	0.70	0.79	1.11	1.09	0.98	1.61	1.31	1.47
Gd	0.86	3.01	3.01	2.72	3.17	2.76	2.53	3.81	3.64	3.69	3.47	3.85	2.59	2.48	2.68	2.60	3.66	3.73	3.72	5.73	4.69	5.94
Tb	0.13	0.49	0.59	0.43	0.51	0.40	0.39	0.54	0.58	0.56	0.57	0.56	0.39	0.36	0.38	0.38	0.64	0.56	0.50	0.66	0.55	0.71
Tm	0.08	0.27	0.35	0.25	0.63	0.25	0.22	0.33	0.27	0.34	0.33	0.34	0.22	0.24	0.32	0.32	0.48	0.31	0.79	0.32	0.33	0.42
Yb	0.59	1.76	2.56	1.85	1.69	1.79	1.53	2.28	1.89	2.12	2.10	2.29	1.57	1.69	2.30	2.42	2.39	2.12	1.97	2.20	2.31	2.80
Lu	0.09	0.27	0.38	0.31	0.25	0.28	0.23	0.33	0.30	0.34	0.32	0.34	0.23	0.29	0.35	0.45	0.36	0.31	0.27	0.34	0.34	0.46
Hf	2.46	5.19	5.93	5.56	6.76	7.38	5.10	7.94	7.47	5.03	6.25	7.32	5.40	5.94	5.33	4.72	7.13	7.53	6.03	6.01	5.13	6.30
Ta	0.16	0.24	0.36	0.43	0.38	0.21	0.32	0.44	0.39	0.56	0.31	0.53	0.27	0.34	0.26	0.20	0.45	0.33	0.43	0.74	0.64	0.67
Ir (ppb)	< 1	5	< 2	< 1	1	< 8	< 10	< 1	< 3	< 1	< 6	< 1.5	< 5	< 3	< 4	< 7	< 8	< 9	< 14	< 2	< 1	< 6
Au (ppb)	1	< 6	7	< 2	3	5	4	3	10	< 2	9	16	7	6	7	< 11	3	3	< 1	7	6	9
Th	2.06	4.96	5.88	4.58	5.28	5.08	4.36	6.85	6.40	7.71	7.72	8.92	5.76	7.65	6.87	6.72	8.50	8.43	7.89	7.56	6.66	8.38
U	0.68	3.41	1.94	1.30	2.37	0.67	1.81	1.85	2.01	2.79	1.01	1.91	3.04	3.83	2.83	0.84	3.23	1.72	2.31	0.46	2.48	2.34
K / U	n.d.	6405	8647	9911	6108	20133	5557	5746	5700	2971	13397	7867	3932	5137	5045	18085	n.d.	9653	6073	46488	10783	10770
Th / U	3.03	1.46	3.03	3.52	2.23	7.61	2.41	3.71	3.18	2.76	7.64	4.67	1.89	2.00	2.43	8.00	2.63	4.90	3.42	16.3	2.69	3.59
La / Th	4.90	4.24	4.92	5.27	5.02	4.97	4.60	4.52	4.80	3.90	4.30	5.47	5.00	3.40	4.41	4.48	3.66	3.84	4.17	6.67	6.69	5.64
Zr / Hf	29.7	20.0	6.4	37.0	65.6	18.4	42.4	53.4	47.4	38.0	43.4	32.5	21.1	38.2	27.6	29.9	34.2	40.1	37.8	41.5	34.0	43.7
Hf / Ta	15.4	21.9	16.4	12.9	17.8	35.2	15.8	18.3	19.2	9.00	20.2	13.8	20.0	17.5	20.5	23.6	15.8	22.8	14.0	8.09	7.98	9.43
La_N/Yb_N	17.1	11.9	11.3	13.0	15.7	14.1	13.1	13.6	16.2	14.2	15.8	21.3	18.3	15.4	13.2	12.4	13.0	15.3	16.7	22.9	19.3	16.9
Eu / Eu*	0.81	0.72	0.53	0.67	0.68	0.81	0.85	0.45	0.77	0.78	0.65	0.69	0.89	0.68	0.63	0.76	0.83	0.78	0.70	0.81	0.73	0.72

Table A1. (Cont.).

	Cpx-Related Microtektites											
	High-Si							Low-Si				High-Al
Site	DSDP 216	DSDP 216	DSDP 216	DSDP 216	DSDP 216	DSDP 216	DSDP 167	DSDP 292	DSDP 292	DSDP 292	DSDP 167	DSDP 162
No.	774-4	774-5	774-6	774-7	774-8	774-9	799-1	789-1	789-4	789-9	798-1	801-1
weight	73.1	40.1	38.2	94.6	46.1	49.5	174.8	9.0	2.5	40.0	41.5	15.4
SiO_2	81.84	81.77	82.95	89.66	80.25	73.86	73.74	67.78	68.57	71.16	63.64	54.33
TiO_2	0.47	0.41	0.56	0.28	0.46	0.52	0.78	0.44	0.53	0.42	0.44	1.64
Al_2O_3	13.01	11.64	12.64	6.45	12.82	14.91	22.52	9.48	11.83	9.12	10.12	30.37
FeO	0.51	0.69	0.48	0.99	0.73	6.11	0.54	6.75	6.09	6.28	6.82	4.06
MgO	0.28	1.07	0.50	0.53	1.07	0.78	0.77	4.85	3.24	5.23	7.81	6.93
CaO	0.12	1.43	0.18	0.67	1.54	0.57	0.12	4.94	2.94	4.41	8.26	1.71
Na_2O	0.01	0.04	0.02	0.03	0.03	0.24	0.04	2.19	2.39	1.10	1.30	0.62
K_2O	3.75	2.94	2.64	1.34	3.08	3.01	1.49	3.57	4.40	2.28	1.60	0.34
Sc	4.73	6.17	6.65	4.13	6.06	8.87	9.05	12.6	15.8	14.1	11.1	40.9
Cr	25.4	21.1	23.3	17.8	26.3	37.1	5.11	725	329	457	417	415
Co	8.53	8.00	9.25	5.01	9.6	12.9	0.06	101	72.0	66.2	49.7	9.15
Ni	16	20	8	11	32	26	15	1715	1410	910	293	61
Zn	20	22	18	8	23	39	6	107	108	21	< 1	23
Ga	2	8	19	5	6	49	4	8	27	6	45	13
As	2.9	1.2	2.8	0.4	2.4	2.8	0.2	0.6	< 0.8	0.2	1.1	0.4
Br	0.7	1.2	< 1	0.2	0.8	0.6	< 0.2	0.9	< 1.2	0.3	0.6	0.4
Rb	96.5	70.4	71.0	45.9	79.2	103	29.3	157	192	91.9	45.1	10.3
Sr	143	137	121	85	117	176	210	160	216	258	166	337
Zr	272	281	377	273	297	269	615.0	224	198	246	54.4	853
Sb	0.16	0.19	0.02	0.07	0.16	0.24	0.17	0.50	0.14	0.05	1.45	< 0.1
Cs	1.29	1.32	1.10	1.01	1.42	2.30	0.74	1.62	4.15	0.72	0.34	0.26
Ba	1140	2100	884	567	985	1210	1840	n.d.	419	551	514	1225
La	37.2	45.2	54.8	25.8	44.3	49.7	57.9	49.1	63.7	51.2	40.6	109
Ce	61.3	78.7	96.1	44.2	79.1	84.2	98.9	96.3	123	100.3	65.9	205.0
Nd	29.9	42.0	40.4	17.4	34.9	39.5	45.7	41.1	52.8	38.9	37.4	107
Sm	5.12	6.65	7.47	3.42	6.58	6.96	8.74	6.47	8.06	6.72	5.70	20.6
Eu	1.13	1.49	1.54	0.69	1.42	1.45	1.77	1.39	2.05	1.27	1.15	4.07
Gd	3.87	4.81	5.26	2.44	4.49	5.32	6.25	5.13	7.06	5.91	4.34	17.2
Tb	0.52	0.71	0.75	0.36	0.69	0.74	0.95	0.81	1.21	0.98	0.72	2.75
Tm	0.29	0.39	0.39	0.20	0.34	0.41	0.51	0.49	n.d.	0.59	0.43	1.46
Yb	1.99	2.76	2.45	1.39	2.50	2.79	3.50	3.38	5.07	4.03	2.89	9.82
Lu	0.31	0.40	0.37	0.21	0.36	0.43	0.55	0.52	0.76	0.61	0.43	1.58
Hf	6.51	6.48	9.79	7.35	6.23	7.11	11.80	6.02	7.97	7.07	8.33	25.5
Ta	0.69	0.65	0.81	0.55	0.67	0.78	1.26	0.77	0.35	0.60	0.38	2.00
Ir (ppb)	< 1	< 2	< 2	< 1	< 2	< 2	< 1	< 6	< 10	< 2	< 1	< 1.5
Au (ppb)	3	5	5	3	6	3	3	6	< 1	5	11	5
Th	7.19	7.44	9.07	6.09	7.38	9.19	13.0	7.99	10.5	9.70	8.04	22.8
U	1.68	1.46	1.91	1.06	1.54	2.45	1.80	1.83	1.52	0.40	1.02	0.98
K / U	18598	16581	11372	10515	16507	10189	6780	15869	23317	45805	12854	2880
Th / U	4.28	5.10	4.74	5.76	4.80	3.75	7.22	4.37	6.92	24.0	7.88	23.3
La / Th	5.18	6.08	6.04	4.23	6.00	5.40	4.45	6.15	6.04	5.27	5.05	4.78
Zr / Hf	41.9	43.5	38.5	37.1	47.7	37.8	52.1	37.3	24.9	34.8	6.5	33.5
Hf / Ta	9.41	10.0	12.1	13.3	9.31	9.08	9.37	7.78	23.0	11.8	21.8	12.8
La_N/Yb_N	18.7	16.4	22.3	18.6	17.7	17.8	16.5	14.5	12.6	12.7	14.0	11.1
Eu / Eu*	0.77	0.81	0.75	0.73	0.80	0.73	0.73	0.74	0.83	0.62	0.71	0.66

Major element data (wt. %) by EDX-analysis, recalculated to 100%, and then standardized. Trace element data (in ppm, except as marked) by INAA; all Fe as FeO; n.d. = not determined.